EXPERIMENTAL STUDIES ON FRACTURE TOUGHNESS OF SHORT FIBRE COMPOSITES

A Thesis Submitted

In Partial Fulfilment of the Requirements
for the Degree of

DOCTOR OF PHILOSOPHY

?8୧୧୨

by

B. SEETARAMA PATRO

to the

DEPARTMENT OF MECHANICAL ENGINEERING
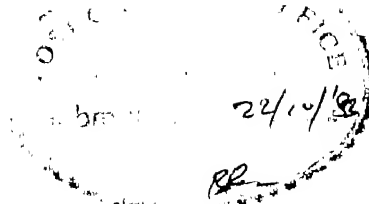INDIAN INSTITUTE OF TECHNOLOGY KANPUR
OCTOBER, 1983

ME-1983-D-PAT-EXP

Dedicated

to

MY MOTHER

CERTIFICATE

This is to certify that the thesis entitled "EXPERIMENTAL STUDIES ON FRACTURE TOUGHNESS OF SHORT FIBRE COMPOSITES", by B. SEETARAMA PATRO is a record of work carried out under our supervision and has not been submitted elsewhere for a degree.

B. D. AGARWAL
Professor
Department of Mechanical Engg.
Indian Institute of Technology
Kanpur 208 016

PRASHANT KUMAR
Assistant Professor
Department of Mechanical Engg.
Indian Institute of Technology
Kanpur. 208 016
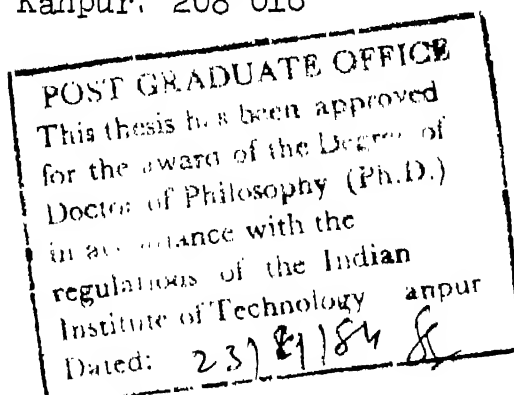
ACKNOWLEDGEMENT

I express my deep sense of gratitude and
appreciation to Professors B.D. Agarwal and Prashant Kumar
for their valuable guidance throughout the present work.
Their generous attitude has been a constant source of
inspiration and encouragement.

I am thankful to Prof. P.C. Das for his valuable
suggestions and also to Professors A.K. Jena, A. Ghosh,
N.G.R. Iyengar, G.S. Murthy, V. Sinha, M.B. Nayak and
B. Rath for their interest in my work.

I highly value the association with my friends
especially Messrs K Srinivasan, R.K. Nakrani, L.J. Rao,
I.K. Bhat , B.K. Mishra, S.K. Khanna and A.K. Dalai with
whom I shared many ideas.

Thanks are due to Mr. B.K. Jain of Advanced
Centre of Material Science and Mr. S.L. Srivastava of
Experimental Stress Analysis Laboratory for the cooperation
and help rendered throughout the experimental investigations.

Thanks are also due to Messrs. D.K. Sarkar,
D.P. Saini, Swaran Singh, R.M. Jha, S.N. Yadav, B.D. Pandey
and S.N. Dwivedy of Mechanical Engineering Department for
their help.

Thanks are due to Mr. J.D. Varma for the excellent
typing of the manuscript. Thanks are also due to Messrs.

S.J. Kushwaha and G.K. Shukla of Design and Development Cell for the tracings and Mr. R.S. Shukla for making photographs.

B.S. Patro

October, 1983

TABLE OF CONTENTS

LIST OF FIGURES

NOMENCLATURE

A	Area
a	Crack length
a_e	Equivalent or effective crack length
a_o	Initial crack length
a_d	Equivalent crack length at unloading
a_{or}	Equivalent crack length at the beginning of reloading
a_{dr}	Equivalent crack length corresponding to straight line portion of load - COD curve
COD	Crack mouth opening displacement
C	Compliance based on COD
C_o	Initial compliance
C_d	Compliance at unloading
C_{or}	Initial compliance during reloading
C_{dr}	Compliance corresponding to straight line portion of load-COD curve during reloading
d	Generalised displacements
F	Generalised force
G	Energy release rate
I_n	Constant
J	J integral
J_c	Critical value of J integral
K	Stress intensity factor
K_c	Critical stress intensity factor

K_I Stress intensity factor in mode I

K_1 Crack extension force

K_R Crack growth resistance

$K_{R(Ins)}$ Crack growth resistance at instability

LEFM   Linear elastic fracture mechanics

l   Length of specimen

n   Strain hardening exponent

n_i Direction cosines of a normal vector

P   Load

R-curve   Crack growth resistance curve

r   Near tip crack field length parameter

S   Boundary of a two dimensional body

S_T Portion of boundary where traction is prescribed

SEN   Single edge notched specimen

T_i Traction vector

t   Thickness

U   Potential energy per unit thickness

u_i Displacement vector

V_f Fibre volume fraction

W   Strain energy density function

w   Width

X_1, X_2 Coordinates

Y   K calibration factor

σ Stress along load direction, standard deviation

σ_{ij} Stress tensor

$\tilde{\sigma}_{ij}(\theta)$ Function of θ

$\bar{\sigma}_1$ Constant

$\bar{\sigma}$ Equivalent stress

ϵ Strain along load direction

ϵ_{ij} Strain tensor

$\tilde{\epsilon}_{ij}(\theta)$ Function of θ

$\bar{\epsilon}_p$ Equivalent strain

δ Crack mouth opening displacement

Γ J integral contour

SYNOPSIS

EXPERIMENTAL STUDIES ON FRACTURE TOUGHNESS
OF SHORT FIBRE COMPOSITES
A Thesis Submitted in Partial Fulfilment
of the Requirements for the Degree of
DOCTOR OF PHILOSOPHY
by
B. SEETARAMA PATRO
to the
Department of Mechanical Engineering
Indian Institute of Technology Kanpur
Kanpur, October, 1983

Fracture toughness of short glass and carbon fibre reinforced epoxy composites has been investigated experimentally. The composite material plates were fabricated in the laboratory and single edge notched specimens were used. The tests were conducted in tension in a 10 Ton MTS machine. The instantaneous value of load, displacement and crack mouth opening displacement (COD) were measured on all the specimens so that analysis could be carried out using J integral and R curve approaches. However, emphasis was placed on developing J integral as a fracture criterion. A total of 1000 specimens were tested at different stages of the investigations.

     The R curve approach has been applied to composites widely by investigators. Since the crack length in composites is not well defined, application of this approach

requires estimation of instantaneous crack length indirectly
through the compliance matching procedure. Validity of this
procedure has been examined and established. Further, it
has been mathematically established and experimentally
verified that the peak load point on the load-COD curve is
the instability point and the fracture toughness can be
determined at this point. This eliminates the necessity
of obtaining the full R curve through a tedious and time
consuming process.

Short glass fibre composites do not exhibit self
similar crack growth because of local heterogeneity ahead
of the crack. Instead, a damage zone is formed with multi-
ple cracks in the matrix and along the fibre-matrix
interface. In such a case, characterization of the crack
tip area by a parameter calculated without focussing atten-
tion directly at the crack tip would provide a more useful
method for analyzing fracture. The well known J integral,
which is often used to characterize fracture of metals
under conditions of large scale yielding, is such a para-
meter. Its value depends on the near tip stress strain
field but its path independent nature allows an integra-
tion path, taken sufficiently far from the crack tip, to
be substituted for a path close to the crack tip region.
With this in mind, the experimental data have been analysed
using the J integral approach through its energy rate
interpretation.

Critical value of J integral (J_c) is found to be independent of crack length when the ratio of crack length to specimen width (a_0/w) is larger than 0.4. For smaller cracks, general material damage away from crack tip also influences the energy absorbed significantly. However, an extrapolation method has been developed through which the crack tip energy may be separated from the energy absorbed due to general material damage. J_c thus obtained for $a_0/w < 0.4$ is also independent of crack length and its value is the same as that obtained earlier without extrapolation for $a_0/w > 0.4$. The J_c values have been compared with the critical crack growth resistance, K_c, obtained through R curve approach. The results compare very well and thus, validate each other. Appropriate modelling of the constitutive relation and observation of damage zone through scanning electron microscope also justify the use of J integral to characterize fracture behaviour of short fibre composites.

The specimen width has been varied between 15 and 40 mm and thickness between 1.8 and 9 mm. J_c is found to be independent of specimen width and thickness. Earlier it has been shown that J_c is independent of specimen length and crack length. Thus, J_c can be regarded as a material property which can be used to characterize fracture toughness of short fibre composites.

In the present investigations, the fracture
toughness of short glass fibre composites has been deter-
mined for varying fibre volume fractions. In the range
V_f = 23.6 to 47.2 %, J_c increases linearly with fibre
volume fractions.

Investigations on short carbon fibre composites
show that they exhibit more brittle behaviour than the glass
fibre composites and have much lower fracture toughness.
The J integral approach appears to be equally applicable.

" I personally believe that the 'mechanics of
fracture' and 'mechanics of composites' are the two
foremost branches of modern applied mechanics. Fracture
of composite materials includes a combination of the two
and should pave the way for the development of applied
mechanics."

V.V. Bolotin[*]

in the Second USA - USSR
Symposium held at Lehigh University,
Bethelehem, Pennsylvania, USA
March 9 - 12, 1981

[*]Mechanical Engineering Research Institute
USSR Academy of Sciences
Moscow, USSR

CHAPTER I

INTRODUCTION

1.1 INTRODUCTION TO FRACTURE OF COMPOSITES

Composite materials are a result of engineering combination of two or more materials to achieve certain physical properties not realizable by the constituent materials individually. These materials offer high strength and stiffness coupled with low density. The manufacture of composites requires comparatively low labour and generates less waste in addition to ease of processing structural forms that are otherwise inconvenient to manufacture. Composite structures are destined for many future applications as they have many other desirable properties such as good vibration, fatigue and corrosion resistance, low heat conductivity, good electrical insulation properties, favourable cost effectiveness etc. in addition to the earlier mentioned impressive properties.

The employment of composite materials in vital structural applications requires material selection criteria and design procedures. Global properties such as modulus and deformation are well understood. Strength criteria, although not well founded, are generally agreed upon. Consequently research emphasis has shifted towards gaining

an understanding and common acceptance of the fatigue and fracture response of composites.

Fracture mechanics has now been widely accepted as a useful discipline which recognises the likelyhood of presence of inherent macroscopic cracklike defects in materials. It concerns with the study of fracture of materials by crack initiation and propagation under various service conditions. It does provide guidelines for tolerable size of crack like defects and inspection requirements to prevent catastrophic failures. The development in fracture mechanics, so far, has led to established methods for predicting fracture toughness of traditional materials such as metallic and ceramic materials. The modern fibre reinforced composite materials also seek reliable means of characterizing fracture behaviour as a part of establishing the fundamental properties.

In view of the appreciable heterogenity of the composite materials and the complexity of interaction between constituents, fracture is accompanied by several processes, each of which requires special representation. These processes include the breaking of the fibres, their extraction from the matrix, debonding between fibres and matrix, fracture of the matrix etc. Some fibre composites fracture during stretching along the fibres by breakdown of the integrity i.e., by multiple fracture of structure

without formation of macroscopic cracks. In other cases
where steady growth of cracks is observed, they differ
substantially from the cracks in traditional materials.
The cracks are greatly dispersed owing to multiple exfo-
liation of the fibres from the matrix.

The problem of characterizing fracture properties
of composite materials is challenging as the cracks in them
differ substantially from the cracks in homogeneous isotro-
pic materials which exhibit self similar crack growth. The
additional complexities in composites underscore the need
for parallel or combined experimental and theoretical
analyses. Fracture mechanics of composite materials,
together with its initiation, propagation and controlling
parameters, represents a significant problem.

1.2 LITERATURE REVIEW

Since the advent of fracture mechanics, two basic
approaches, namely, the energy and stress approaches have
emerged. The first approach was initiated by Griffith [1]
who on the basis of thermodynamic considerations derived a
criterion for fracture by taking account of the total change
in energy of a cracked body. The second approach is due
to Irwin [2] who relied on stress analysis of a cracked
body. According to him, the behaviour of a crack could be
fully characterized through elastic stress intensity factor,
K, and it is equivalent to Griffith's energy release rate, G.

The salient definitive features of fracture in isotropic homogeneous solids were identified by Griffith [1] and skillfully extended by Orowan [3] and Irwin [2] for engineering materials. Orowan recognised that in metals that undergo plastic deformation additional work is required for producing plastic zone ahead of the crack tip and that the surface energy is small in its comparison and can be neglected. He proposed a modification to the analysis on this basis. Irwin carried out stress analysis of cracked bodies assuming the material to be linear elastic. The approach which assumes the material to be linear elastic is known as linear elastic fracture mechanics (LEFM). The LEFM approach has also been used, through an appropriate correction, for small scale yielding where the crack tip plastic region is atleast an order of magnitude smaller than the physical dimensions of the component.

Rice [4, 5] used a different energy approach applicable to linear as well as nonlinear elastic materials and also applicable under conditions of large scale yielding. He used a two dimensional energy line integral, now commonly termed as J integral, to characterize the crack tip. The basis of J integral is provided by the works of Hutchinson [6] and Rice and Rosengren [7] . They have shown that a singularity in stress and strain does exist at the crack tip which is uniquely dependent upon the material

flow properties. McClintock [8] has demonstrated that
the crack tip stress and strain field can be described in
terms of J integral. The use of the J integral as an
elastic-plastic fracture criterion has also been discussed
by Broberg [9] from an analytical standpoint. Begley and
Landes [10 - 12] through extensive experiments have shown
the applicability of J integral as a fracture criterion
for metals.

Since the early seventies, linear elastic fracture
mechanics concepts have been applied to composite materials
[13 - 27]. Several investigators have obtained critical
value of energy release rate of composites through compliance
tests. Others have found out critical stress intensity
factors from fracture loads and initial crack lengths. Many
researchers have observed that fracture toughness was not
independent of initial crack length and they used a method,
similar to plastic zone correction in metals, to take into
account the effect of damage zone at the crack tip. They
proposed a new two parameter LEFM model, in place of the
usual one parameter model, with the length of the damage
zone as the second parameter.

By a consideration of hole size effect, Nuismer
and Whitney [28, 29] proposed two alternative approaches
for fracture of laminated composites. The point stress
criterion is based on the stress at a certain distance away

from the crack tip. The average stress criterion is based on the average stress over a characteristic length ahead of the crack tip. They carried out experiments on glass and carbon fibre reinforced laminates and observed that the predictions of both the criteria agreed well with the experimental results. Like the two parameter LEFM model, the size of the crack is increased to account for the damage zone. Nuismer and Labor [30] have shown that the average stress criterion leads to acceptable strength predictions for counter sinks and slant cracks in graphite-epoxy laminates. Giare [31] and Agarwal and Giare [48] have found notched strength of short glass fibre reinforced epoxy resin composites to be in agreement with Whitney - Nuismer criteria. Performing experimental studies on laminated graphite-epoxy composites Brinson and Yeow [32] found that the characteristic dimension, mentioned in the Whitney - Nuismer models, changes with Laminate type. Pipes [33] assumed the material characteristic dimension to be an exponential function of crack size.

Wu [34] formulated a phenomenological failure criterion where fracture initiates under a complex state of stress. Depending upon the fibre volume fraction and the material properties of the constituents, Sih [35] modeled the composite system by invoking the assumption of homogeneous anisotropy or nonhomogeneous isotropy. Fracture is assumed

to occur when the strain energy stored in an element ahead
of crack reaches a critical value.

Daniel, Rowlands and Whiteslide [36] conducted
research on laminates using various experimental stress
analysis procedures. They observed that stacking sequence
plays an important role on fracture phenomenon to an extent
that it can alter the mode of failure from catastrophic to
noncatastrophic. Beaumont [37] presented models for the
dissipation of energy for different fracture micromechanisms
in composites such as fibre breakage, matrix cracking, fibre
pullout etc. By comparision of experimental data from
flexural beam tests with the models, he has shown that post
debond fibre sliding mechanism, that is, frictional energy
due to differential displacement between fibre and matrix
in the debonded region, is primarily responsible for the
toughness of glass fibre-epoxy composites.

Slow crack growth is a minor consideration in the
fracture of high strength and relatively frangible materials
under conditions of plane strain. In case of thin metal
sheets, considerable stable crack growth takes place prior
to catastrophic failure. It has been postulated [38, 39]
that there is a unique relationship between the amount of
crack growth and the applied stress intensity factor repre-
sented by the crack growth resistance curve (R curve).

Among the earliest applications of R curve approach to composites was the one on randomly oriented short glass fibre composites which are considered isotropic [40 - 44] in the plane of the composites. Gaggar and Broutman [41 - 44] considered damage zone at the crack tip as a self similar crack extension. The instantaneous crack length is estimated by a compliance matching procedure. Morris and Hahn [45] demonstrated the possibility of using R curve concepts for graphite-epoxy laminates. Mahishi and Adams [46] have used R curve concepts to a micromechanical model of Boron - Aluminium composites to predict initiation and propagation of a matrix crack at a broken fibre. Ochiai and Peters [47] have applied R curve concepts to study fracture behaviour of centre notched graphite epoxy laminates.

Agarwal and Giare [48 - 51] have used R curve approach to characterize fracture behaviour of short glass fibre reinforced epoxy resin for different test parameters including temperature variation. They also evaluated fracture toughness in shear modes (Modes II and III) by testing single edge notched specimens. Garg [52] has obtained an approximate expression for critical stress intensity factor for short fibre composites. Yanada and Homma [53] conducted fracture tests on short glass fibre composites taking compact tension and centre cracked tension specimens. They observed that the stress intensity factor corresponding to

maximum load and initial crack length is independent of thickness, initial crack length and specimen configurations.

There is a continuing search for a parameter to characterize fracture behaviour of a composite material, which is independent of test variables. Carrying out experiments on carbon fibre and hybrid laminates, Lee and Phillips [54] observed that the candidate stress intensity factor provide guidelines for the development of better damage tolerant systems. Fracture toughness does not appear to vary with specimen thickness and there is no apparent transition from plane stress to plane strain. Owen and Cann [55] have conducted fracture tests on centre notched composites with glass chopped strand mat and woven roving fabric. They observed negligible change in critical stress intensity factor with specimen thickness varying between 1.5 and 5.8 mm. However, critical stress intensity factor increases with width and varies with crack length. Recently, Harris and Morris [56] studied the fracture toughness of graphite/epoxy laminates as a function of specimen thickness using center cracked tension specimens. The fracture toughness of the $[0/\pm 45/90]_{ns}$ quasi-isotropic laminates at thickness ranging between 8 and 96 plies decreases with increasing specimen thickness and approaches a lower value asymptotically at a thickness of approximately 10 mm. This behaviour is similar to that of metals.

Griffith, Kanninen and Rybicki [57] have presented a critical look at the application of linear elastic fracture mechanics to the failure of fibre reinforced composites. They point out that the application of LEFM to fibre composites has not met with the same degree of success that has been achieved for metals and other homogeneous materials. In most instances, techniques successful for metals have been applied to composites without regard for the special character of crack growth in these materials. The LEFM approach is unable to cope with the complexity of the crack extension process:

Smith, Green and Bowyer [58] attempted to apply J integral approach to glass fabric reinforced polyester resins. More recently Agarwal, Patro and Kumar [59, 60] have applied J integral method to short glass fibre composites. This approach has the advantage that the analysis of very complex crack tip region is avoided since the integration path can be taken away from the crack tip. It has been demonstrated that critical value of J integral is independent of crack length.

1.3 SCOPE OF PRESENT WORK

The current studies are an attempt to characterize fracture behaviour of composite materials. As seen from the preceding section, researchers are far from agreeing on applicability of a particular fracture mechanics principle

to composite materials. The opinion is so widely varying on' the topic that some authors even wonder if the concepts of LEFM can be extended to composites at all. So far, there is no accord on a fracture toughness criteria even for randomly oriented short fibre composites which being quasi-isotropic may be more amenable to such an endeavour.

The material chosen for the present investigation is randomly oriented short glass or carbon fibre reinforced epoxy resin. The short fibre composites have assumed considerable importance for manufacture of many moulded components. These composites have the additional advantage of being easily processed. Moreover, short fibre composites are isotropic in the plane of the composite materials. These materials are intermediate between isotropic materials such as metals, polymers and ceramics and anisotropic composite laminates. Thus, it may offer insight into fracture behaviour of laminated composites.

Details concerning material and specimen preparation and fracture toughness testing system are given in Chapter 2. The J integral analysis is conducted on single edge notched specimens. The effects of crack length and specimen length on critical value of J integral are reported in Chapter 3 for short glass fibre reinforced composites. Scanning electron microscope studies on damage zone ahead

of crack tip have been done to establish the dominating
fracture mechanisms. The effect of width and thickness on
J critical is investigated in Chapter 4. The effect of
glass fibre volume fraction is also presented.

The R curve approach has, so far, been more
widely used by investigators to obtain fracture toughness
of short glass fibre composites. The experiments were
conducted such that the data could be analysed using J
integral as well as R curve approach. The results using
R curve approach are given in Chapter 5 and compared with
those using the J integral approach given in Chapter 3.
The validity of different steps involved in the application
of R curve approach has also been examined in Chapter 5.

The fracture behaviour of short carbon fibre
reinforced composites is different from that of short glass
fibre composites. Fracture toughness of short carbon fibre
composites has been investigated in Chapter 6. Finally,
important conclusions and some suggestions for further work
are included in Chapter 7.

CHAPTER II

EXPERIMENTAL DETAILS

2.1 MATERIALS AND SPECIMENS

The present investigations have been performed
on randomly oriented short glass fibre reinforced epoxy
resin. The composite material plates were fabricated in
the laboratory using chopped strand mat of glass fibres
having a weight of 0.6 Kg/m^2, an average fibre length of
50 mm and manufactured by Fibre Glass Pilkington Ltd.,
India. Tests were also conducted on composites with ran-
domly oriented carbon fibre (Torayca Mat BO-30) having a
weight of 30 gms/m^2. The matrix material was an epoxy resin
commercially designated as Araldite CY 230 cured with 10 %
by weight of hardener HY 951, both supplied by Ciba-Geigy
of India Ltd.

Composite material plates were cast between two
25 mm thick mild steel mould plates lined with mylar sheets
and separated by steel bars acting as spacers which control
the thickness of the plates being cast. Chopped strand mat
was first cut into pieces of required size and placed on
the lower mould plate, one by one. Resin was spread on
the lower mould plate and on the top of each mat piece.
The resin was spread on the glass fibre mat by a rubber
roller to enhance impregnation and it was brushed on the

carbon fibre mat. Pressure between the two plates was maintained for 24 hours. The plates were cured at room temperature for atleast 10 days before specimens were cut by a diamond impregnated wheel, cooled by running water.

All the fracture tests were conducted in Mode I on single edge notched (SEN) specimens (Fig. 2.1) in tension. The notches were machined using a high speed steel slit cutter of 0.2 mm thickness. A lathe available in the laboratory was suitably modified for this purpose. The experimental arrangement is shown by a photograph (Fig. 2.2). Fracture toughness for short fibre reinforced composites was obtained for different materials for various test variables as described below.

1. Reinforcement material

   Glass and Carbon fibres

2. Specimen width (w)

   $w = 15, 25, 30$ and 40 mm

3. Initial crack length (a_o)

   $a_o/w = 0.1$ to 0.7

4. Specimen length

   Specimen length between grips varied between 3 and 6 times the specimen width.

5. Specimen thickness (t)

   $t = 1.8, 3, 6$ and 9 mm
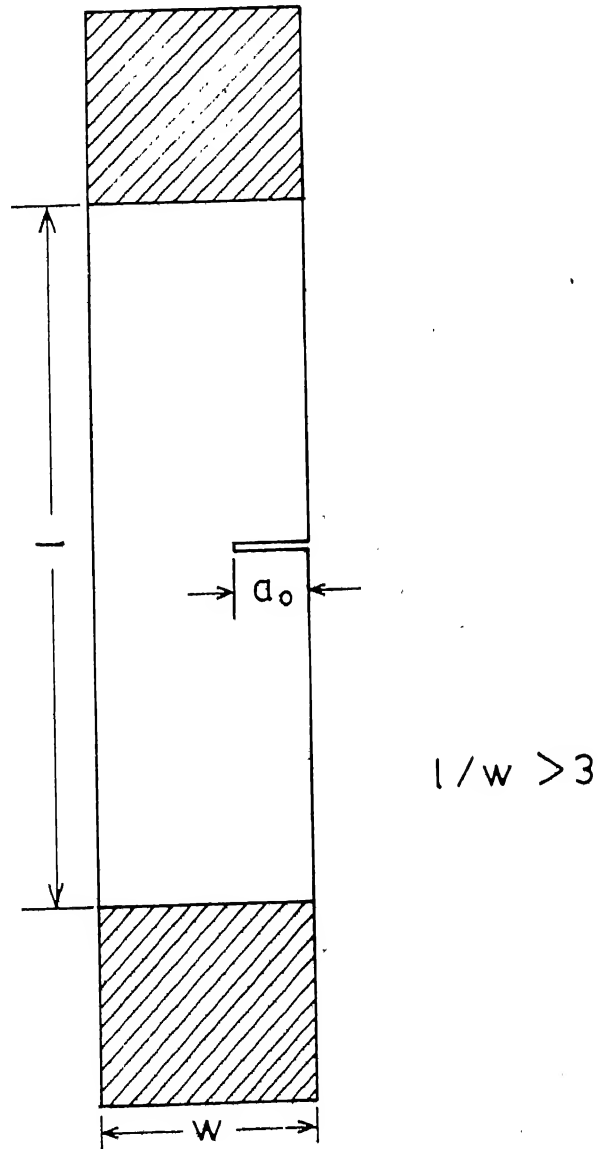
Fig. 2.1 Single edge notched specimen
for tests in mode I .
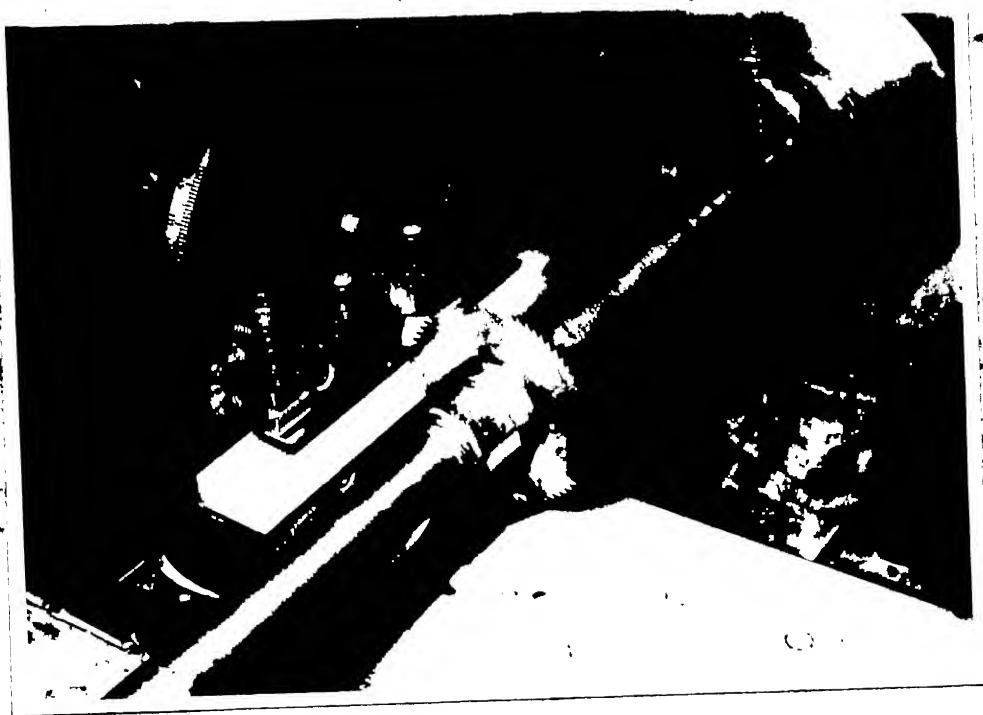
Fig. 2.2 Experimental arrangement for
cutting notches.

6. Volume fraction (V_f).

$\qquad V_f$ = 23.6, 31.5, 39.4, and 47.2 percent (for glass)

$\qquad V_f$ = 20.7 percent (for carbon)

2.2 TESTING SYSTEM

The fracture toughness tests were conducted on SEN specimens in a 10 Ton MTS (Material Test System) testing machine. The general experimental arrangement is shown in Fig. 2.3. Figure 2.4 shows a specimen in the hydraulically actuated grips of MTS. The upper grip is fixed and the lower grip can move in a vertical direction. The tests can be conducted in load controlled or in displacement controlled modes. Instantaneous values of load, displacement of lower grip (henceforth called displacement) and crack mouth opening displacement (COD) were measured. Load versus displacement and load versus COD were monitored on two X-Y recorders.

The instantaneous load is measured by a load cell located above the upper grip. The displacement is sensed by a linearly variable differential transformer (LVDT) located below the movable lower grip. Crack mouth opening displacement may be measured by a clip gauge. MTS clip gauge having gauge length of 4 to 8 mm was available. The clip gauge is suitable for thick metal specimens but not for thin SEN composite specimens because it is too stiff. More importantly, for fixing the clip gauge attachment, V –
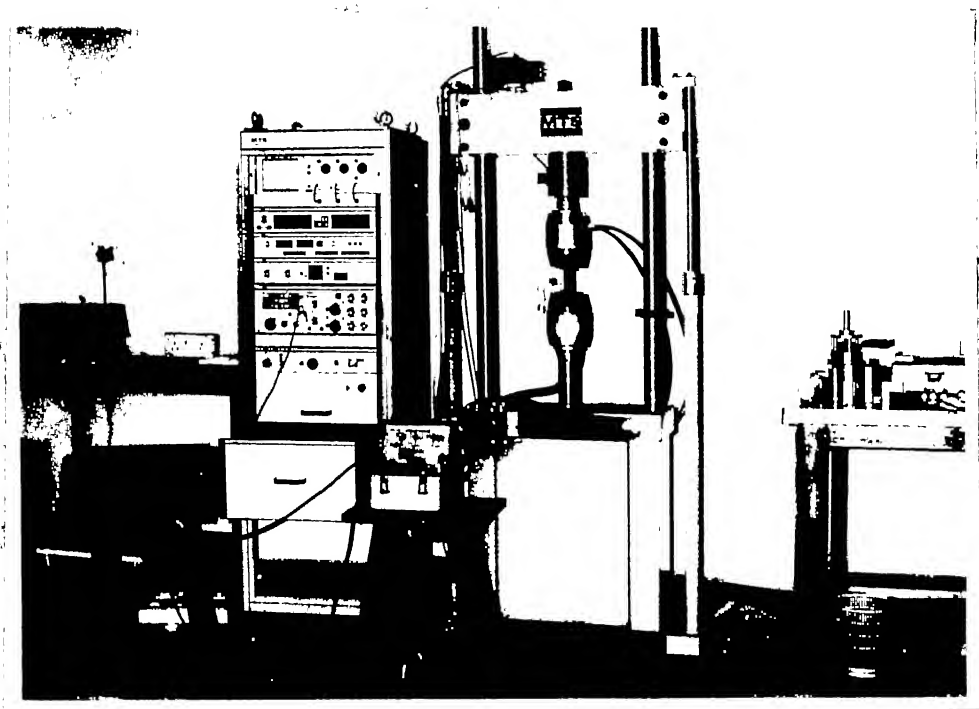
Fig. 2.3 Fracture toughness testing on MTS.

Fig. 2.4, SEN specimen under inflexible grips of MTS.

edges are needed along the thickness on both sides of the notch. This is not possible for thin composite specimens where it is required to tap 3 mm diameter holes for fixing the attachments. Therefore, a clip gauge with low stiffness and fixing arrangements suitable for even 1.8 mm thick composite material specimen was designed and fabricated in the laboratory.

The requirements of a clip gauge are that it be sensitive and linear. There should be no lost motion between gauge and the specimen. The gauge must be released without damage when the specimen breaks. Keeping these points in view, a clip gauge was made. The schematic diagram and the photograph of the clip gauge are shown in Figs. 2.5 and 2.6 respectively. It consists of two 0.4 mm thick, 7.5 mm wide and 44 mm long spring steel strips clamped 10 mm apart at one end through a spacer. Four 120 ohm electrical resistance strain gauges are bonded to the two strips near the fixed ends. The free ends of the strips are machined to a V edge so as to seat them into two 0.25 mm deep grooves made on the specimen located 2.5 mm away on either side of the notch. The clip gauge presses against the specimen by rubber bands and stays in place.

The calibration fixture supplied by MTS was suitably modified to calibrate the clip gauge as shown in Fig. 2.7. Output of the clip gauge was monitered on a
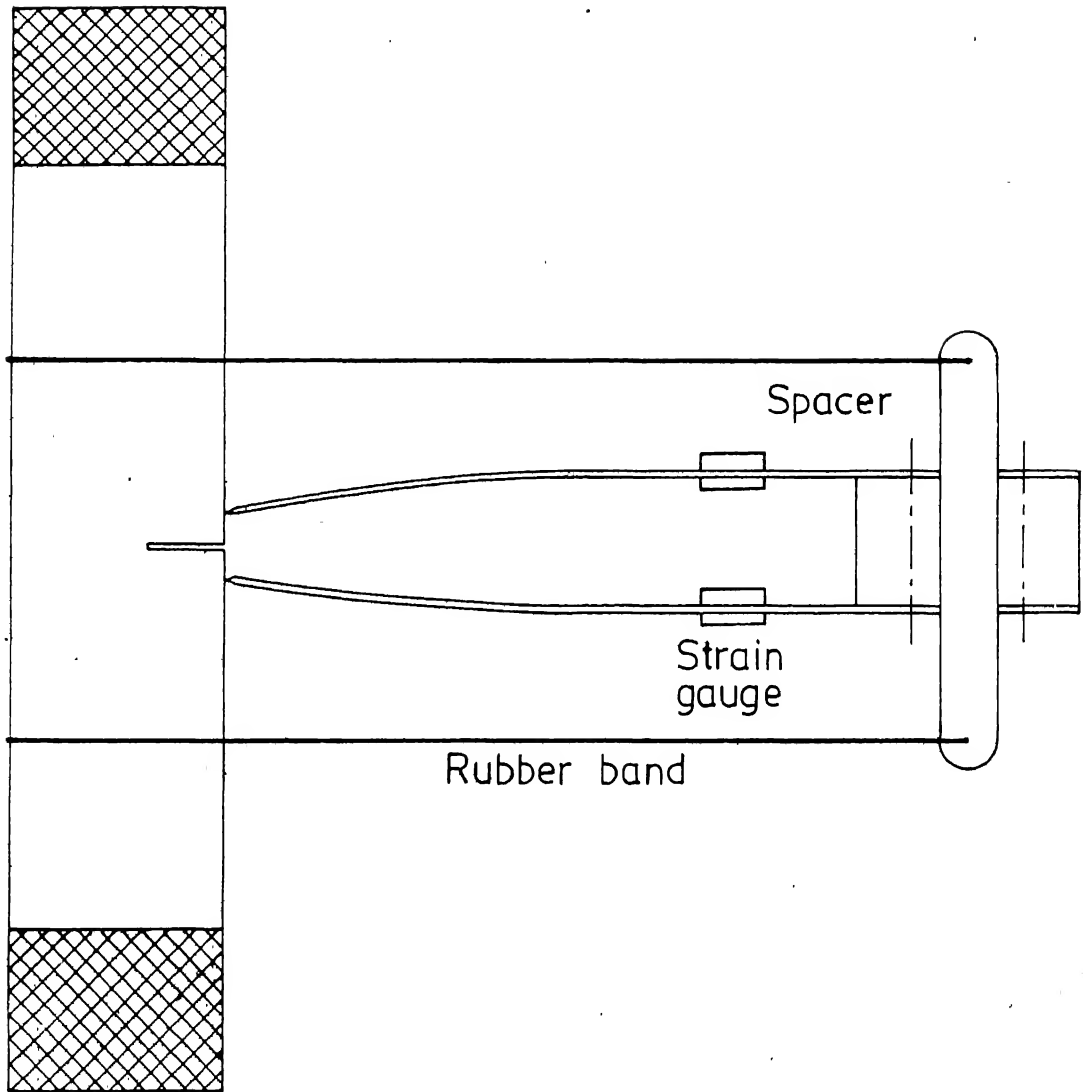
Fig. 2.5 Schematic diagram of clip gauge attached
to a specimen.
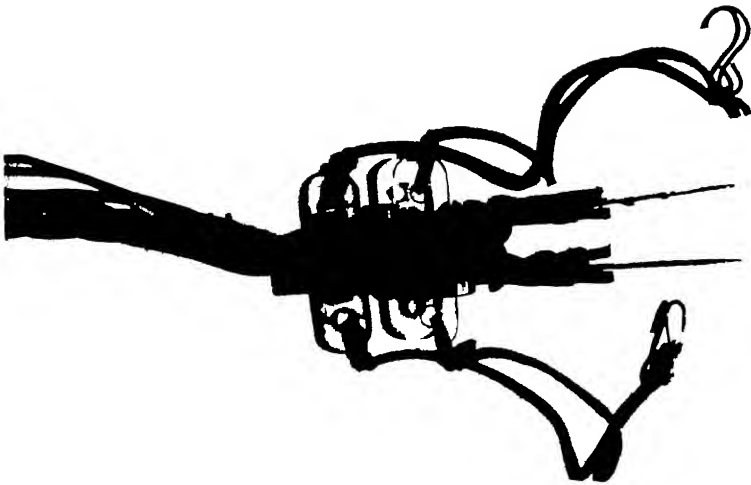
Fig. 2.6 Photograph of a clip gauge.
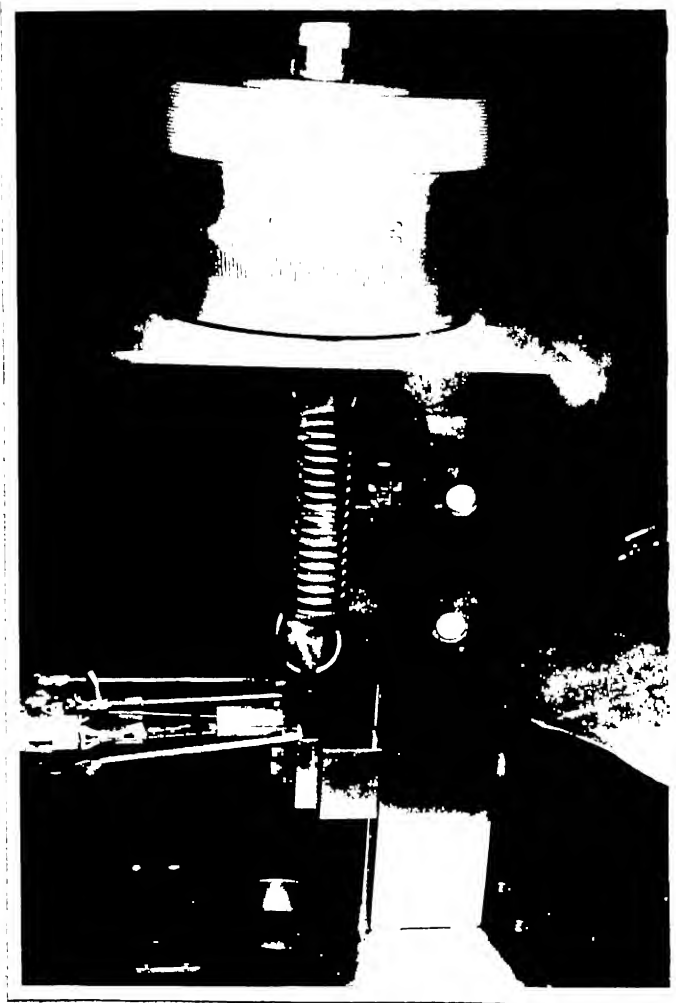
Fig. 2.7 Calibration arrangement for
clip gauge .

X - Y recorder through a strain indicator. The relative
displacement between the two free ends of the clip gauge
indicates crack mouth opening displacement. The relation
between COD and the output in X - Y recorder can be adjusted
by the sensitivity knob in the strain indicator. By increa-
sing the sensitivity, the range decreases. Keeping this in view,
a suitable value of sensitivity was chosen. Output of the
clip gauge is plotted against displacement in Fig. 2.8.
The input-output relationship of the clip gauge is observed
to be linear. The accuracy of the gauge is within
2.5×10^{-3} mm over the working range.
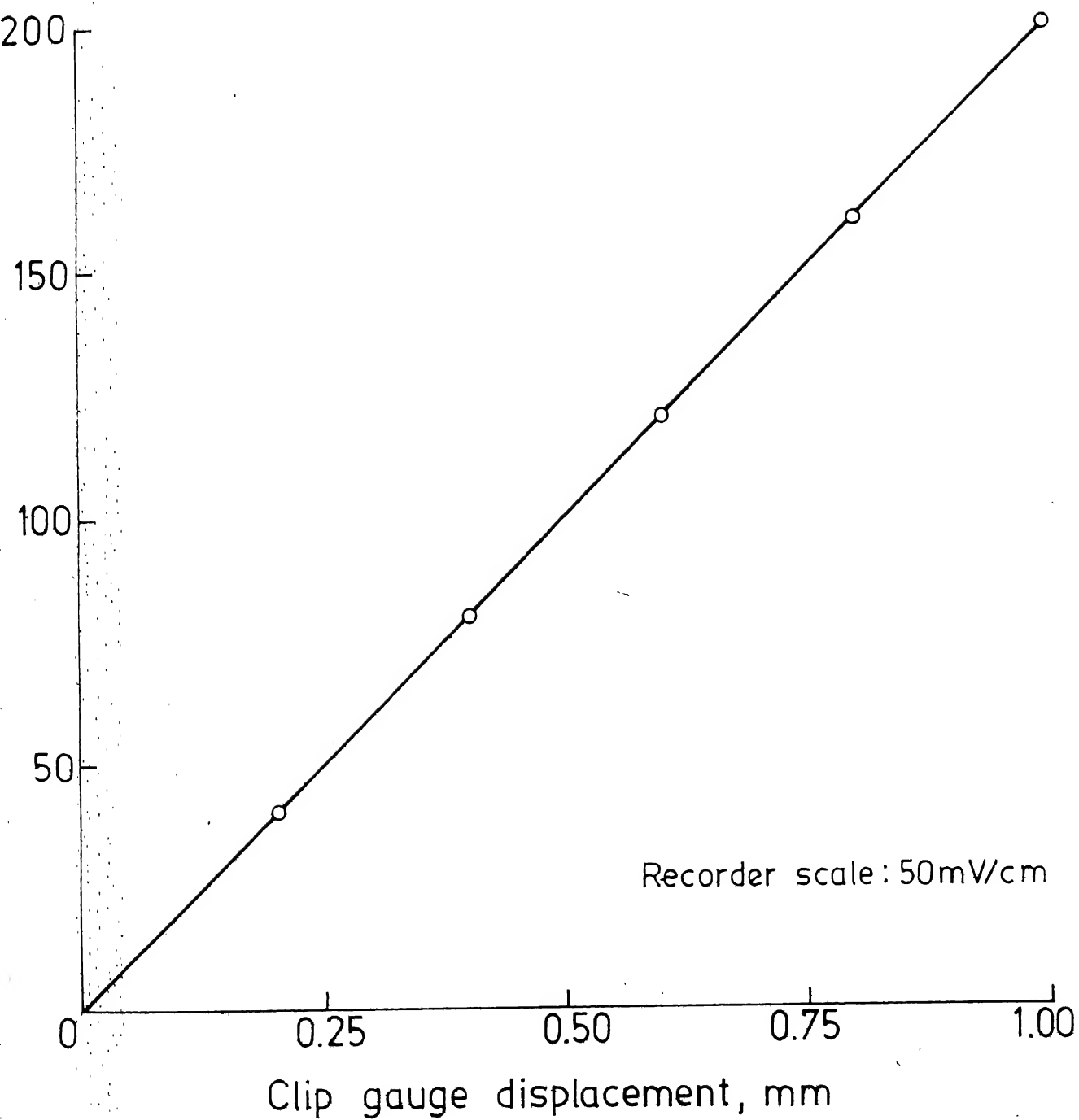
Fig. 2.8 Calibration curve for clip gauge.

CHAPTER III

J INTEGRAL AS FRACTURE CRITERION FOR
SHORT GLASS FIBRE COMPOSITES

3.1 INTRODUCTION

Manifold theoretical refinements and experimental implementations have led to the general acceptance of fracture toughness as an important material property for many homogeneous materials. The successful application of fracture mechanics to metals has led to its extension to composites. Fracture of materials is a highly complex process even for idealized homogeneous isotropic materials. Criteria for fracture are prudently selected by emphasizing the primary physical factors and excluding the secondary. Such a compromise for composite materials, having a much more complex fracture process is critical.

In composite materials, the fibres and matrix interact in a number of different ways, sometimes coopera-ting to increase the work of fracture and sometimes acting cohibitively. The factors affecting work of fracture include the cohesive energies of fibres and matrix and adhesive energy between fibres and matrix. Functional relationship between crack orientation, material orienta-tion and loading direction need be established in addition to mechanical dissipative processes such as fibre pull out

and shrinkage. Microvoids and fibre ends also affect
fracture process. Reviewing and categorizing specific and
combined effects of such a large number of variables here
may confuse rather than clarify the perspective of composite
fracture.

An important difference between mechanisms of
crack propagation in isotropic materials and composites
arises from the fact that isotropic materials such as metals
or polymers exhibit self similar crack growth. In lamina-
tes, the direction of crack extension in each ply is generally
expected to be different depending on fibre orientations.
Randomly oriented short glass fibre composites, which are
macroscopically isotropic, also do not exhibit self similar
crack growth because of the local heterogeneity ahead of
the crack. Instead, a damage zone is formed with multiple
cracks in the matrix and along the fibre-matrix interface.

Fracture characterization by strain energy release
rate assumes a prescribed crack extension trajectory
(usually collinear with the original crack) whereas another
energy release rate approach, namely J integral, does not
require such an assumption and hence more amenable to
characterize cracks in composite materials where the crack
trajectory is not well defined. Further, J integral is
a path independent line integral and does not require
accurate analysis of the most complicated crack tip region.

In this chapter, the use of J integral as a fracture
criterion for short fibre composites has been explored.

3.2 BASIS FOR J INTEGRAL

The J integral, as proposed by Rice [4, 5], is a
two dimensional energy line integral

$$J = \int_{\Gamma} (W \, dx_2 - T_i \frac{\partial u_i}{\partial x_1} \, d \, S) \qquad (3.1)$$

where Γ is any contour traversing in a counter clockwise
sense and enclosing the crack tip as shown in Fig. 3.1.
The components of the traction vector are $T_i = \sigma_{ij} n_j$
where σ_{ij} is the stress tensor and n_j the normal vector
to Γ; u_i is the displacement vector and S the arc length
along Γ. W, the strain energy density, is defined as

$$W = W (\epsilon_{mn}) = \int_{o}^{\epsilon_{mn}} \sigma_{ij} \, d\epsilon_{ij} \qquad (3.2)$$

where ϵ_{ij} is the strain tensor.

The J integral characterizes the crack tip field,
the basis of which is provided by the works of Hutchinson
[6] and Rice and Rosengren [7]. They have extended frac-
ture mechanics concepts to cases of large scale yielding
which also assumes the existence of a crack tip singularity.
They indicate that the product of plastic stress and strain
approaches a 1/r singularity; r being a near tip crack
field length parameter. The crack tip singularity is
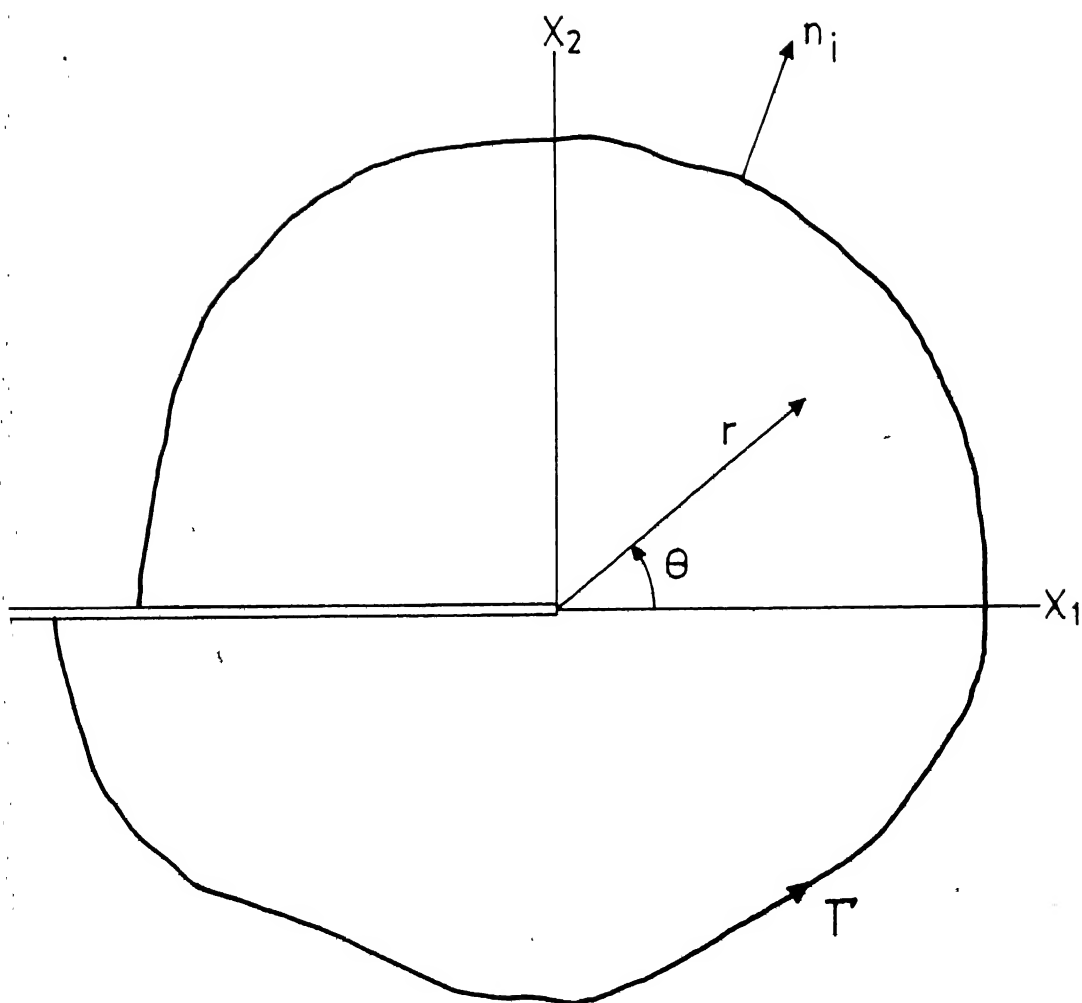
Fig. 3.1 Crack tip coordinate system and arbitrary line integral contour.

uniquely dependent on the material constitutive relations.
Plasticity behaviour of some materials can be modeled by
the Ramberg - Osgood relation

$$\bar{\sigma} = \bar{\sigma}_1 \ (\bar{\epsilon}_p)^n \tag{3.3}$$

where $\bar{\sigma}$ and $\bar{\epsilon}_p$ are equivalent stress and strain respec-
tively and are the instantaneous stress and strain non-
dimensionalised by the yield stress and corresponding strain
respectively. $\bar{\sigma}_1$ is a constant and n is the strain
hardening exponent in Eq. 3.3. McClintock [8] has shown
that the crack tip stress and strain equations, for the
materials following Eq. 3.3, can be expressed from the
Hutchinson-Rice-Rosengren (HRR) singularity

$$\sigma_{ij} = \bar{\sigma}_1 \ (\frac{J}{\bar{\sigma}_1 \ I_n})^{n/(n+1)} \ \frac{1}{r^{n/(n+1)}} \ \tilde{\sigma}_{ij} \ (\theta) \tag{3.4}$$

$$\epsilon_{ij} = (\frac{J}{\bar{\sigma}_1 \ I_n})^{1/(n+1)} \ \frac{1}{r^{1/(n+1)}} \ \tilde{\epsilon}_{ij} \ (\theta) \tag{3.5}$$

where I_n is a function of n and mode of crack opening.
$\tilde{\sigma}_{ij} \ (\theta)$ and $\tilde{\epsilon}_{ij} \ (\theta)$ are functions of θ. These crack
tip stress and strain equations demonstrate a singularity
in r where J is the strength of the singularity.

The J integral has another important advantage
as a fracture criterion. Broberg [9] considered crack
growth criteria for a nonlinear elastic body containing a

crack. For such a body, stress and strain singularities occur at the crack tip. This region ahead of crack tip is termed as the end region outside which the material may be regarded as a continuum. As load is increased, the end region eventually reaches a critical state at which the crack starts moving. One prominent feature of the end region at critical state is that the state is neither dependent on the distribution of loads nor on the crack length. It simply and solely depends on the material itself. The end region can be specified by J integral. Also, J integral reaches a critical value, J_c, as the end region reaches the critical state.

From the foregoing discussions, it is observed that J integral displays three prominent features attractive to its use as a fracture criterion, namely

    i) J integral as a field parameter indicates the stress and strain distribution in a cracked body,

    ii) It describes the crack tip region by specifying the strength of the singularity and

    iii) Critical value of J integral, J_c, is a material property which can be used as a fracture criterion when unstable crack growth occurs.

The J integral can be conveniently evaluated experimentally through its energy rate interpretation. It may be noted that in Eq. 3.1 the two terms in the integrand,

namely W and $T_i \dfrac{\partial u_i}{\partial x_1}$, have the dimensions of energy.
Thus, J is a energy related quantity. In fact, Rice [5]
has shown that the J integral is equal to the change in
potential energy for a virtual crack extension

$$J = -\frac{\partial U}{\partial a} \tag{3.6}$$

where U is the potential energy per unit thickness. For
a two dimensional elastic body of area, A, with a boundary
S, the potential energy is given by

$$U = \int_A W \, dx_1 \, dx_2 - \int_{S_T} T_i \, u_i \, dS \tag{3.7}$$

where S_T is the portion of the boundary over which traction, T_i
is prescribed. A cracked body with prescribed boundary con-
ditions is shown in Fig. 3.2. If the boundary conditions
are given in terms of the generalised force, F, the poten-
tial energy is represented by the shaded area above the
load deflection curve (Fig. 3.3). In this instance the
potential energy is negative and its magnitude is equal to
the complementary energy [10] . When the boundary conditions
are prescribed in terms of generalised displacements the
second term in Eq. 3.7 drops out since S_T is then non-
existent. The potential energy is equal to the strain
energy or the area under the load deflection curve (Fig.
3.4).

The J integral can be evaluated considering the
load deflection diagrams of similar bodies with neighbouring
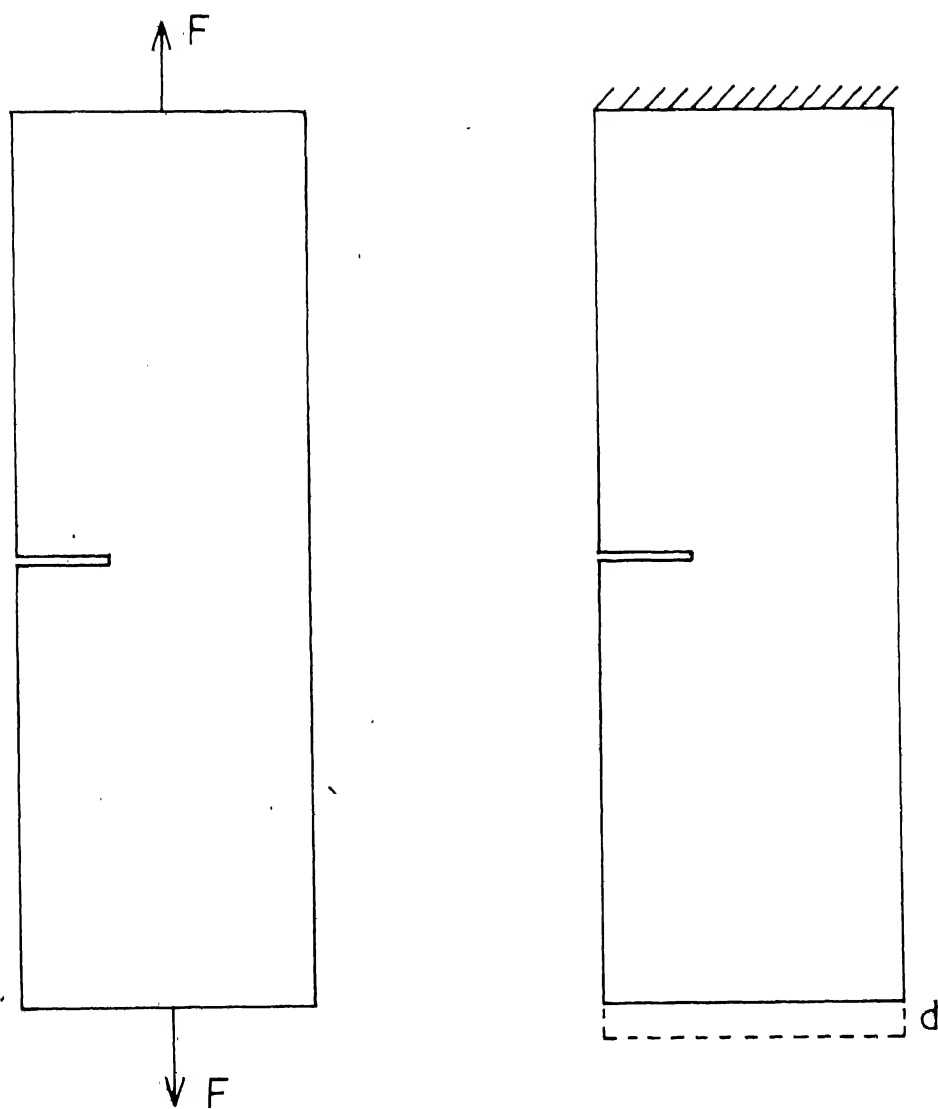
Fig. 3.2 A cracked body with load and displacement
boundry conditions.
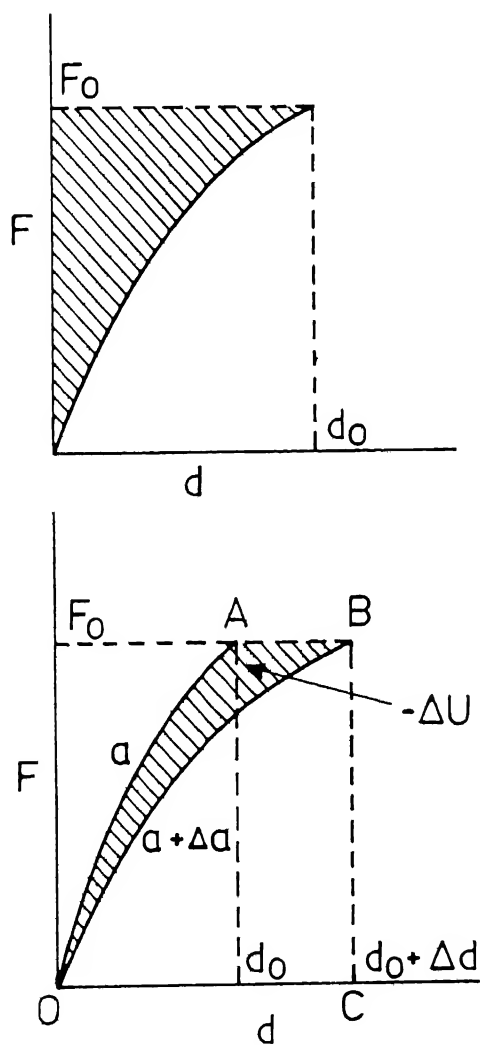
Fig. 3.3 Generalized load deflection
diagram with prescribed load.
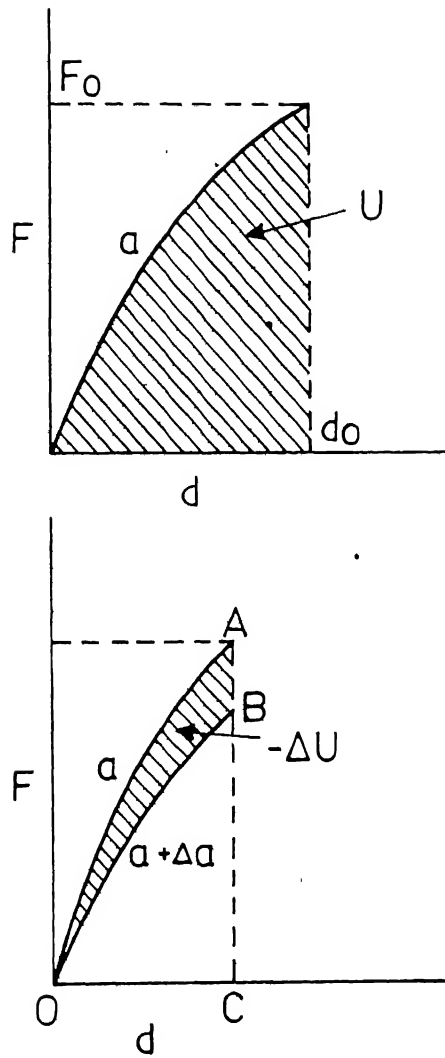
Fig. 3.4 Generalized load deflection diagram
with prescribed displacement.

crack sizes. When two similar bodies with crack lengths, a and a + Δa, are loaded, the load deflection curves are represented by OA and OB. If in the first body, crack extends from a to a + Δa under prescribed load, F_o, the total work done on the body is represented by the area OABCO (Fig. 3.3). Because of reversibility, the unloading curve from point B is the same as the loading curve of the body starting with a crack length, a + Δa. The strain energy of the body with a crack length, a + Δa, under load F_o is the area OBCO. The shaded area OABO (- Δ U) is the energy available for crack extension. Similarly, when crack extends from a to a + Δa under prescribed displacements, the energy available for crack extension is the shaded area OABO (Fig. 3.4). It may be mentioned that the difference in energy obtained by the two methods is approximately equal and of the second order. However, for an experimental evaluation of J integral, the prescribed displacement boundary condition is preferable since, for two specimens of neighbouring crack sizes, the displacements at fracture are observed to be nearly equal, where as the fracture loads are found to be quite different. Furthermore, for higher crack length specimens, at which J integral is evaluated, the load-deflection diagrams become flat and it is more appropriate to evaluate J in terms of displacement. In such a case, Eq. 3.6 can be written as

$$J = - \frac{\partial U}{\partial a} \bigg|_{\text{constant displacement}}$$ (3.8)

Begley and Landes [10 - 12] have used the above relation to evaluate J integral as a failure criterion for metals. They demonstrated the applicability of J integral for the case of large scale yielding at the crack tip through experimental results on an intermediate strength rotor steel. They observed that the J integral at failure for fully plastic behaviour was equal to the linear elastic value of strain energy release rate (G) at failure for extremely large size specimens. Thus, the J integral approach eliminates the necessity of testing very large specimens. In the following section J integral approach is extended to short fibre composites.

3.3 EXPERIMENTAL EVALUATION OF J_c

Fracture toughness studies have been performed on randomly oriented short glass fibre reinforced epoxy resin exhibiting a fibre volume fraction of 39.4%. Single edge notched specimens 25 mm wide, 100 mm long, 3 mm thick and crack lengths varying between 0.1 and 0.7 of the specimen width were tested in displacement controlled mode, in a MTS machine. The upper grip is fixed and the lower grip moves with constant rate of displacement (0.4 mm/min).

The MTS machine grips are inflexible causing uniform displacement along the width of the specimen. A schematic diagram of a SEN specimen showing the imposed displacement boundary conditions and J integral contour is shown in Fig. 3.5.

Typical load displacement (at load point) curves for specimens with different initial crack lengths are shown in Fig. 3.6. The tests were conducted under displacement controlled conditions so that the load displacement behaviour beyond maximum load is also clearly indicated. Specimens with small cracks fracture suddenly causing an abrupt drop in load whereas the specimens with larger cracks show a more gradual fracture process beyond maximum load. The behaviour is similar to that observed in metals [11]. This is because the strain energy stored during loading in a small crack length specimen is sufficient to cause catastrophic failure. It is not the case for longer crack length specimens.

The observed fracture load is plotted against crack length in Fig. 3.7 along with the fracture load that would be expected if the strength was unaffected by the crack i.e. the fracture load obtained by multiplying the net cross-sectional area and the unnotched strength. The observed fracture load is smaller than the expected, indicating that the crack reduces the fracture load far greater
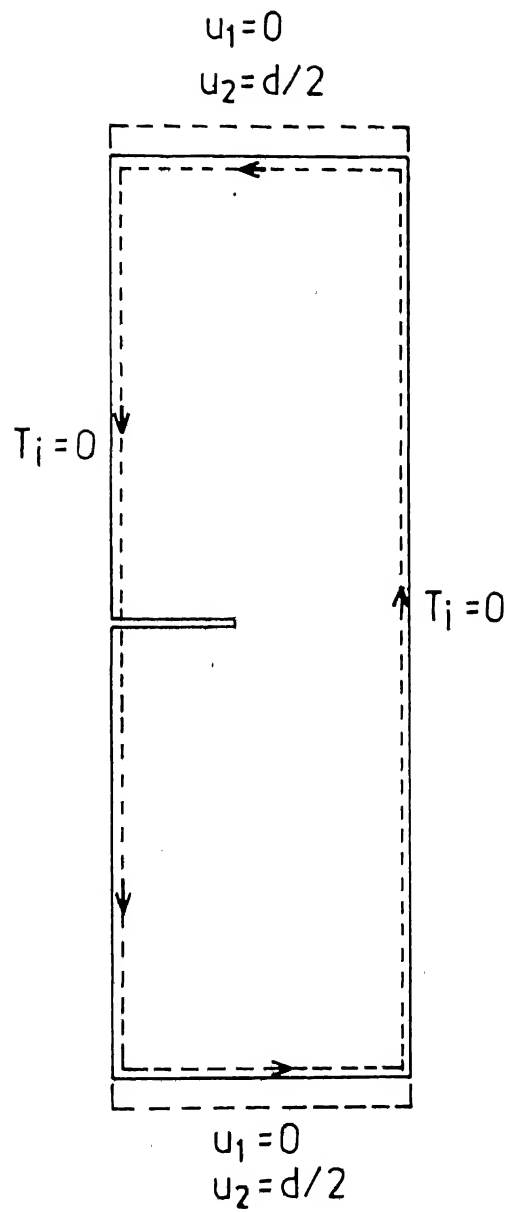
Fig. 3.5 A SEN specimen showing
J integral contour.
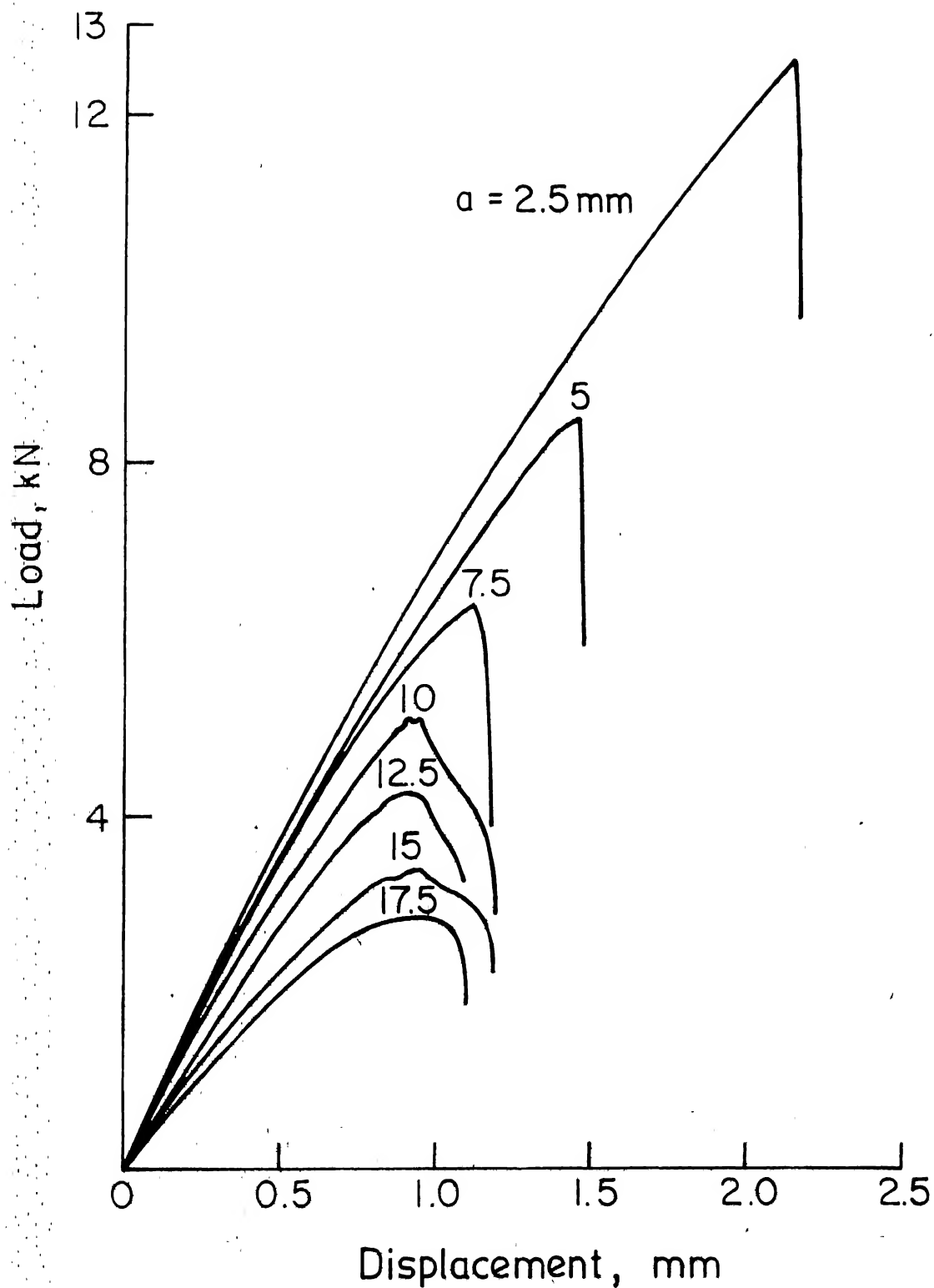
Fig. 3.6 Load displacement curves for different
initial crack lengths.
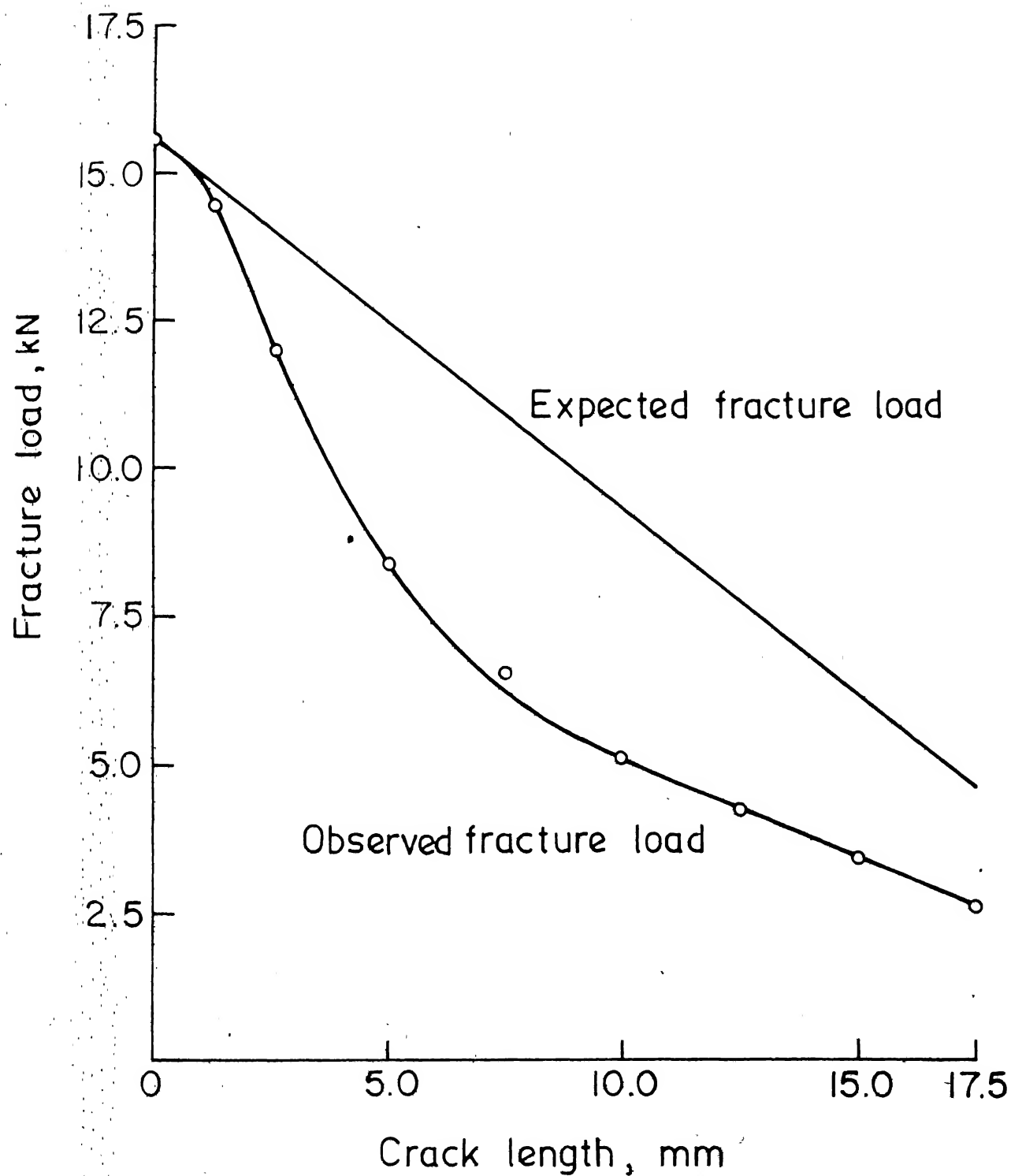
Fig. 3.7 Observed and expected (based on net cross section area) fracture loads for notched specimens.

than can be accounted for by the reduction in cross -
sectional area. The extent of this influence is illus-
trated in Fig. 3.8 through the ratio of observed to
expected fracture loads. The decreasing ratio indicates
the increasing influence of cracks which stabilizes for
crack lengths 10 mm or longer.

The fracture process becomes unstable at a dis-
placement beyond which the load decreases monotonically.
This displacement may be referred to as the critical
displacement. It is plotted against the crack length in
Fig. 3.9. Initially the critical displacement decreases
with increase in crack length and remains constant for
10 mm or larger cracks. The initial variation in critical
displacement occurs due to the significant deformations
away from the crack plane because of large loads. This
point will be further explained in the next section. The
critical value of J integral is to be obtained correspond-
ing to the constant critical displacement of 0.96 mm as
shown in Fig. 3.9.

The load displacement curves can be used to
obtain the value of J integral experimentally through its
energy rate interpretation (Eq. 3.8). To this end, area
under the load displacement curves is obtained graphically
to determine the work done in loading the specimen for a
given displacement. For each specimen the strain energy
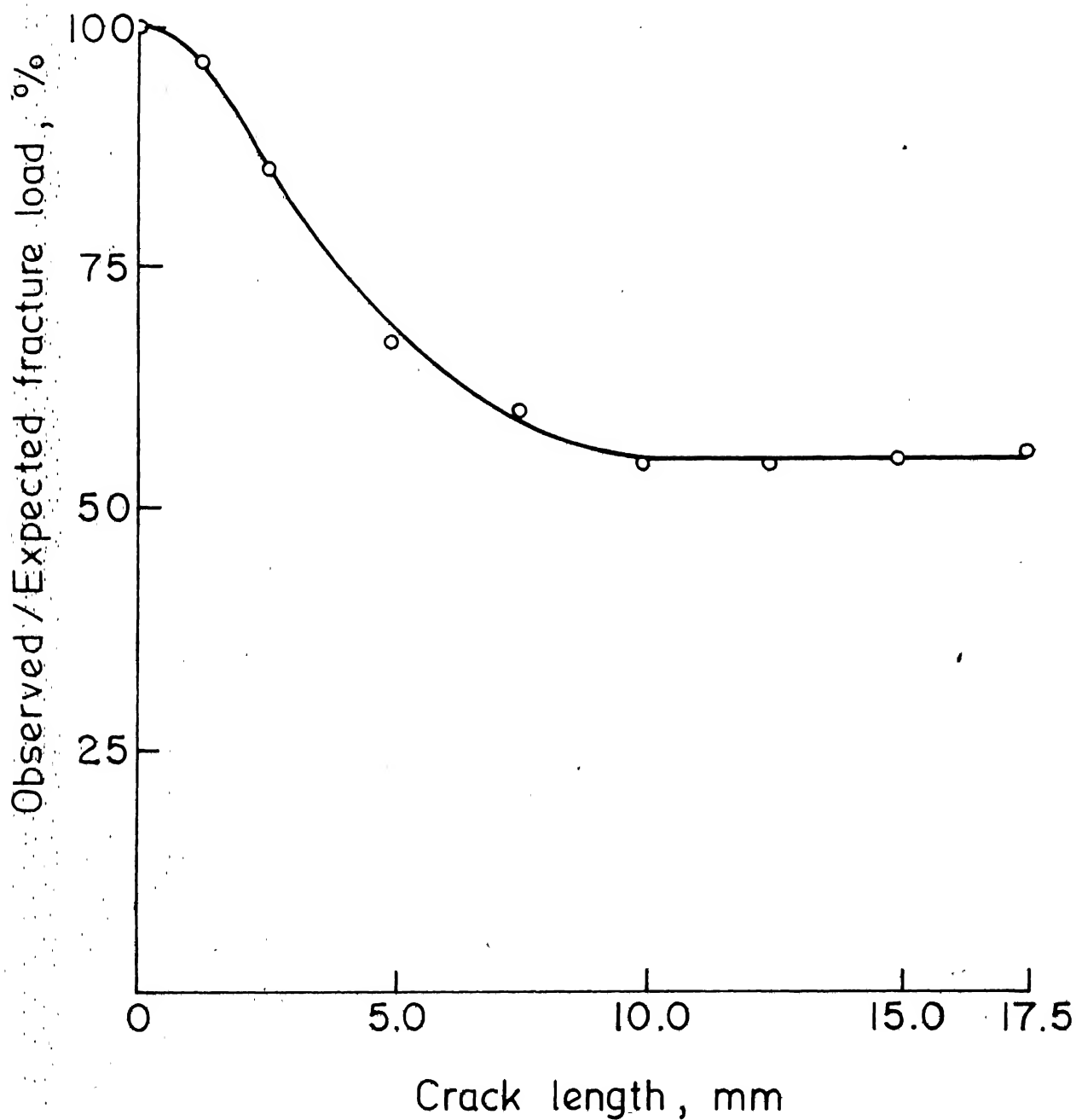
Fig. 3.8 The ratio of observed to expected fracture
load as a function of crack length.
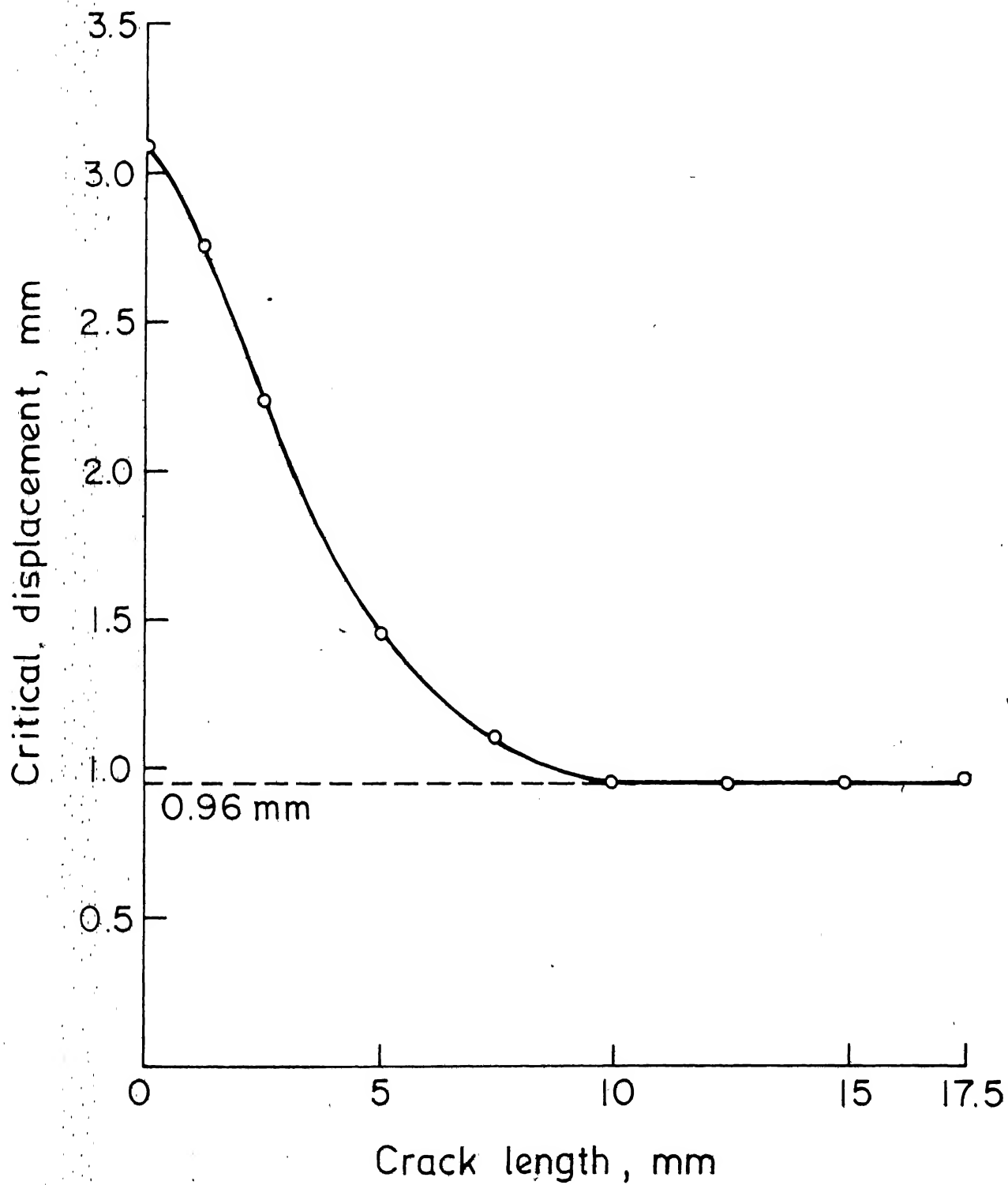
Fig. 3.9 Variation of critical displacement with initial crack length.

per unit thickness is obtained for displacements at intervals of 0.05 mm. It is plotted in Fig. 3.10 as a function of crack length for different displacements. For a given displacement, energy absorbed by a specimen decreases as the crack length increases (Fig. 3.10) because smaller loads are required. The variation in energy absorbed is less for cracks shorter than 10 mm compared to that for longer cracks because in specimens with longer cracks the energy absorbed is essentially in the vicinity of the crack tip and is thus, strongly influenced by the crack length.

The J integral is obtained from Eq. 3.8 through slopes of the energy curves in Fig. 3.10. The J integral is independent of crack length for cracks equal to or larger than 10 mm since the energy curves are straight lines in this range. The variation of J with displacement is shown in Fig. 3.11. The critical value of J corresponding to the critical displacement of 0.96 mm is 51.8 kJ/m^2. The variation of J for cracks smaller than 10 mm has not been shown because it is not unique. However, in view of Fig. 3.10 it may be stated that in this region J will be smaller for a given displacement but defined for a greater range of displacement. Its apparent critical value is also expected to be larger in these cases. The applicability of J integral in this region is further discussed in the next section.
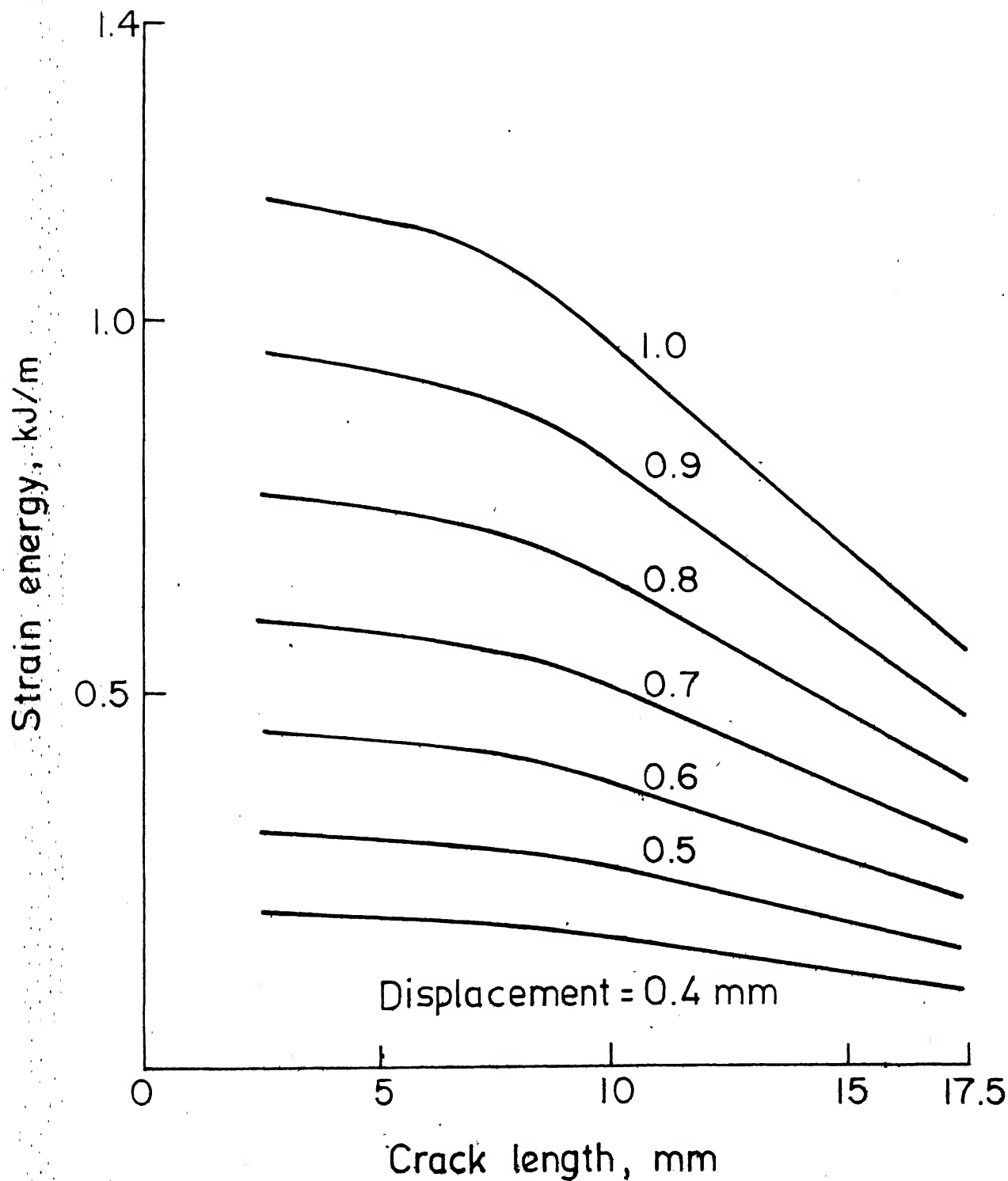
Fig. 3.10 Strain energy per unit thickness for different displacements.
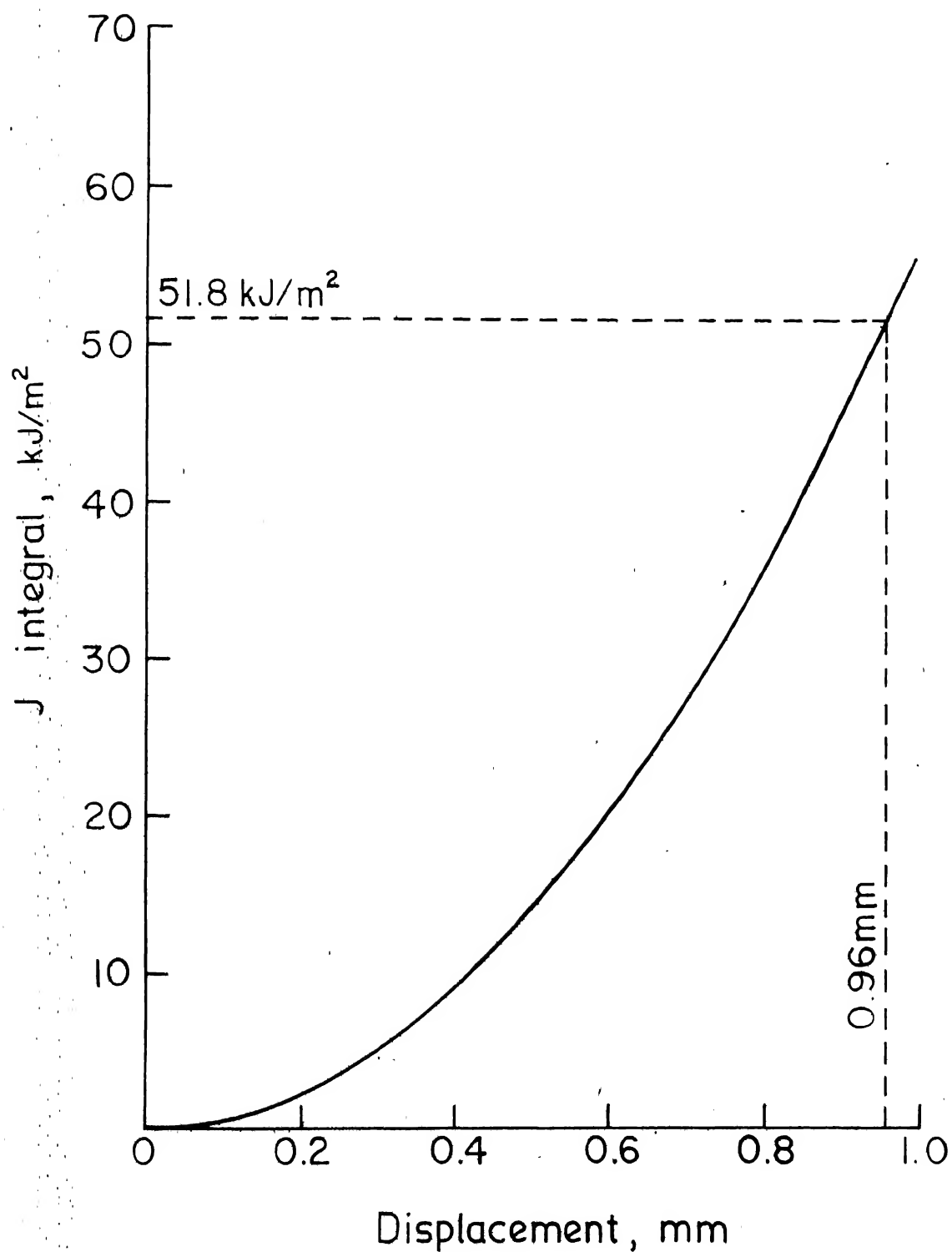
Fig. 3.11 J integral as function of displacement.

From the previous discussion, it has been established that when the crack is equal to or longer than 10 mm (or a/w $\geq$ 0.4) in 25 mm wide specimens, the fracture behaviour is governed essentially by the crack tip environment resulting in a constant critical displacement and a unique value of J integral. For these crack lengths, the fracture load is small which does not cause any general material damage away from the crack tip region. On the other hand when cracks are small (a < 10 mm or $\frac{a}{w}$ < 0.4), the J integral and critical displacement depend upon the crack length, indicating that in addition to the crack tip environment, the region away from it also influences such quantities as the energy absorbed and displacement at fracture. This may be attributed to the fact that the fracture loads are high enough to cause general material damage.

3.4   EFFECT OF SPECIMEN LENGTH

In order to study the influence of the general material damage in specimens with smaller cracks, additional specimens with varying specimen lengths were tested. These tests also establish the effect of specimen length on J integral at higher crack lengths. Four crack lengths 5, 7.5, 10 and 12.5 mm were chosen such that two crack lengths were in the range where J can not be evaluated directly and the other two crack lengths are in the range where J can directly be obtained. The length of each

specimen between grips was varied from 3 to 6 times the specimen width (25 mm). The load-displacement records for different crack lengths are shown in Figs. 3.12 to 3.15 for different crack lengths. The critical displacements for specimens with different initial crack lengths are plotted against specimen length in Fig. 3.16. As expected, the rate of increase of critical displacement is higher for specimens with smaller crack lengths. For longer cracks, straight lines overlap and their slope is less. This observation is consistent with Fig. 3.9.

For smaller crack lengths, the total displacement of the specimen is the sum of the displacement in the crack tip region, which may be expected to be independent of the specimen length, and displacement in the region away from the crack tip which should be a function of specimen length. The intercept on the ordinate obtained through extrapolation of a straight line in Fig. 3.16, may be regarded as the displacement in the crack tip region alone. Interestingly, all the straight lines in Fig. 3.16 intercept the ordinate at the same point. This common intercept may be regarded as a critical displacement due to the presence of the crack and whose value is independent of crack length and specimen length.

Variations of energy absorbed upto fracture are shown in Fig. 3.17 for different crack lengths. The total energy absorbed may also be thought of as the sum of the
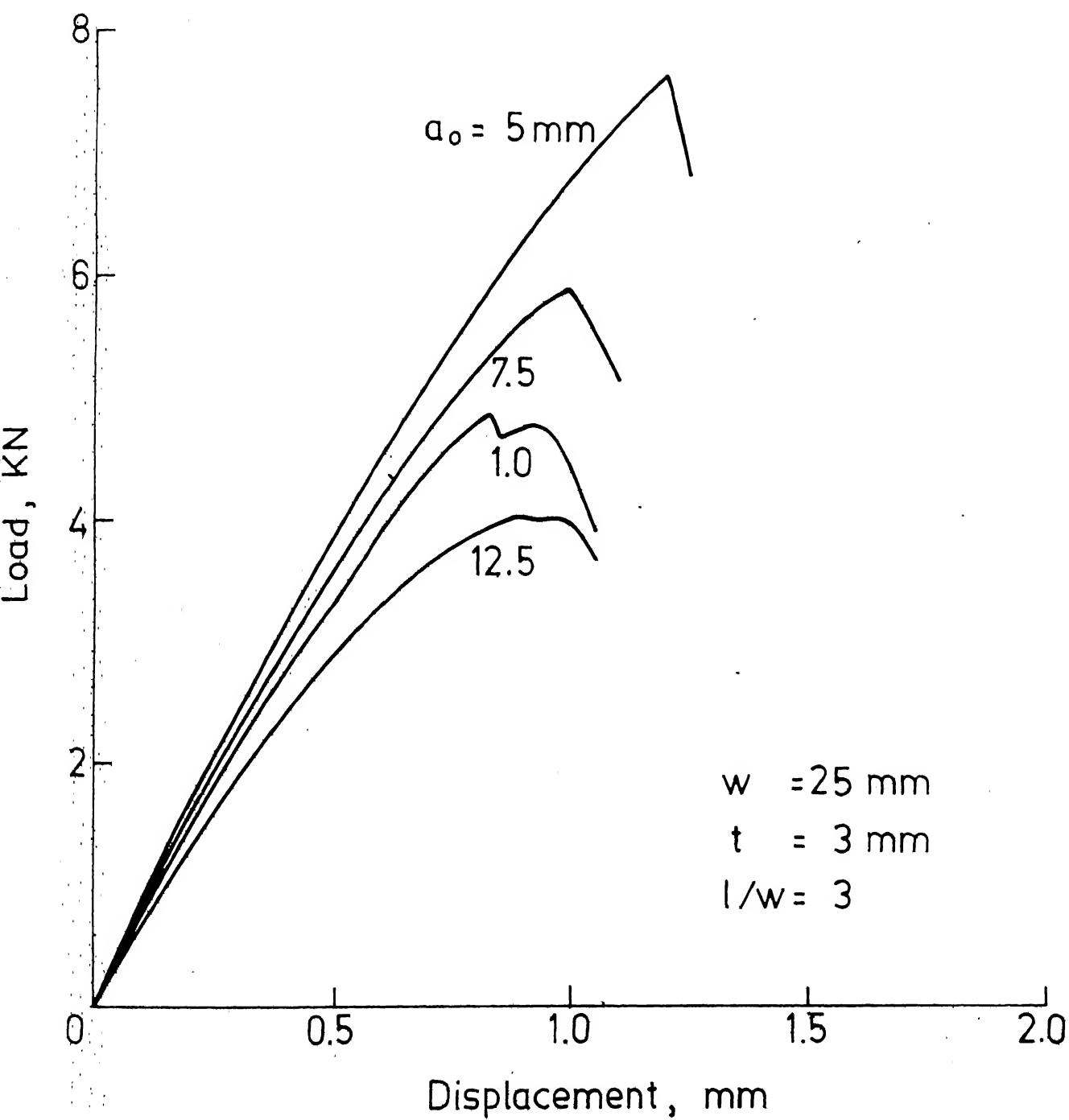
Fig. 3.12 Load displacement curves for 75mm long specimens.
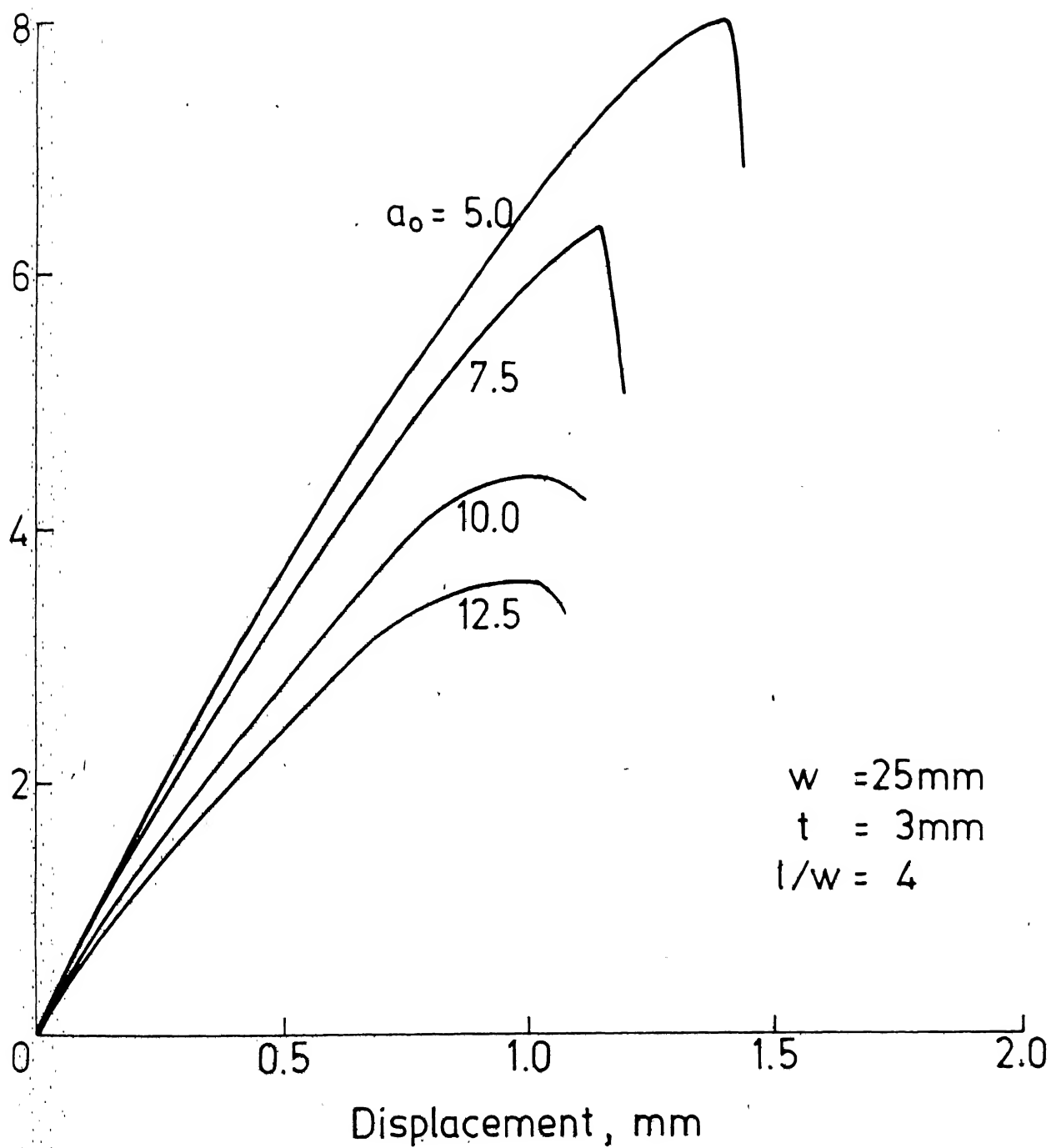
Fig. 3.13 Load displacement curves for 100 mm long specimens.

The figure shows load (vertical axis) versus displacement in mm (horizontal axis) curves for four values of a_o: 5.0, 7.5, 10.0, and 12.5. Parameters noted: w = 25 mm, t = 3 mm, l/w = 4.
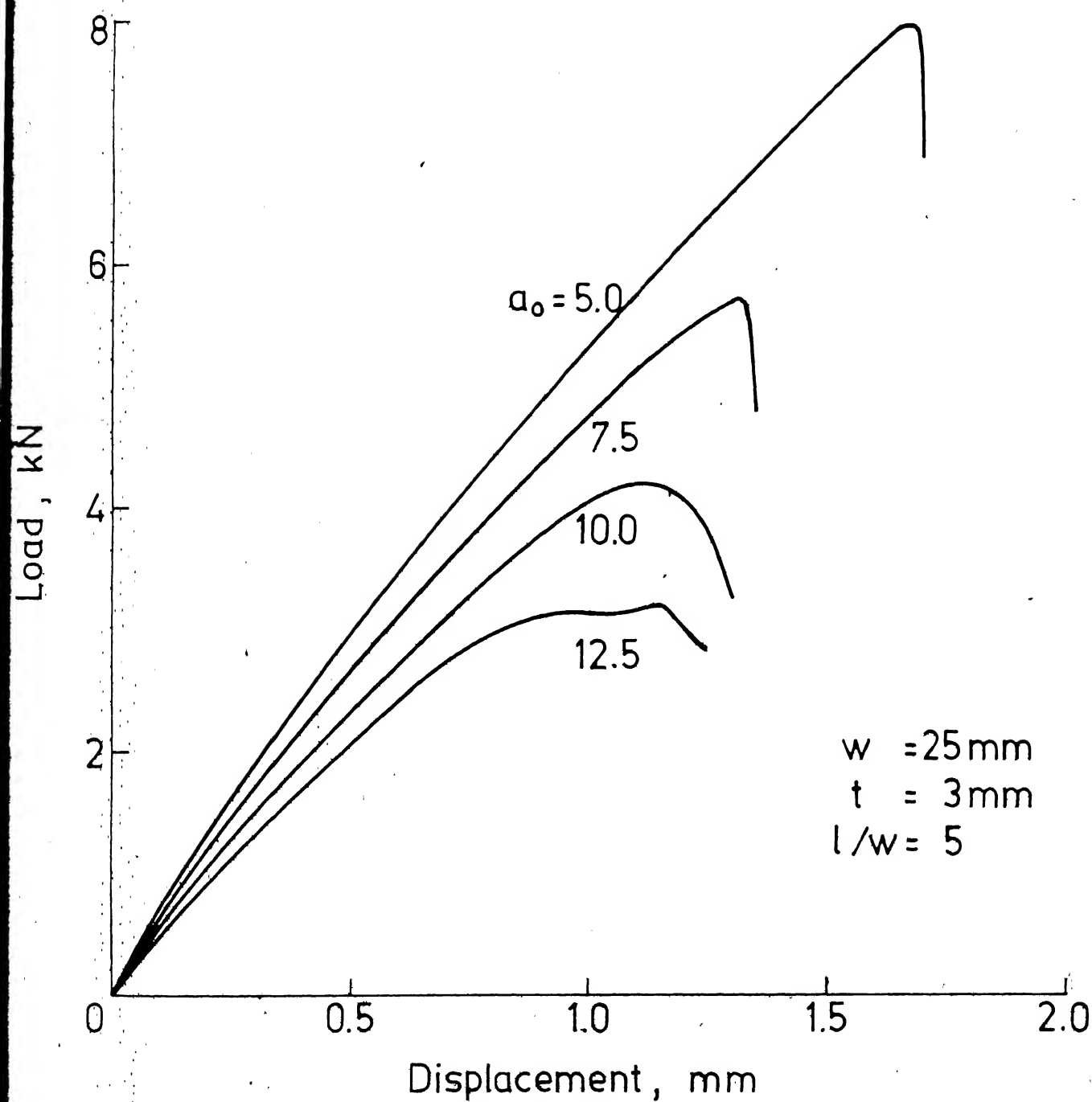
Fig. 3.14 Load displacement curves for 125 mm long specimen
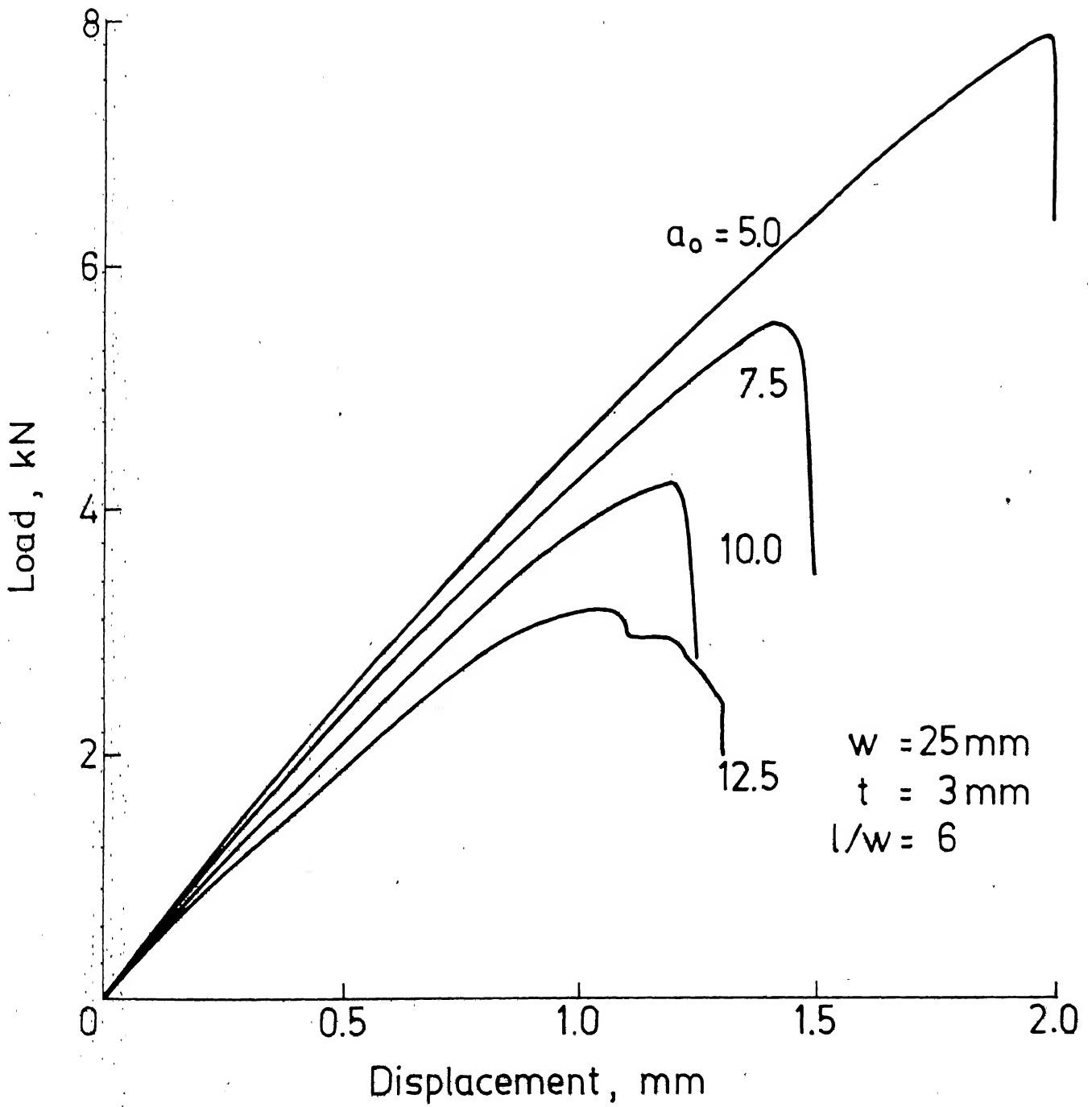
Fig. 3.15 Load displcement curves for 150mm long specimen
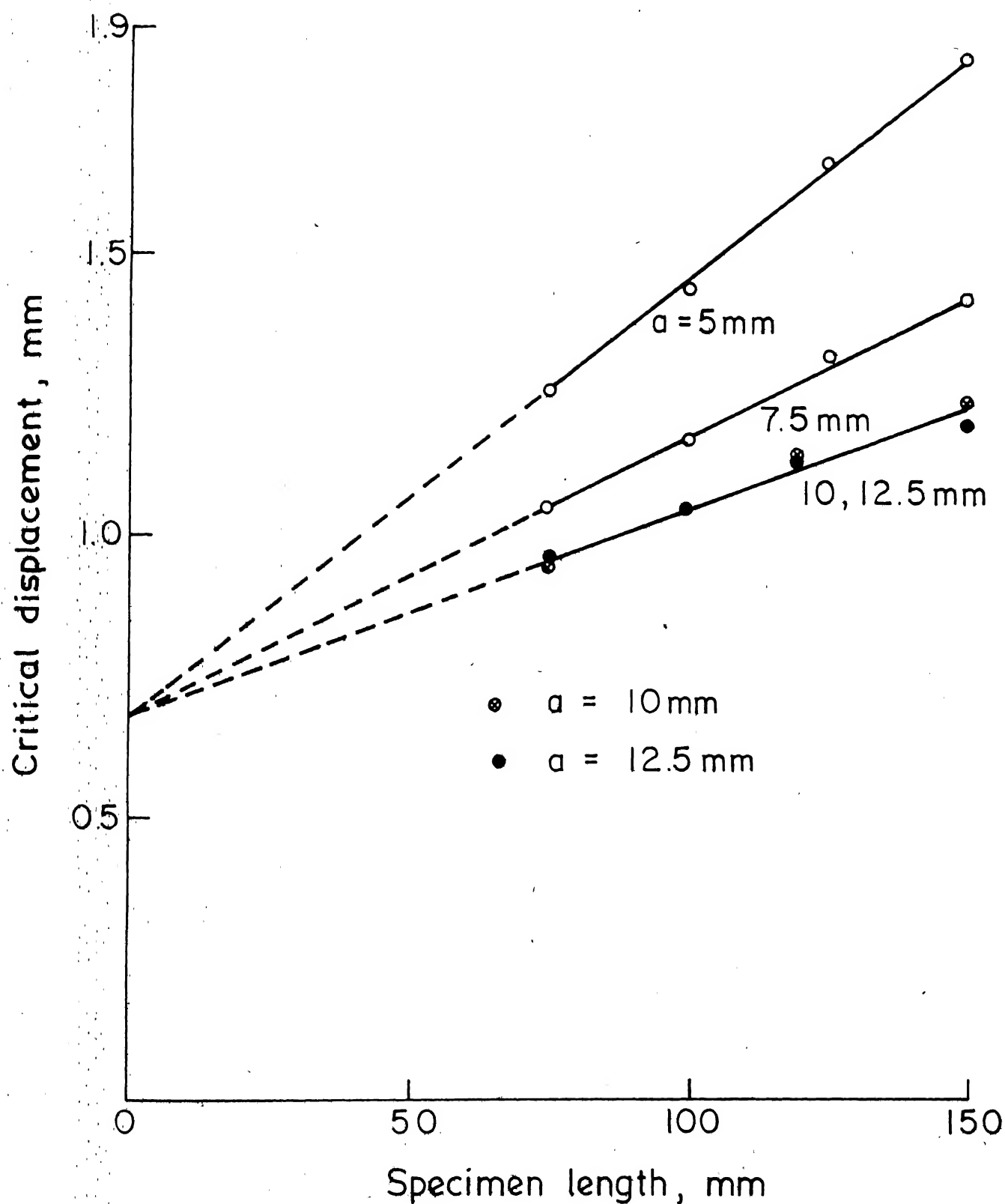
Fig. 3.16 Variation of critical displacement with specimen length for different initial crack lengths.
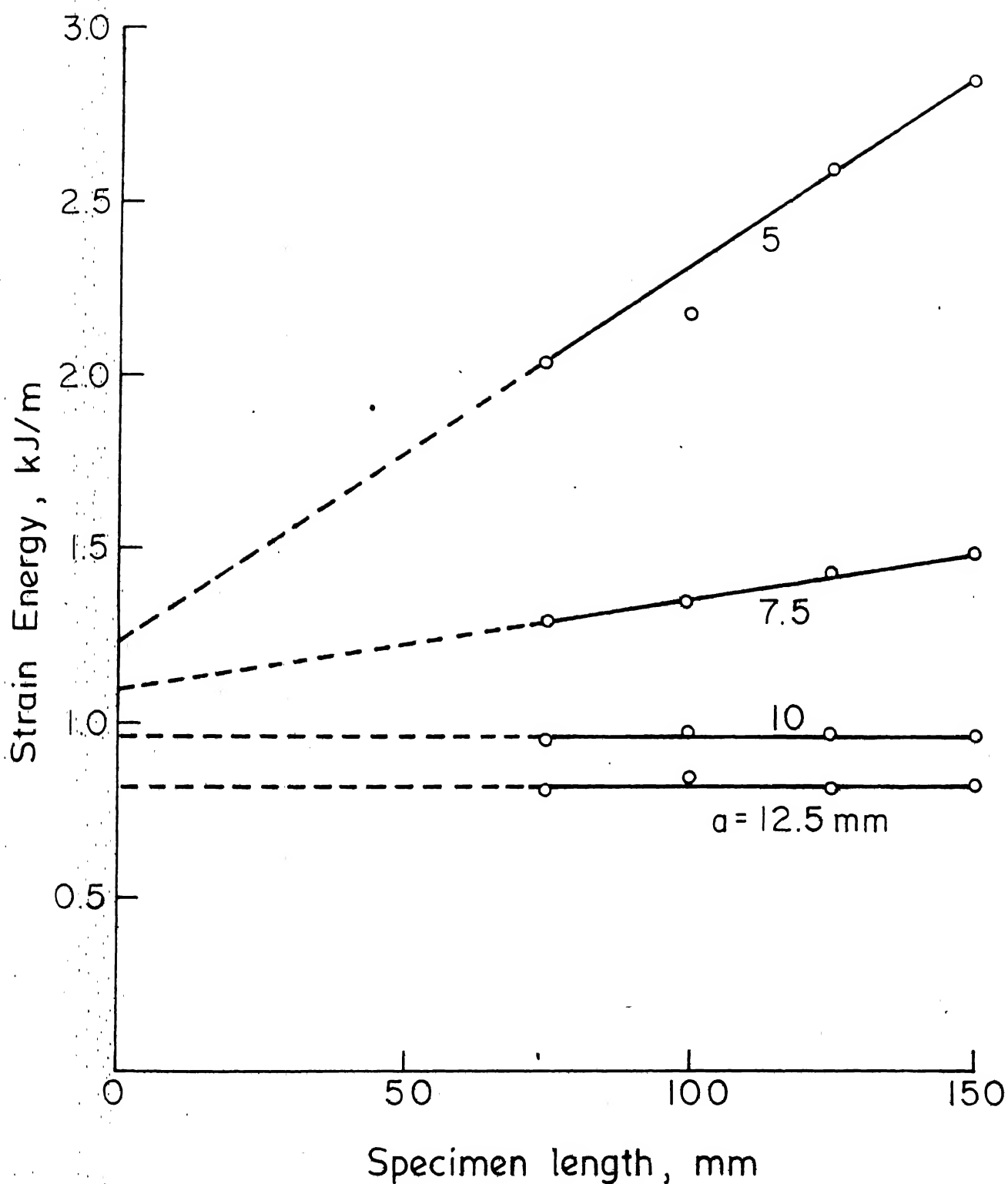
Fig. 3.17 Variation of strain energy with specimen length, for different initial crack lengths.

energies absorbed in the crack tip region and the region away
from it. The energy absorbed in the crack tip region
depends upon the crack length but not on specimen length
whereas the energy absorbed in the region away from the
crack tip depends upon the specimen length. It is observed
that when the crack length is 10 or 12.5 mm, the energy
absorbed is independent of the specimen length signifying
negligible energy absorption in the region away from the
crack tip. For 5 and 7.5 mm crack lengths, the total energy
absorbed increases linearly with the specimen length indi-
cating a significant energy absorption in the region away
from the crack tip as well. These observations are further
supported by visual observations on the specimens. The
damage in the specimens with 10 and 12.5 mm cracks is con-
fined to the crack tip region whereas in specimens with
smaller cracks the material damage is all over. This is
illustrated in Fig. 3.18 through a photograph of two frac-
tured specimens. The photograph was taken in a bright
light background and therefore, the damage (opaque to light)
is indicated by dark areas.

The intercept on the ordinate obtained by extra-
polation of a straight line in Fig. 3.17 may be regarded as
the energy absorbed in the crack tip region. Energy
absorbed thus obtained is plotted in Fig. 3.19. It has
already been explained with respect to Fig. 3.16 that the
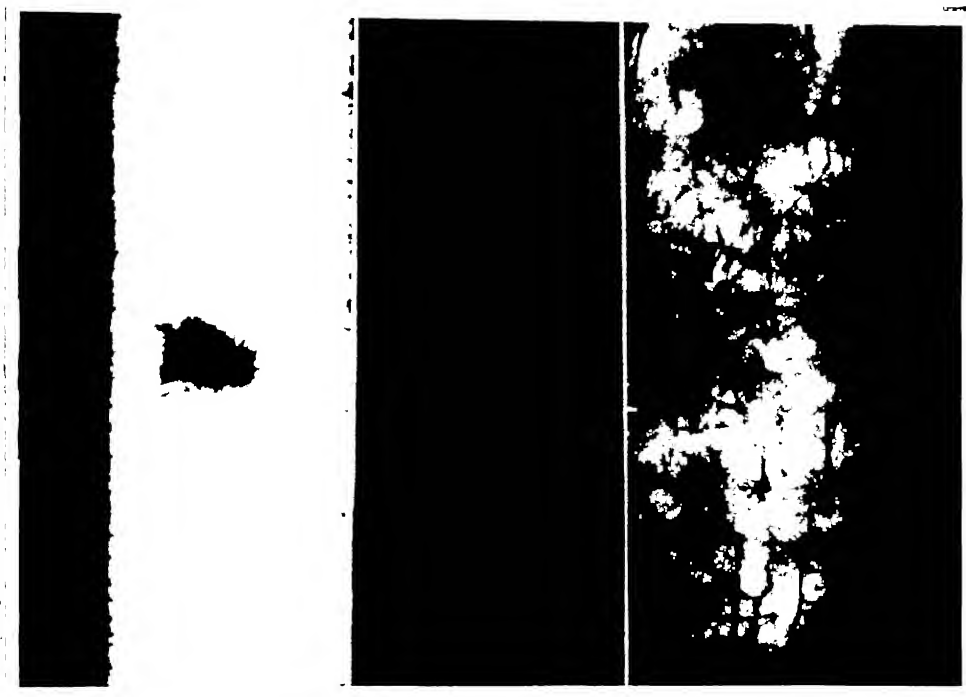
Fig. 3.18 Transmitted light photograph of two specimens with different crack lengths.
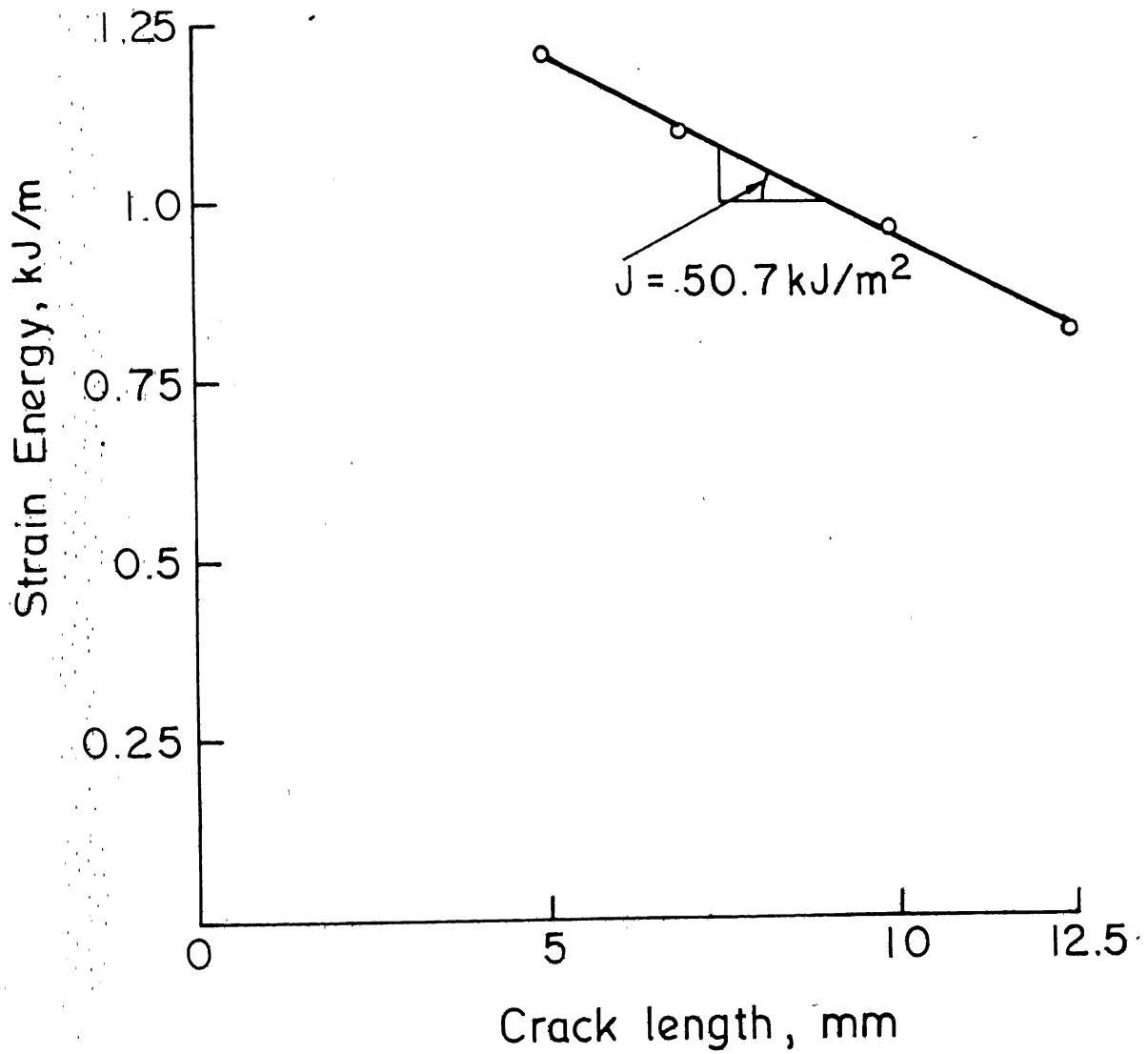
Fig. 3.19 Strain energy at the crack tip for diffrent crack lengths.

critical displacement due to the presence of a crack alone
is independent of crack length. Thus, it may be argued that
the energy absorbed for different crack lengths (Fig. 3.19)
corresponds to the same critical displacement and therefore,
the slope of the straight line may be used to obtain the
critical value of J (J_c), independent of crack length. The
J critical thus obtained is $50.7 \, kJ/m^2$ which is close to
the value $51.8 \, kJ/m^2$ obtained earlier in Fig. 3.11. This
is a significant observation. This shows that the energy
absorbed at the crack tip may be separated from that
absorbed in the region away from it. Thus, a parameter
independent of testing variables (i.e. crack length and
specimen length) is obtained which may be used as a fracture
criterion for the randomly oriented short glass fibre
reinforced epoxy resin.

3.5   JUSTIFICATION OF J CRITERION

A major limitation of the J integral approach
arises from the fact that J is path independent only when
the stress-strain relation is unique. It is truely path
independent for linear and nonlinear elastic materials. It
is also applicable for elasto-plastic materials following
Ramberg-Osgood relation under situations of monotonic load-
ing. This restricts the use of J integral to situations of
zero crack extension since unloading is not permitted. The
above considerations also limit the application of J integral

to metals for crack initiation rather than the crack propagation. It is well known that in composite materials, microcracks at the fibre matrix interface appear at very low loads due to the stress concentrations produced by the fibres lying perpendicular to the load. It is probably this unavoidability of microcracks that has deterred researchers from exploring applicability of the J integral as a fracture criterion for composite materials. In this section the behaviour of short glass fibre composites is investigated and compared with that of metals regarding the applicability of J integral in the light of the aforesaid limitations.

3.5.1 Stress-Strain Behaviour

A typical stress-strain curve for 25 mm wide and 100 mm long short glass fibre reinforced epoxy resin specimen is shown in Fig. 3.20. The stress-strain behaviour can be modeled by the Ramberg-Osgood relation (Eq. 3.3). The curve can be idealized by the following relation shown (dashed lines) superimposed on the experimental stress-strain curve:

$$\frac{\sigma}{25.75} = \left(\frac{\epsilon}{0.225} \right)^{0.83} \tag{3.9}$$

where σ is the composite material stress in MPa and ϵ is the strain in percent. The constants 25.75 MPa for stress and 0.225 percent for strain correspond to the end of linear portion of stress-strain curve. The exponent
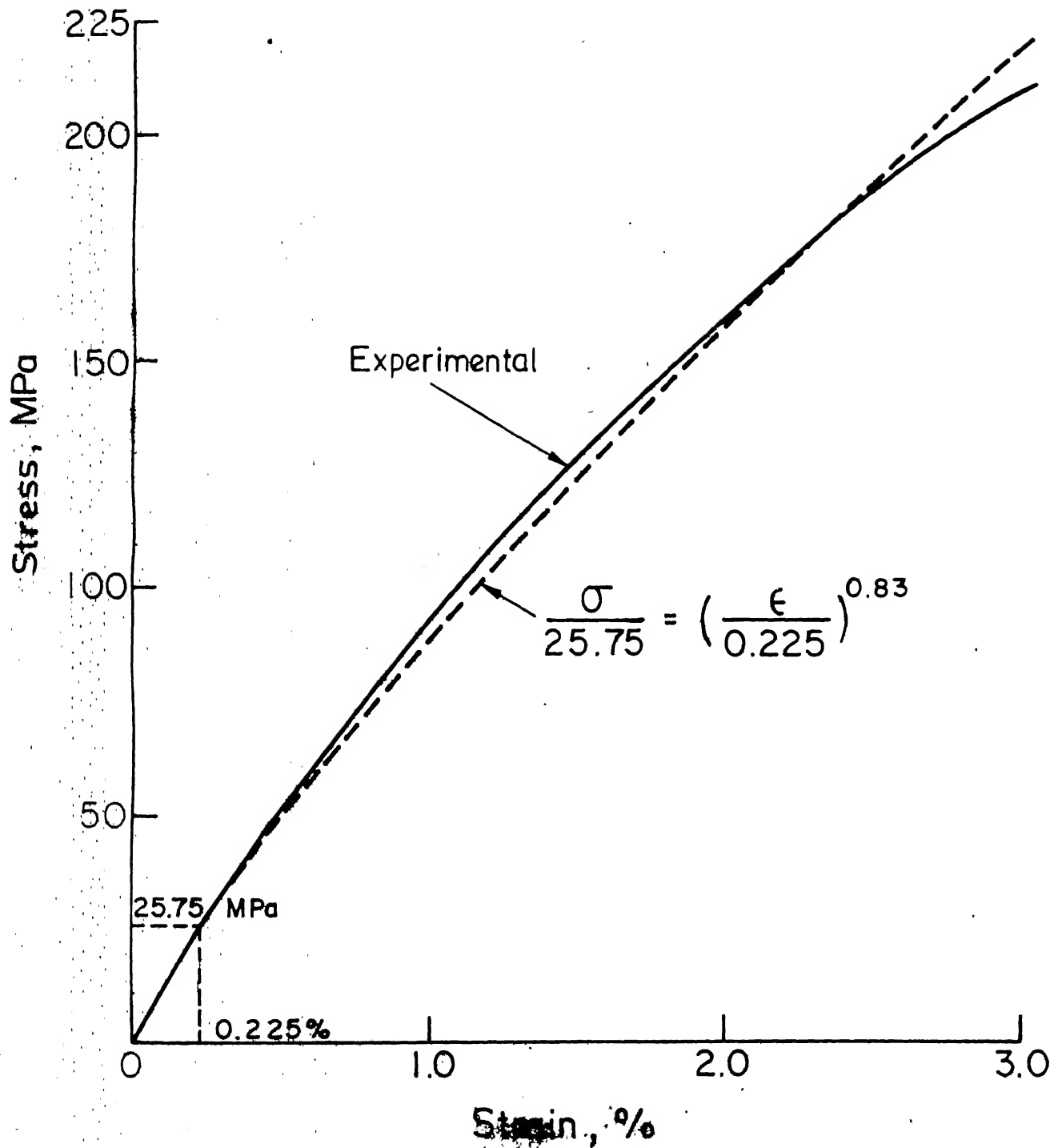
Fig. 3.20 Experimental and idealized stress-strain relation for randomly oriented short glass fibre reinforced epoxy resin composites.

0.83 found out by idealisation of experimental stress-strain curve shows the material to be weakly nonlinear. The two curves in Fig. 3.20 are quite close to each other indicating that the stress-strain behaviour of short fibre composites may be closely approximated by the Ramberg-Osgood relation. This representation of the nonlinear behaviour of the composite provides a justification for exploring the possibility of using J integral as a fracture criterion for composite materials. For metals exhibiting elasto-plastic behaviour, incremental plasticity theory is most appropriate and representation by Ramberg-Osgood relation is only approximate. Thus, if nonlinear behaviour is considered, short fibre composites are better suited than metals for such a representation. The development of J integral as a fracture criterion for short fibre composites is based on test results. Further justification for this empirical development is given in the following paragraphs.

3.5.2 Study of Damage Zone

During fracture tests on short glass fibre composites, as load increases, damage at the crack tip occurs primarily due to matrix cracking and debonding at the fibre-matrix interface, resulting in unloading of the matrix locally but not necessarily of fibres for two reasons. One, the Scanning Electron Microscope observation

of the specimens prior to fracture do not show evidence of
any significant fibre failures even in the crack tip region.
A Scaning Electron Microscope photograph shows (Fig. 3.21)
only debonding cracks and no fibre breaks in a fibre bundle
which is about 1 mm away from the crack tip. Two, even in
the case of short fibre composites like the present one,
the fibres are long enough (average length 50 mm) so that
major part of their length is embedded in the matrix away
from the damage zone. Therefore, debonding at the interface
and few fibre failures do not significantly influence the
load carried by the fibres. Further, since fibres carry
major portion of the load in fibrous composites, this crack
tip damage does not constitute material unloading to the
same extent as a crack extension does in metals. Although
the requirement of no unloading is not completely met, its
influence may be quite small and ignored in an empirical
development of the criterion. Further, J integral as frac-
ture criterion corresponds to crack propagation.

3.5.3   Unloading Behaviour

The implication of elastic behaviour is that the
loading and unloading paths for the material are the same.
In many cases of metals, the material is treated as non-
linear elastic through the deformation theory of plasticity.
In general, however, the deformation theory can not be used
for problems in which unloading occurs, for the obvious
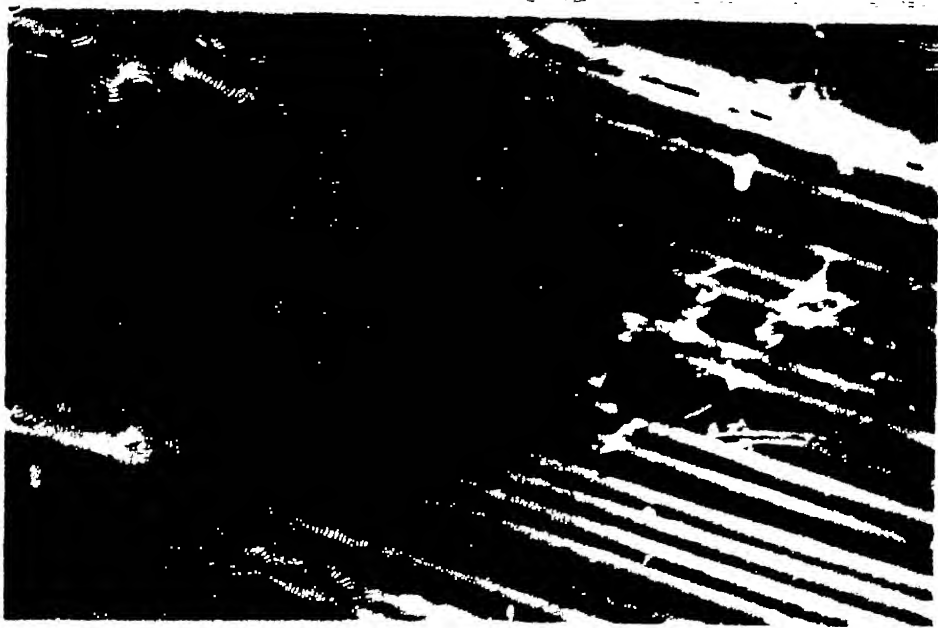
Fig. 3.21 Scanning electron microscope photograph of a fibre bundle near crack tip showing debonding cracks but no fibre breaks.

reason that unloading in a real material follows a different
stress-strain curve. If unloading path is different from
the nonlinear loading path, the recoverable energy is not
given by the areas demarcated in Figs. 3.3 and 3.4.

For a metal like behaviour, the unloading path
would be parallel to initial loading path shown in Fig. 3.22
by dashed lines. The actual unloading path of randomly
oriented short glass fibre reinforced epoxy resin composite
is also shown in the same figure. The residual strain is
only about 40% of the residual strain a metal like behaviour
would have produced. Considering only the unloading aspect,
the application of J integral is expected to be better
suited to short glass fibre composites.

3.6 RELATION OF K_c WITH J_c

Rice energy line integral is expressed only in two
dimensions. J integral approach is, therefore, limited to
problems of plane strain or generalized plane stress. This
approach has been developed after the linear elastic frac-
ture mechanics approach. Several authors [41, 48] have
obtained fracture toughness of randomly oriented short glass
fibre reinforced composites using R curve method. It is
useful to compare the J_c value with critical crack growth
resistance, K_c, obtained by them inspite of the fact that
J_c as a fracture criterion is more general.
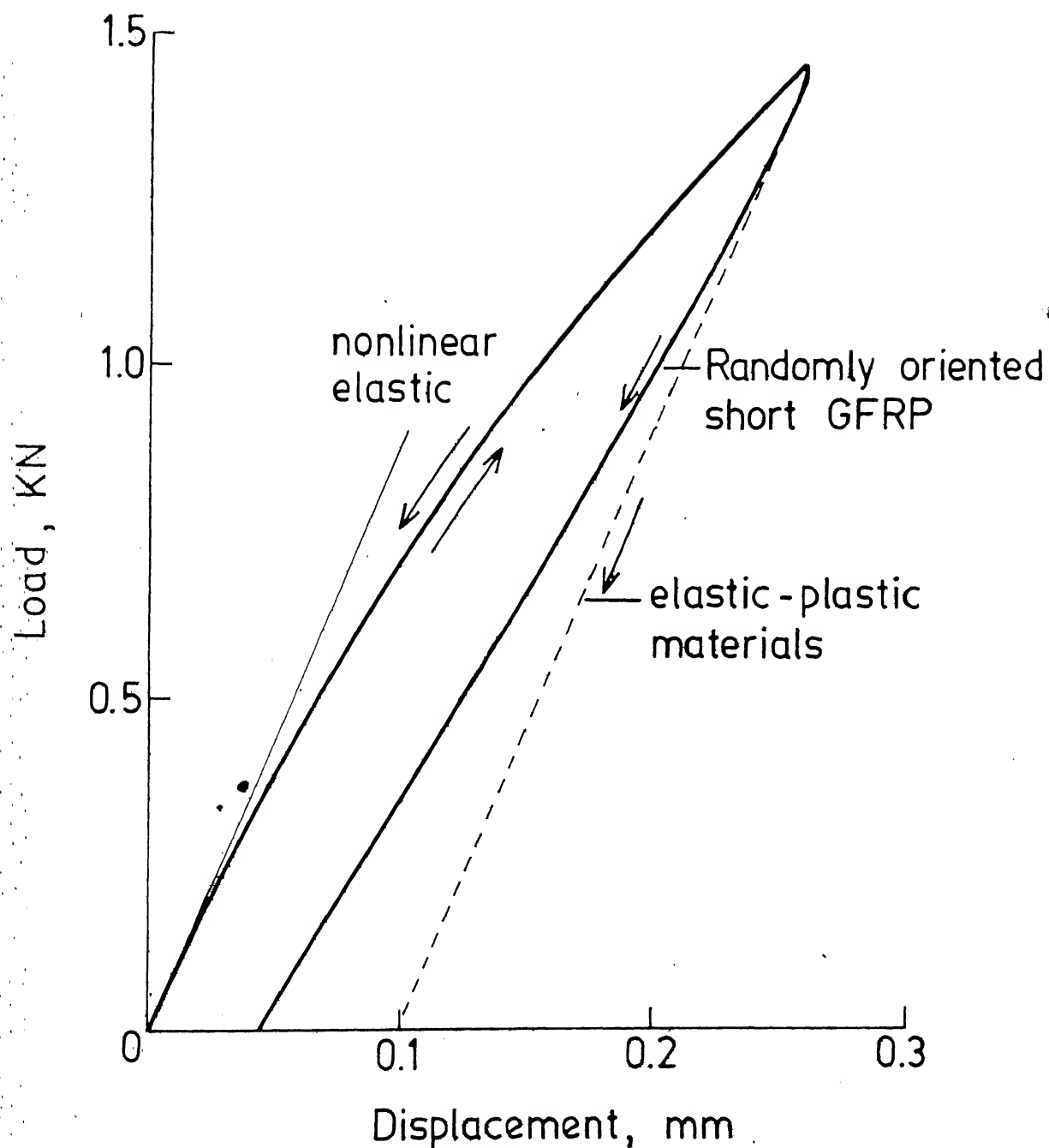
Fig. 3.22 Unloading paths for an elastic-plastic material and short glass fibre composite.

R curve approach is essentially meant for problems of generalised plane stress. Considering that composites are made of thin layers of laminae, plane stress conditions seem to prevail. Again, while measuring displacement and load for evaluation of J, the thickness average values are measured. Therefore, considering the above, the relation between J_c and K_c may be chosen for plane stress case [5]

$$J_c = \frac{K_c^2}{E} \qquad (3.9)$$

where E is the modulus of elasticity. The present material has an average elastic modulus equal to 12.5 GPa. Therefore, corresponding to J_c value of 51.8 kJ/m^2, Eq. 3.9 gives K_c equal to 25.45 MPa√ m. This value of critical crack growth resistance agrees very well with the average value of K_c of 26.2 MPa √m for the same specimens (Chapter 5). Agarwal and Giare [48] have obtained 24.82 MPa √m for similar glass fibre composite. This demonstrates that the J integral method of characterizing fracture toughness is consistent with the R curve method. However, J integral approach is more general and simpler for experimental and analytical evaluation.

3.7 CONCLUDING REMARKS

Fracture behaviour of a short fibre composite has been investigated. J integral has been evaluated using the energy rate interpretation. Its value is found to be

independent of cracklength when the ratio of crack length to specimen width (a_o/w) is larger than 0.4. For smaller crack lengths general material damage away from the crack tip also influences the energy absorbed significantly. However, an extrapolation method has been developed through which the crack tip energy may be seperated from the energy absorbed due to general material damage. The J integral thus obtained is independent of crack length and specimen length and its critical value is the same as obtained for $a_o/w \geq 0.4$ without extrapolation. Further, it also agrees well with the critical stress intensity factor obtained using R · curve approach in an earlier study. Appropriate modelling of the stress – strain curve and observations on damage mode also justify the use of J integral to characterize fracture of short fibre composites.

CHAPTER IV

EFFECT OF SPECIMEN WIDTH, THICKNESS AND
FIBRE VOLUME FRACTION ON J_c

4.1. INTRODUCTION

In the preceeding chapter, critical value of J integral, J_c, has been evaluated for randomly oriented short glass fibre reinforced epoxy resin composites. It has been observed that J_c as a fracture parameter is independent of initial crack length and specimen length. However, before this fracture toughness parameter can be used in design, it is useful to study the size effect, that is, the effect of specimen width and thickness on J_c. In case of composite materials, this is even more relevant since the fracture toughness testing procedures for them are yet to be standardized.

Fibre concentration is the single most important variable influencing the properties of the composites. It can be easily controlled during fabrication. The influence of fibre concentration on J_c has also been studied in this chapter.

4.2 EFFECT OF WIDTH

The effect of specimen width on the fracture toughness (J_c) of the short glass fibre reinforced composite

was studied by varying specimen width between 15 and 40 mm.
The thickness in all the cases was maintained at 3 mm and
the fibre volume fraction at 39.4%. In fact, different
width specimens were cut from the same plates. The length
of specimens between grips was four times the width. For
each width and crack length, at least four specimens were
tested.

The load displacement curves for specimens with
different widths are shown in Figs. 4.1 to 4.4 and they are
quite similar in nature. Nominal fracture stress is plotted
in Fig. 4.5 against crack size (a_o/w). Figure 4.5 shows
that when a_o/w is greater than 0.5, the nominal fracture
stress is independent of specimen width because in this
range the crack dominates the fracture process. When a_o/w
is small, the nominal fracture stress is influenced by the
crack size. That is, for the same a_o/w, the fracture stress
decreases as the specimen width increases since the actual
crack length is larger in the wider specimens. The critical
displacement is plotted against a_o/w in Fig. 4.6. It
decreases as a_o/w increases and remains constant for a_o/w
larger than 0.4. This constant value, however, depends
upon the specimen width; it increases with specimen width.

The J integral for each width is obtained as a
function of displacement using its energy rate interpretation
as discussed in chapter 3. The J curves for different widths
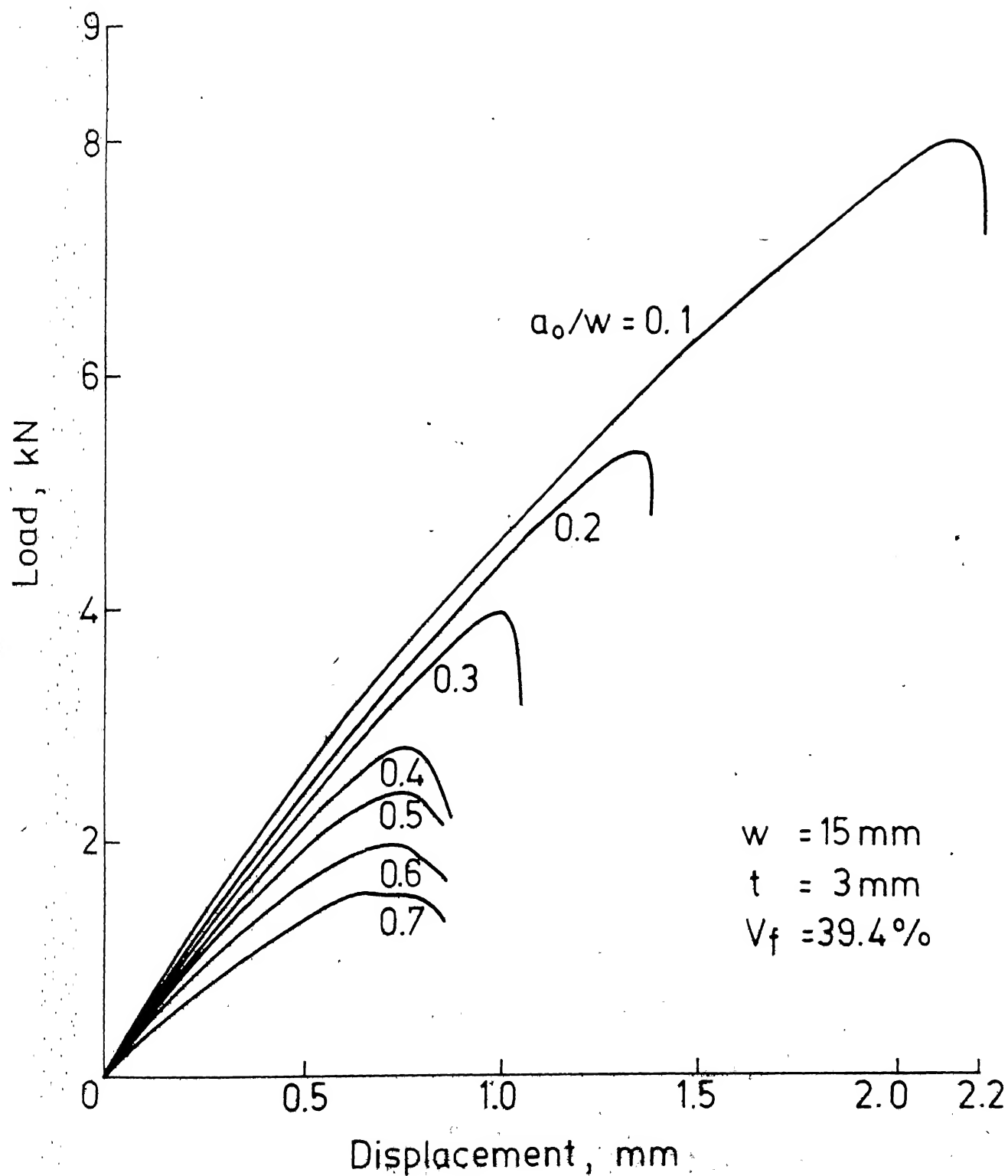
Fig. 4.1 Load displacement curves for 15 mm wide specimens.
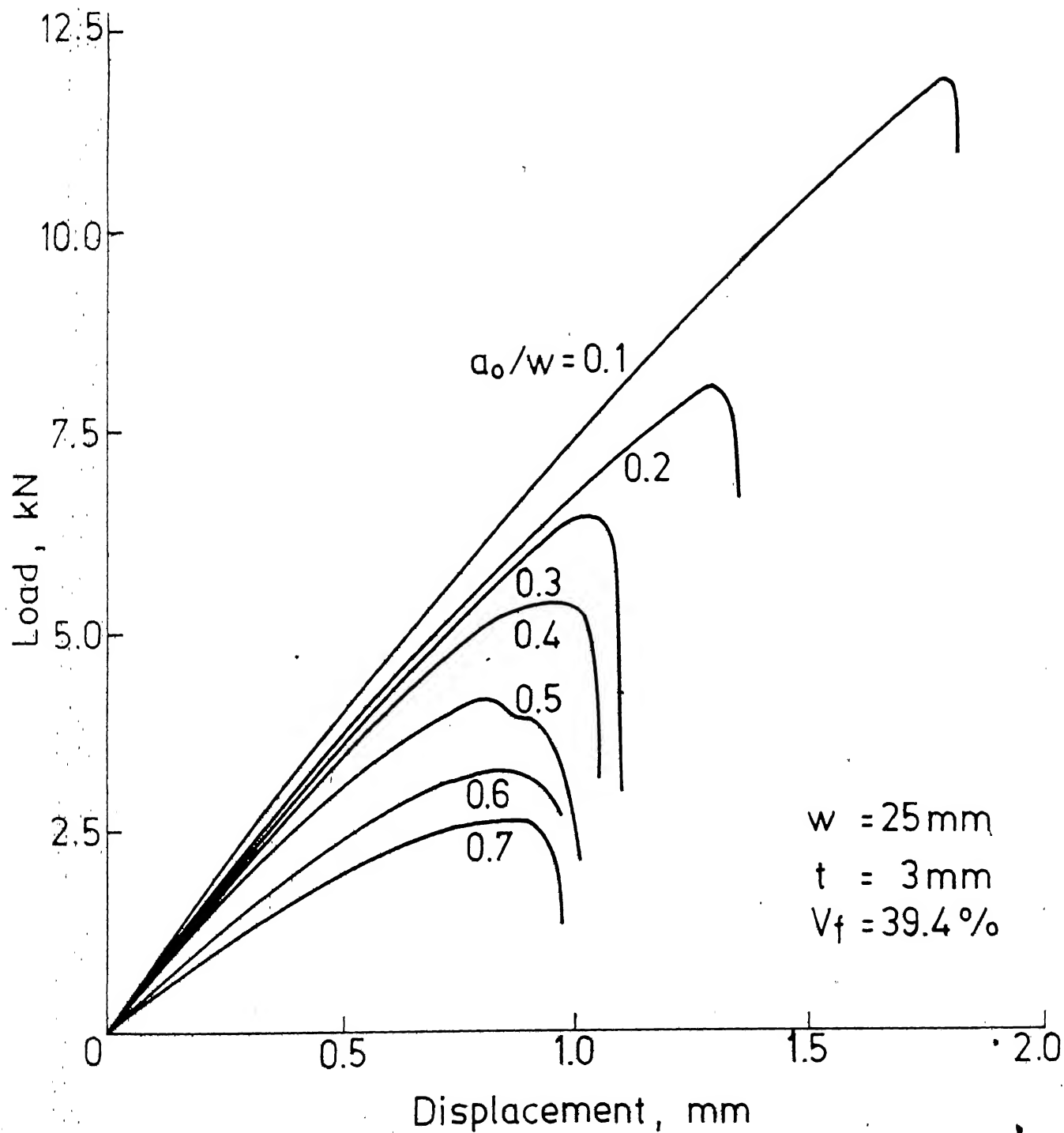
Fig. 4.2 Load displacement curves for 25mm wide specimens.

ig. 4.3 Load displacement curves for 30 mm wide specimens.

Fig. 4.4 Load displacement curves for 40mm wide specimens.
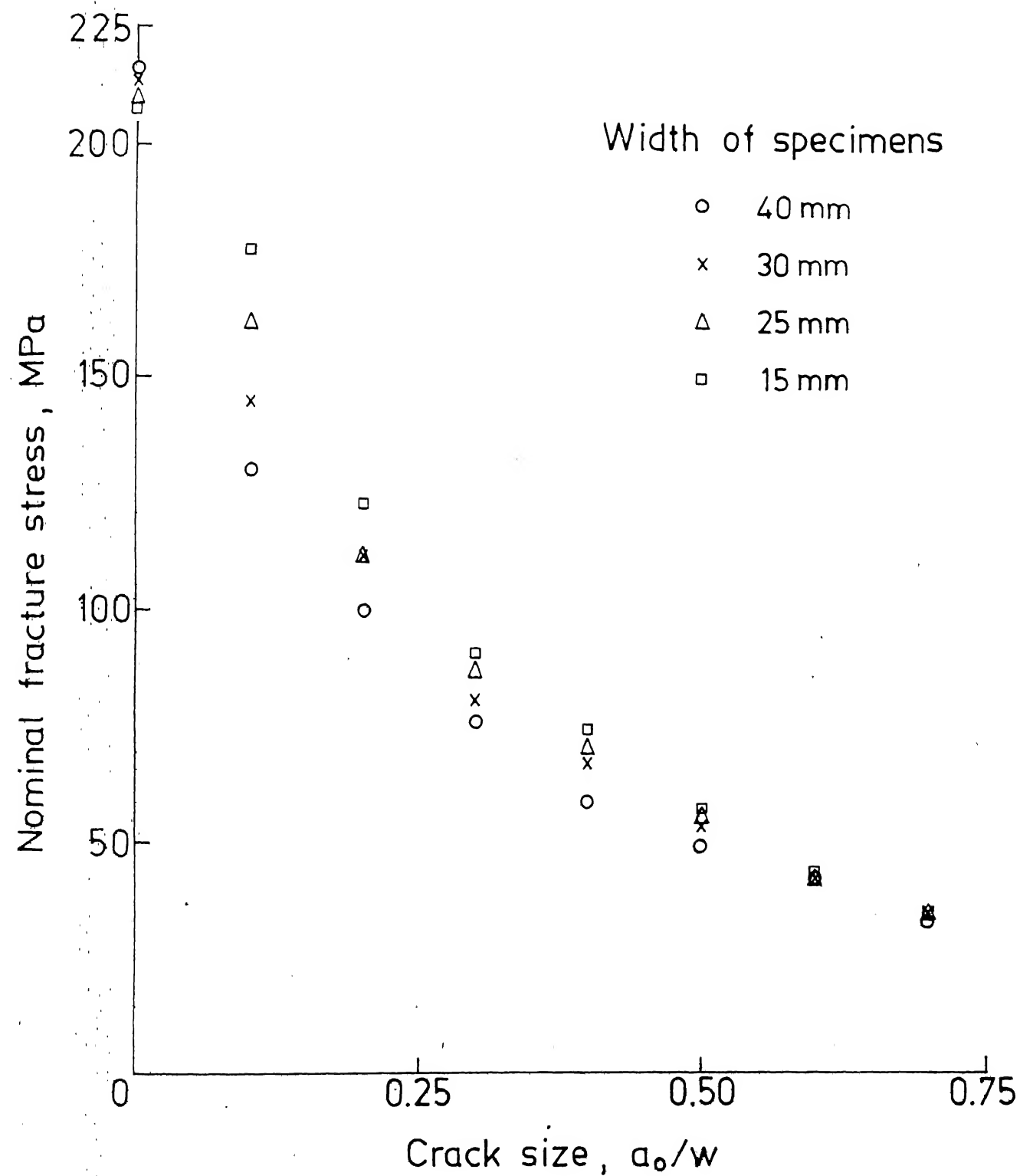
Fig. 4.5 Effect of specimen width on nominal fracture stress.
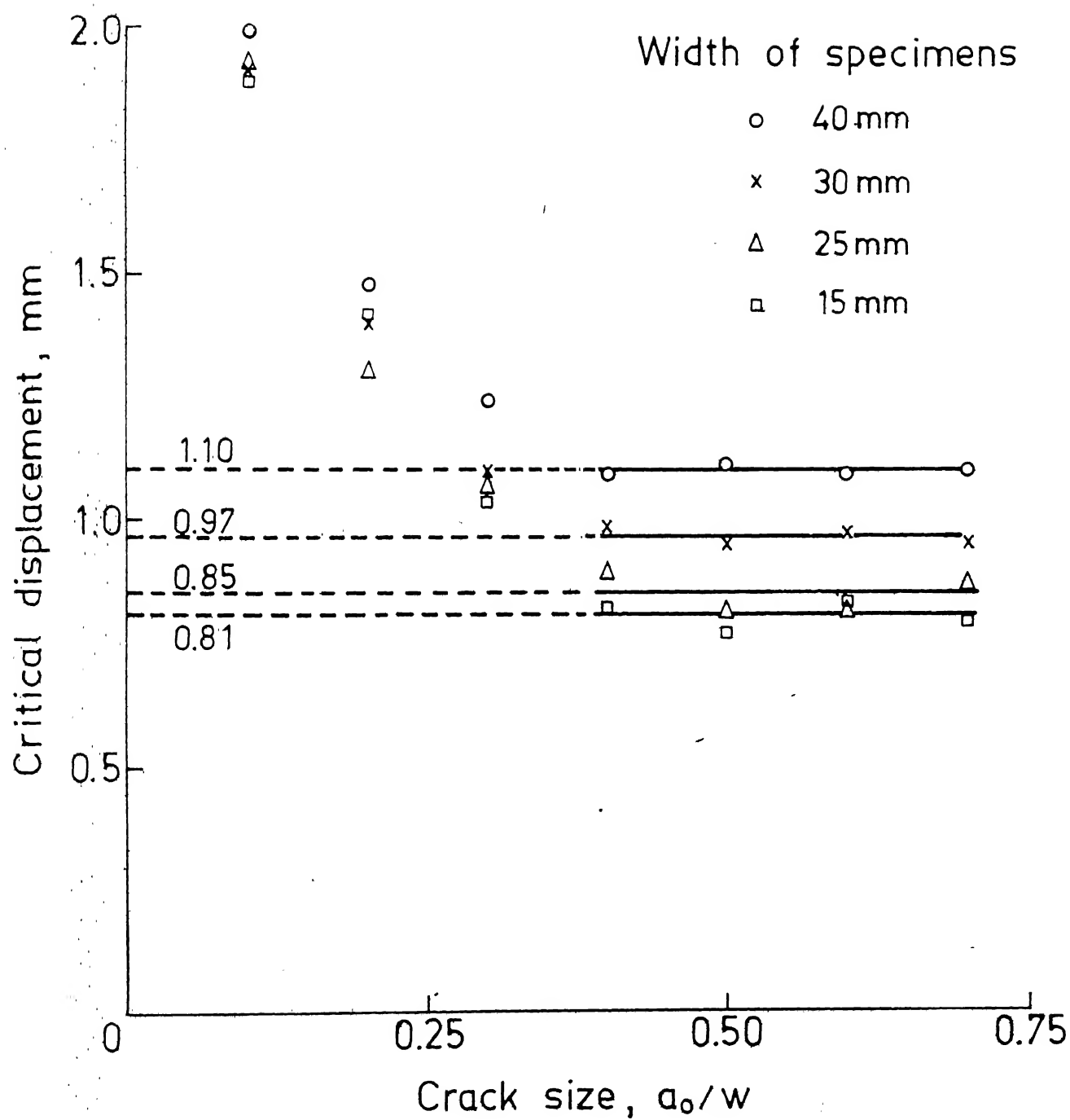
Fig. 4.6 Effect of specimen width on critical displacements.

are shown in Fig. 4.7. Corresponding to the constant critical displacements obtained earlier (Fig. 4.6), the critical value of J integral, J_c, is obtained for each width in Fig. 4.7. These values are plotted against specimen width in Fig. 4.8. The values of J_c do not exhibit any trend with specimen width. The slight variation is random. Thus, J_c, may be taken to be independent of specimen width. An average value of J_c is 47.65 kJ/m^2. This value of J_c is slightly different (about 8% lower) from that obtained in Chapter 3. This may probably be due to the chopped strand mat of glass fibres that came from a different lot.

4.3   EFFECT OF THICKNESS

The effect of specimen thickness on fracture toughness (J_c) was studied by conducting tests on specimens with thicknesses 1.8, 3, 6 and 9 mm. The number of chopped strand mat layers used for 1.8, 3, 6 and 9 mm thickness plates were 3, 5, 10 and 15 respectively. The width in all the cases was 25 mm and the volume fraction 39.4%. The length of specimens between grips was 100 mm. For each thickness and crack length, at least four specimens were tested.

The load displacement curves for specimen thicknesses 1.8, 6 and 9 mm are shown in Figs. 4.9 to 4.11 and those for 3 mm specimen thickness have already been shown in Fig. 4.2. The average fracture stress (Fig. 4.12) is independent of specimen thickness. It may be mentioned that the scatter
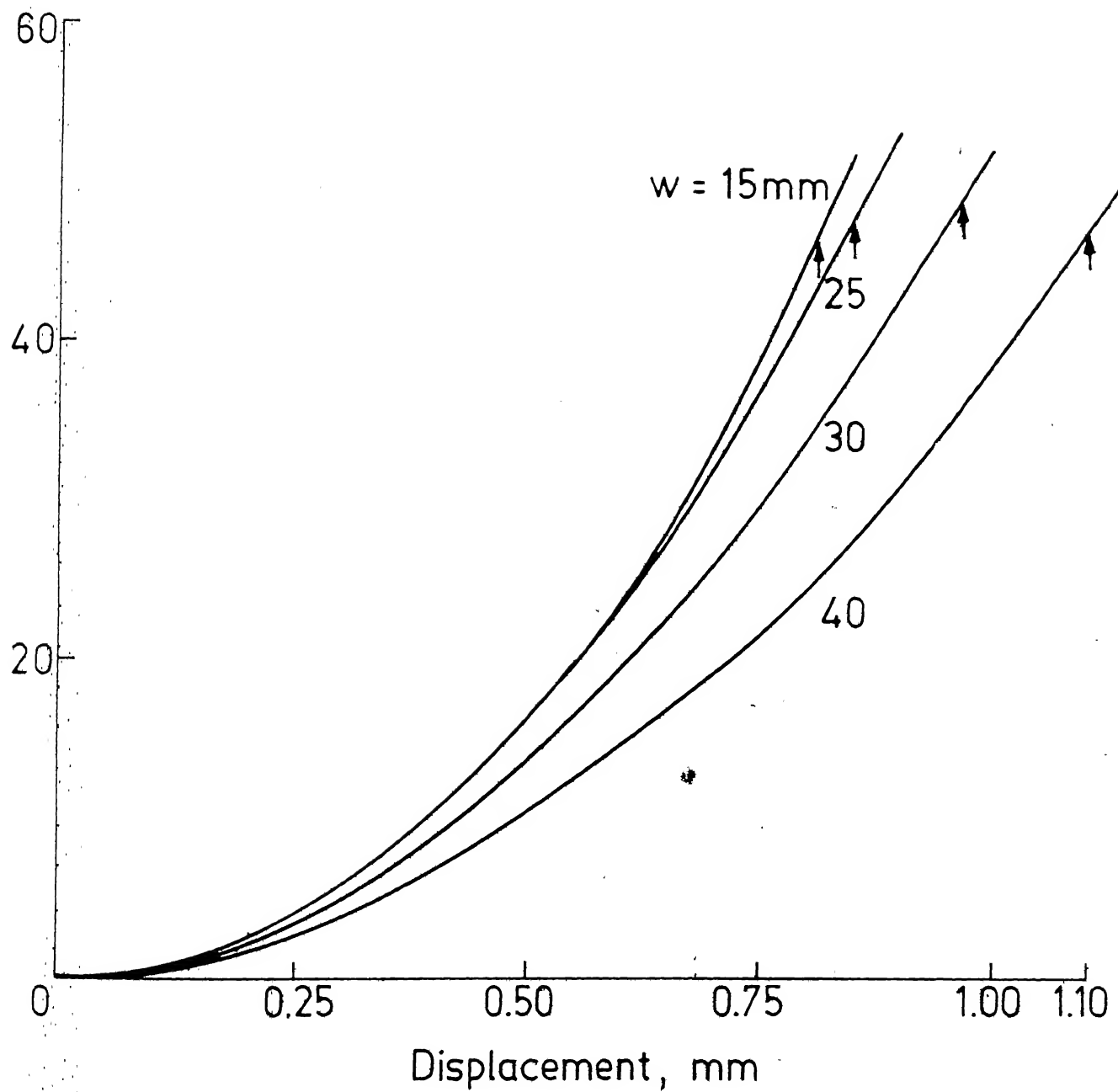
Fig. 4.7 J integral curves for specimens of different width.
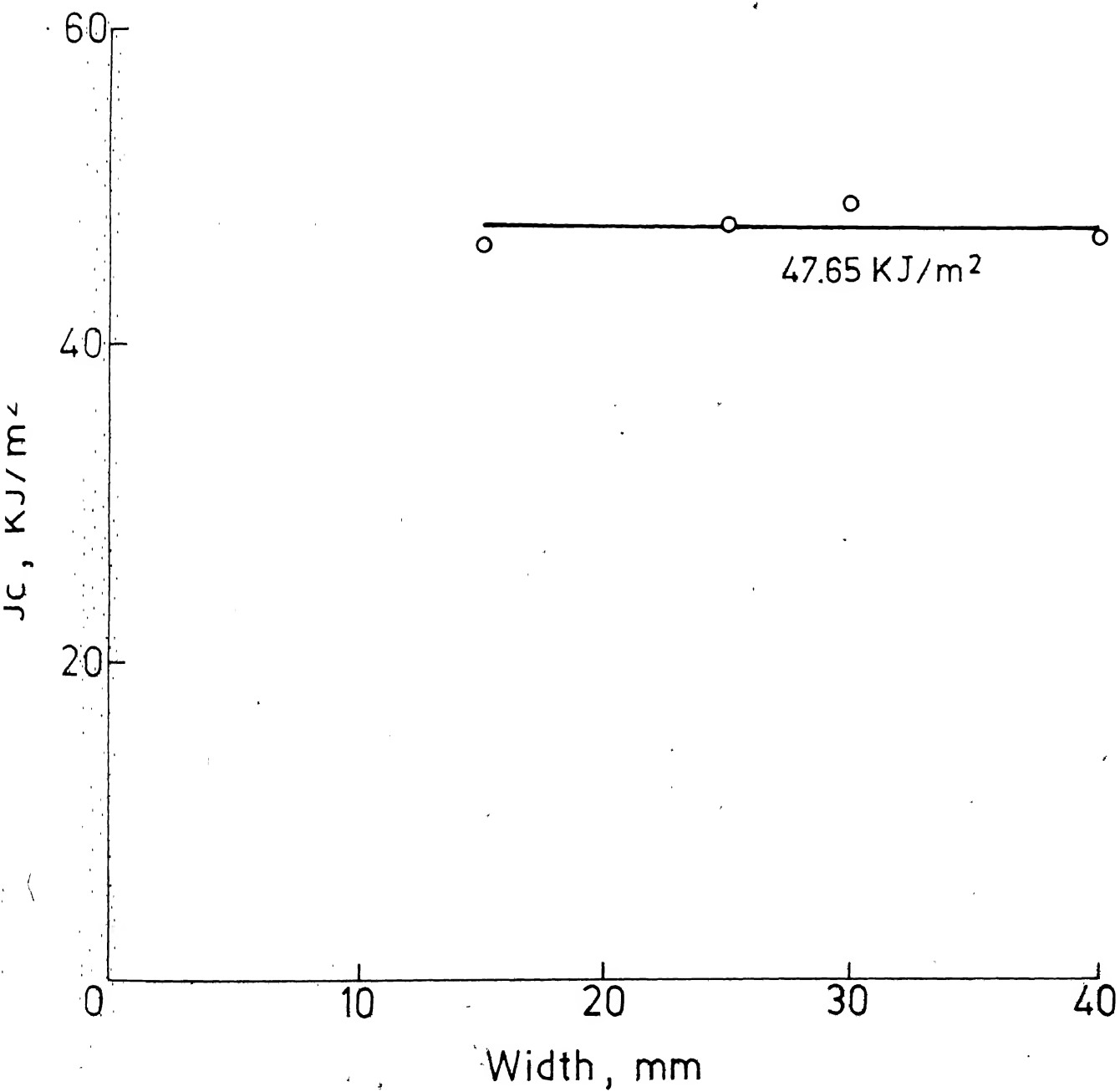
Fig. 4.8 Influence of width on J_c.
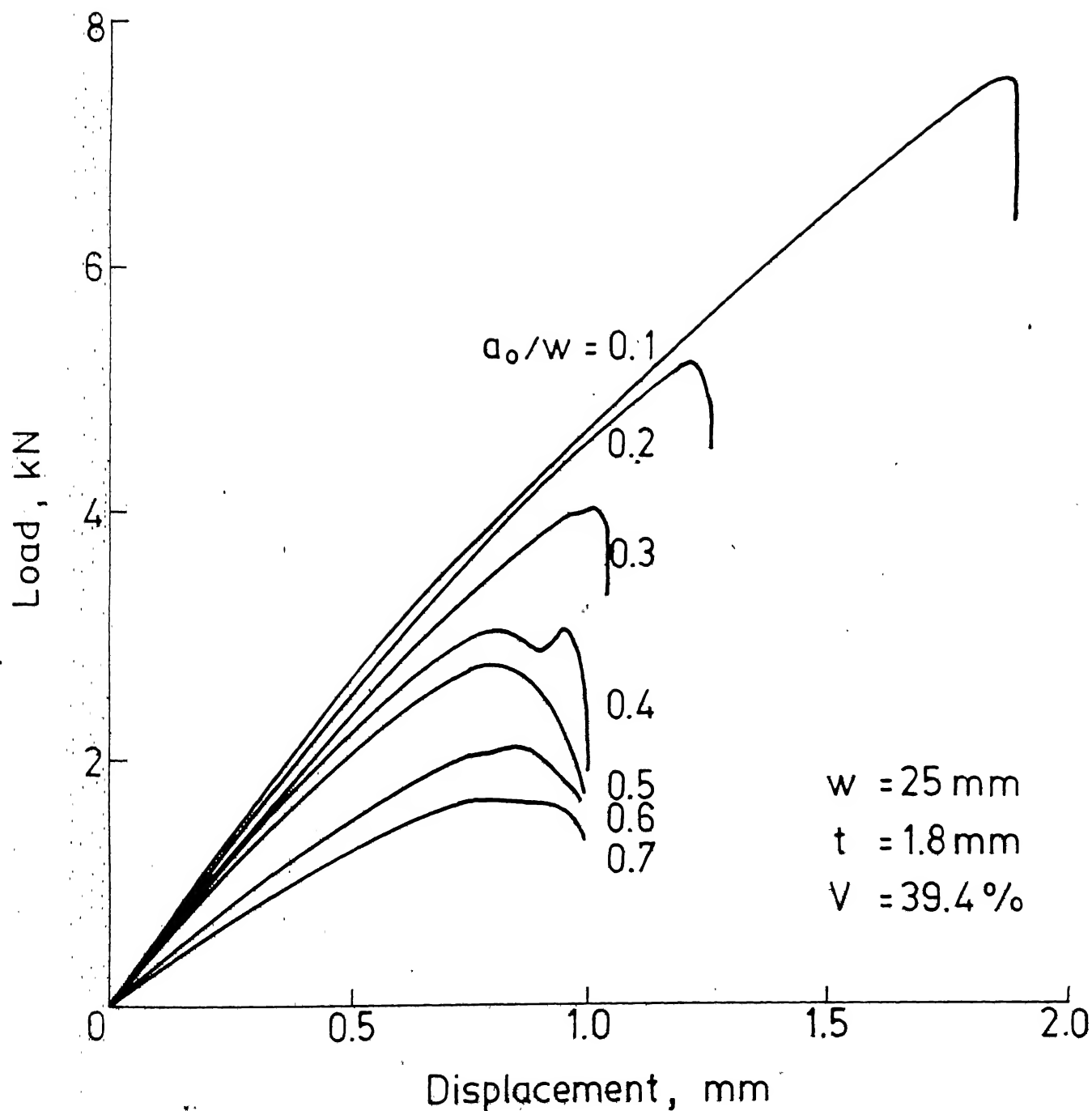
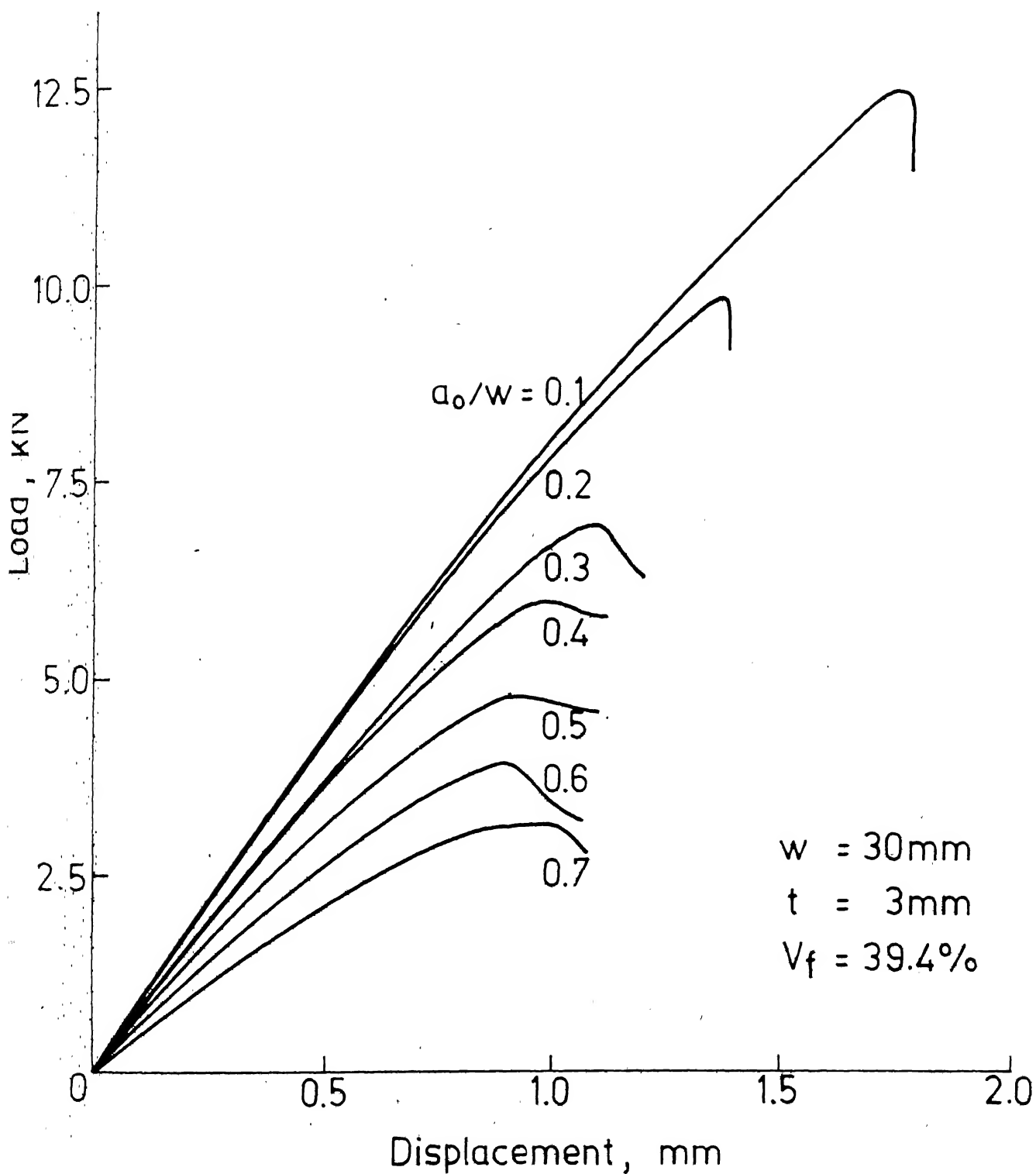Fig. 4.9 Load displacement curves for 1.8 mm thick
specimens.
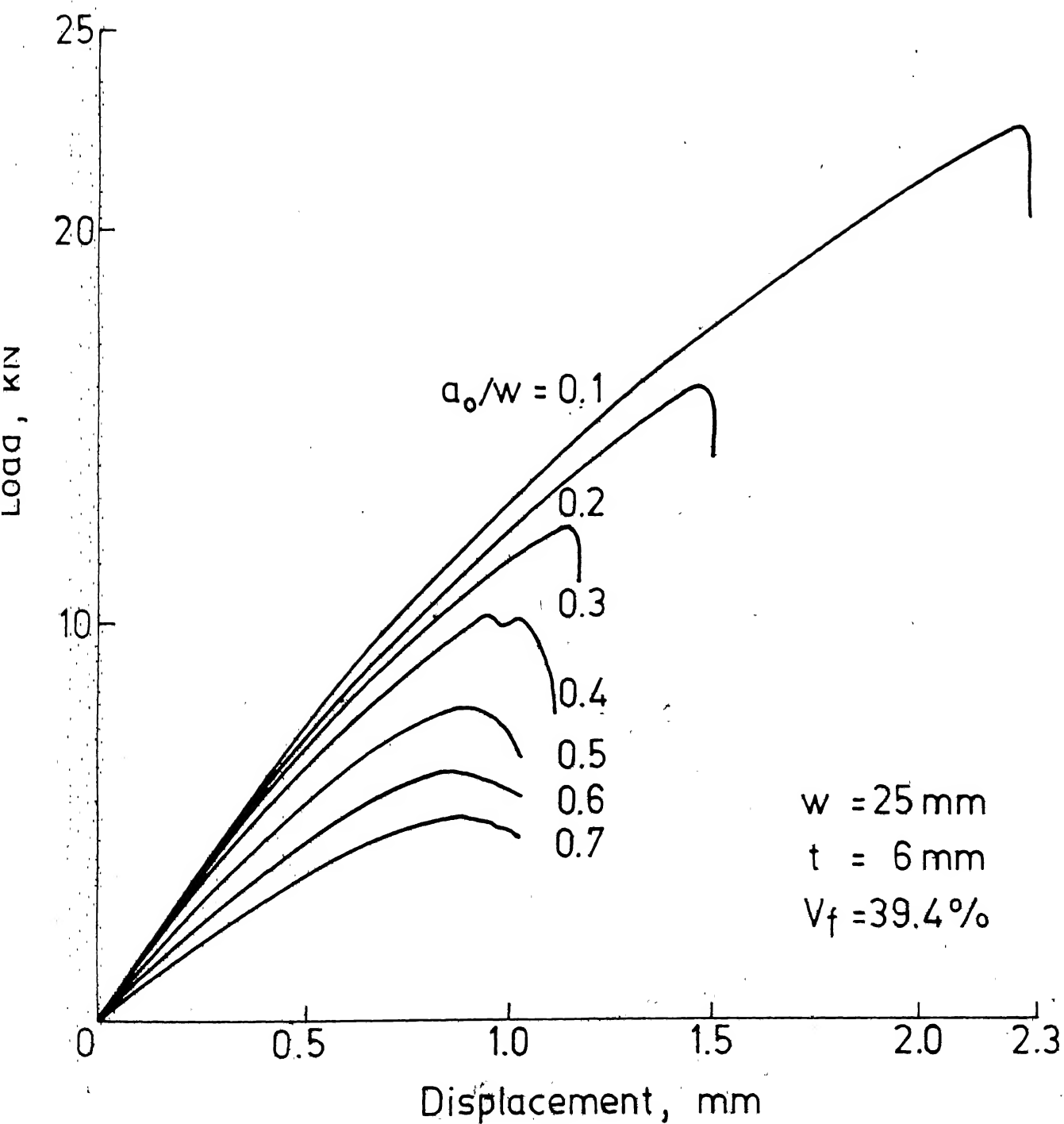
Fig. 4.10 Load displacement curves for 6mm thick specimens.

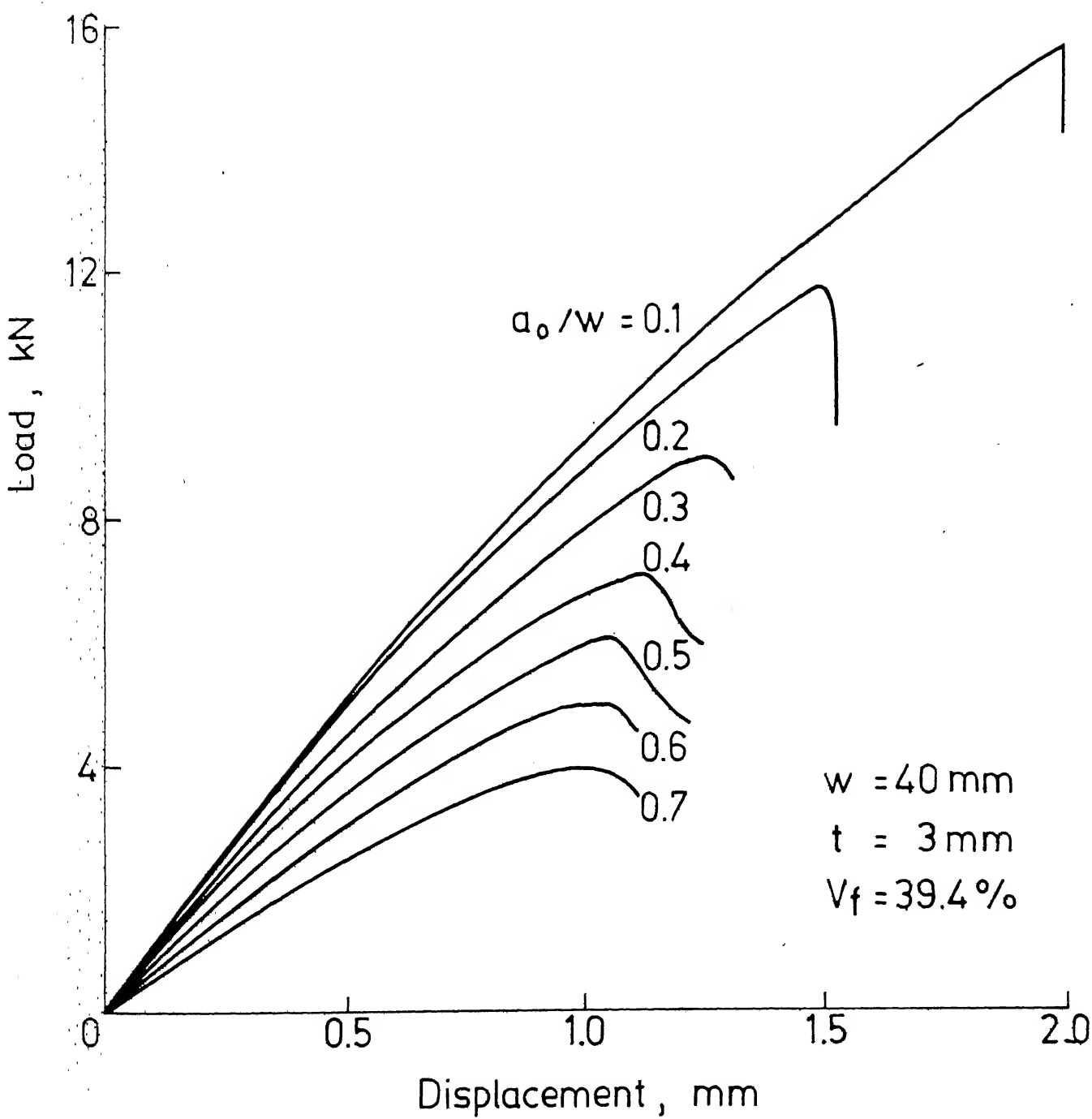Fig. 4.11 Load displacement curves for 9.0 mm thick specimens.
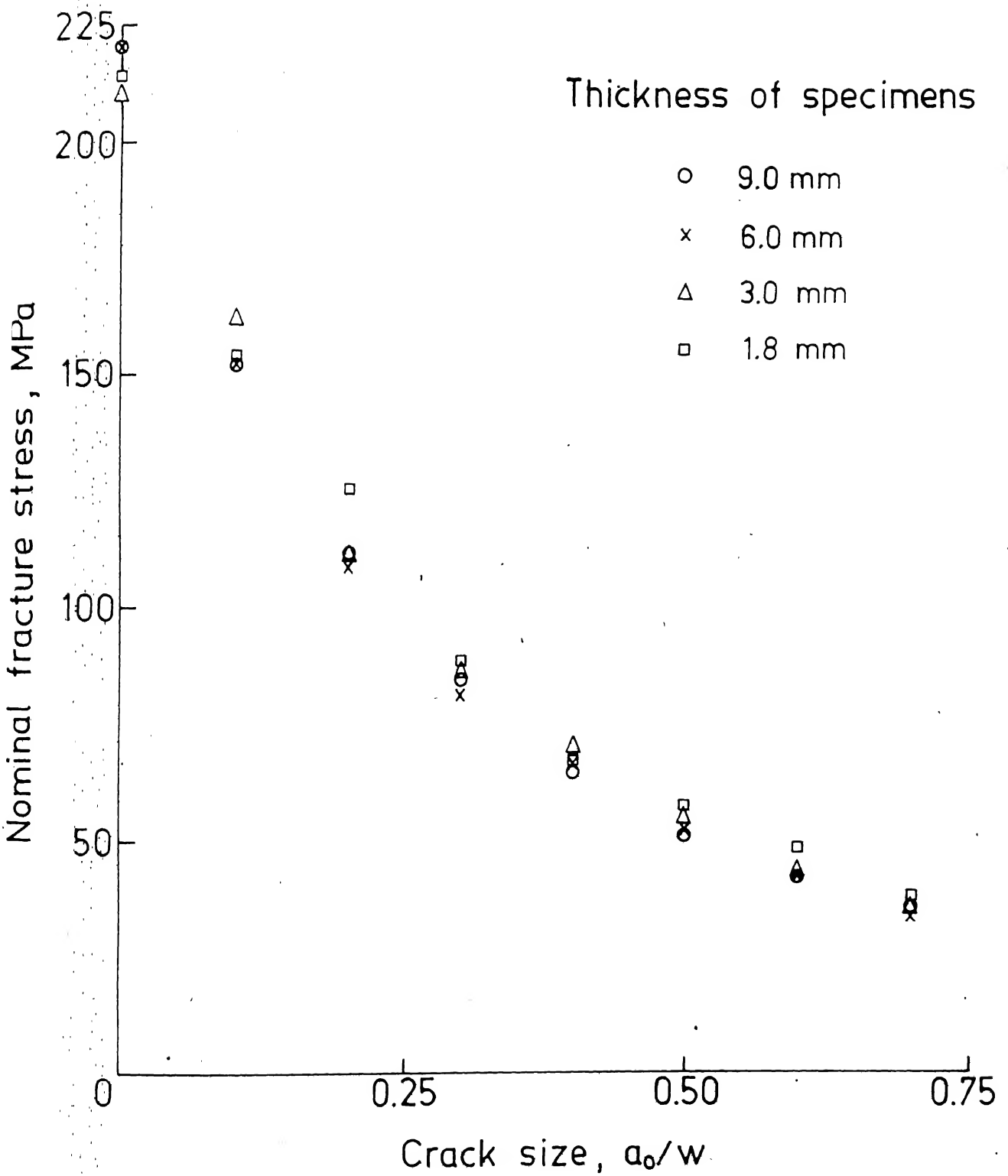
Fig. 4.12 Effect of specimen thickness on nominal fracture stress.

in data was observed to decrease as the specimen thickness
increases because in thicker specimens, the number of layers
of chopped strand mat is larger which promotes randomness
of the fibres over the total thickness and hence better
isotropy. The critical displacements are shown in Fig. 4.13
for different thickness specimens. The variations of critical
displacement with crack length are similar i.e., it decreases
with increase in crack length and reaches a constant value
for cracks larger than 10 mm ($a_o/w \geq 0.4$).

The J integral was obtained using the energy rate
interpretation. The J integral curves are shown in Fig.
4.14. The critical value of J integral for different thick-
nesses are also indicated. The J_c is plotted against thick-
ness in Fig. 4.15. The J_c is observed to be independent of
thickness with an average value of 47.6 kJ/m^2. The fracture
toughness being independent of thickness appears to be
peculiar to randomly oriented short fibre composites. Harris
and Morris [56] found that, like isotropic metals, the
fracture toughness of graphite fibre-epoxy laminates decreases
with increasing laminate thickness. It may be pointed out
that in fracture toughness testing of composite materials,
specimen length may play an important role particularly
when the crack length is small and specimen thickness is
large. It has been observed during the present investigations
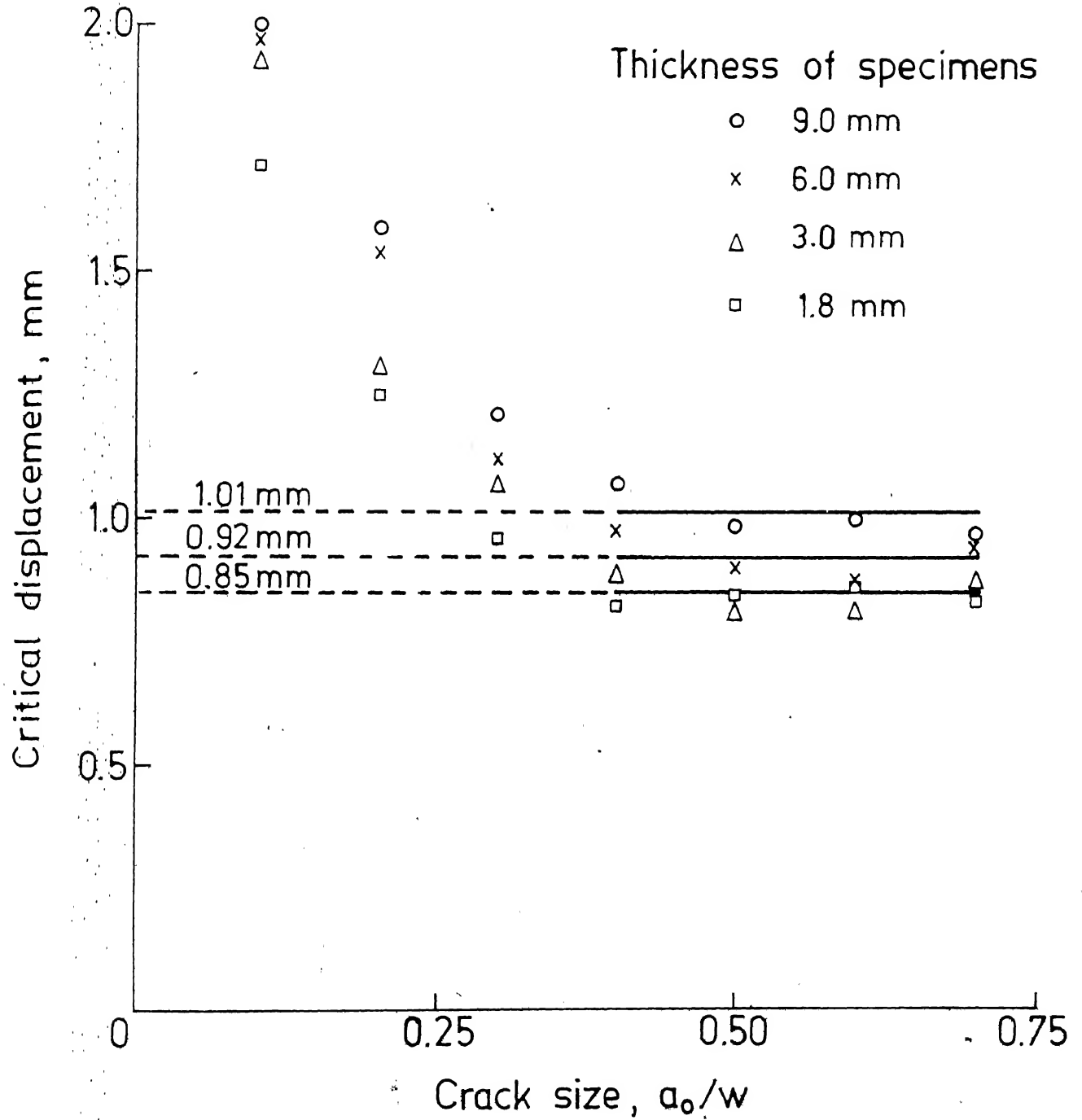
Fig. 4.13 Effect of specimen thickness on critical
displacement.
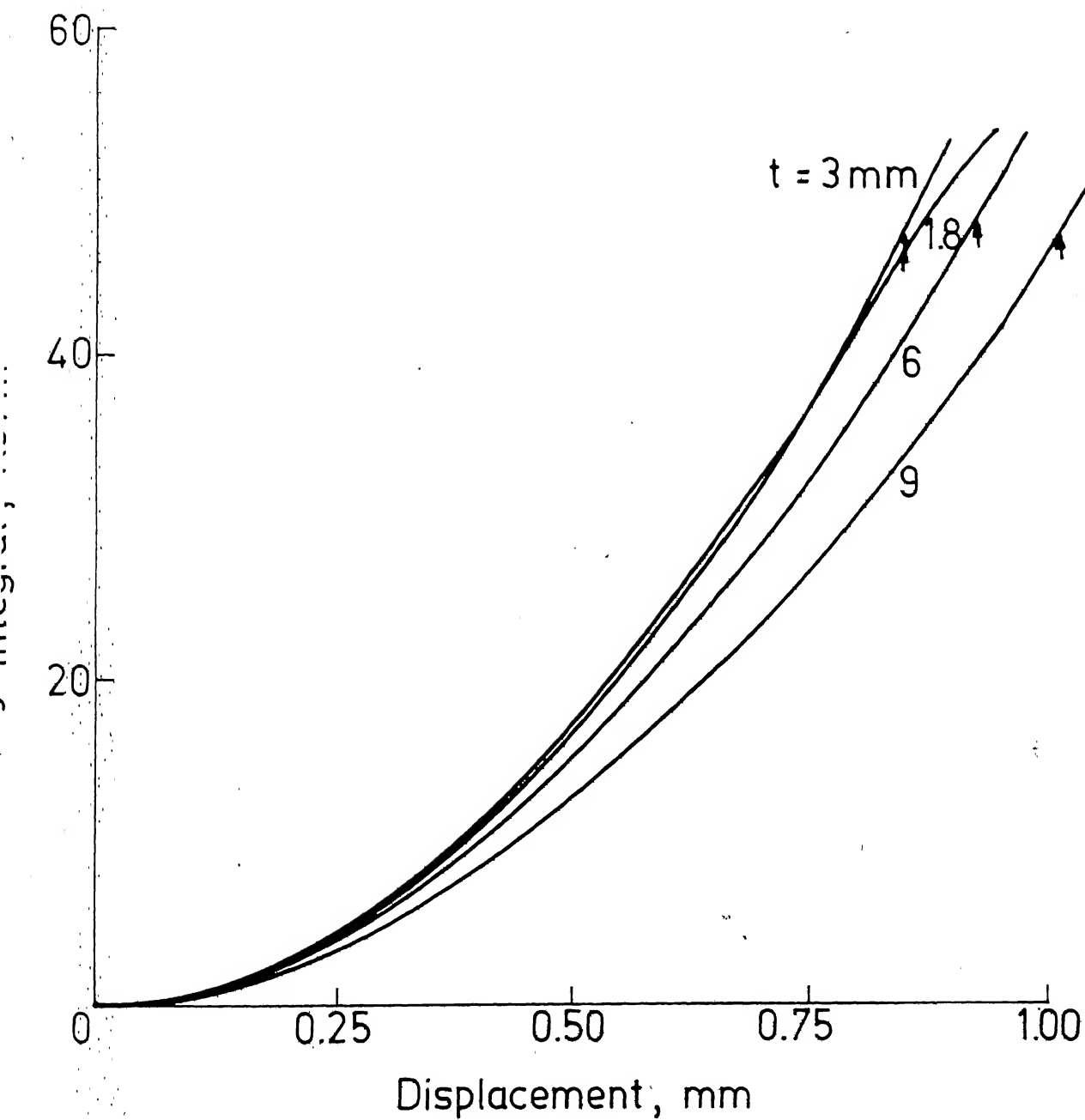
Fig. 4.14 J integral curves for specimens with different
thickness.
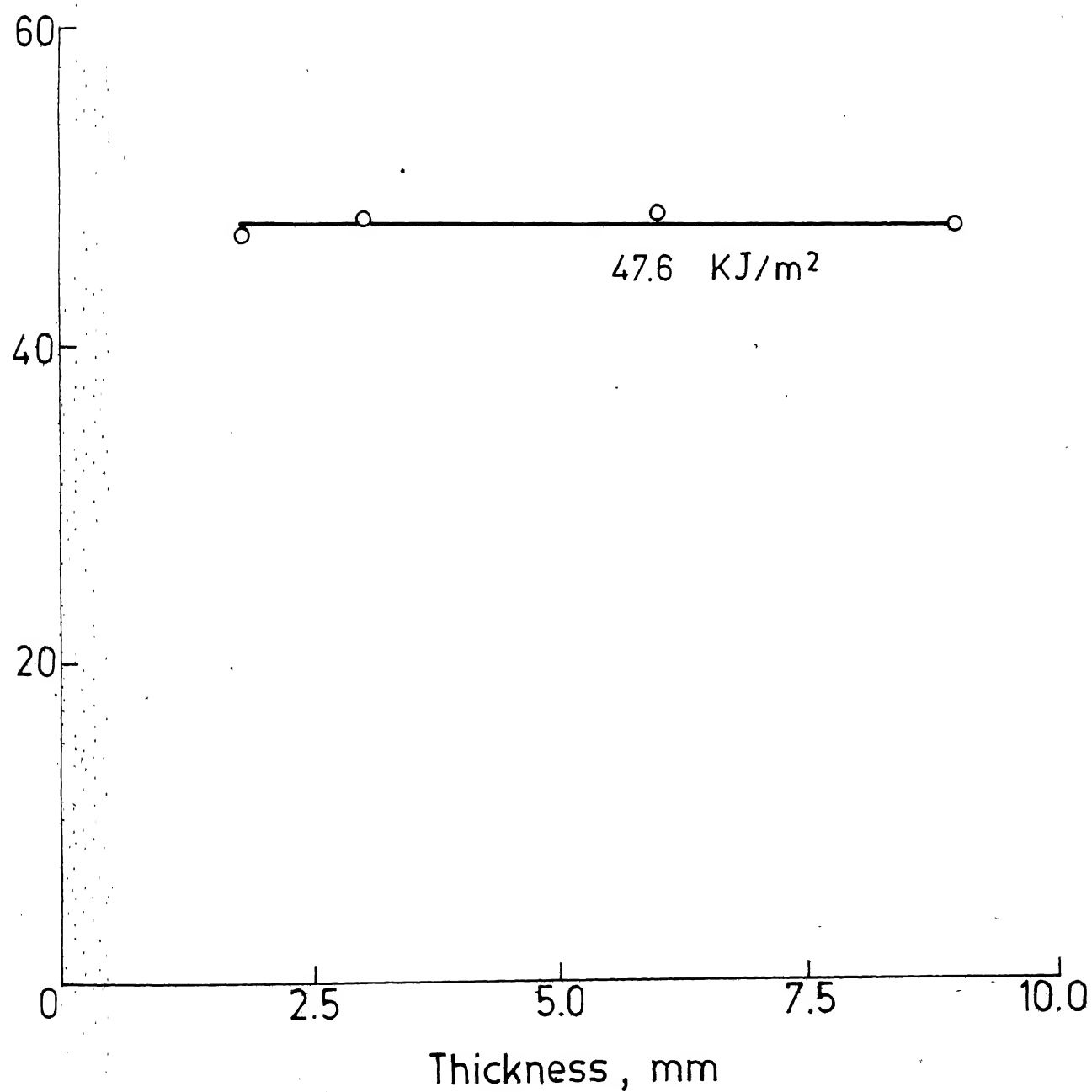
Fig. 4.15 Influence of specimen thickness on J_c.

that in thick specimens with small crack lengths outer
layers tend to fail first because of nonuniform stress dis-
tribution across the thickness. Thus, when fracture tough-
ness is evaluated from small crack length specimens, as in
the case of R curve approach, a lower value of fracture
toughness may result for higher thickness. However, this
does not influence the present critical value of J integral
which has been evaluated from specimens with larger crack
lengths.

4.4 EFFECT OF FIBRE VOLUME FRACTION

In addition to the tests on specimens with a fibre
volume fraction of 39.4%, the tests were conducted for
three other volume fractions namely 23.6, 31.5 and 47.2%.
In all the cases, specimen thickness and width were 3 and
25 mm respectively. The length of specimens between grips
was 100 mm. For a given volume fraction and crack length,
at least four specimens were tested.

The load displacement curves are shown in Figs.
4.16 to 4.18 for specimens with 23.6, 31.5 and 47.2 percent
fibre volume fraction and those for $V_f = 39.4\%$ have already
been shown in Fig. 4.2. The J integral for different fibre
volume fractions are plotted in Fig. 4.19. The critical
values are marked on the curves for the critical displace-
ments corresponding to $a_o/w > 0.4$. The J_c, plotted in
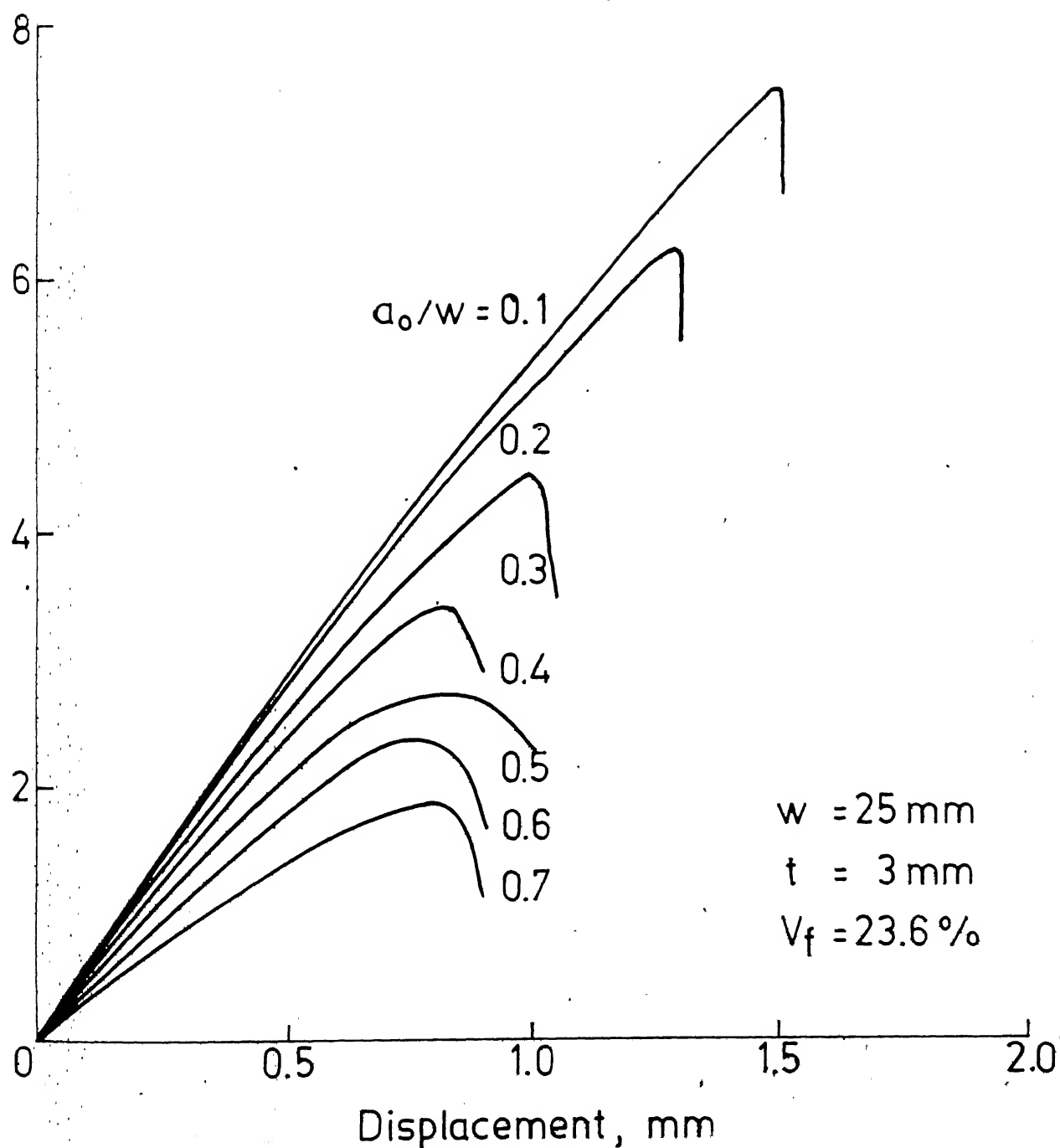
Fig. 4.16 Load displacement curves for specimens with 23.6% fibre volume fraction.
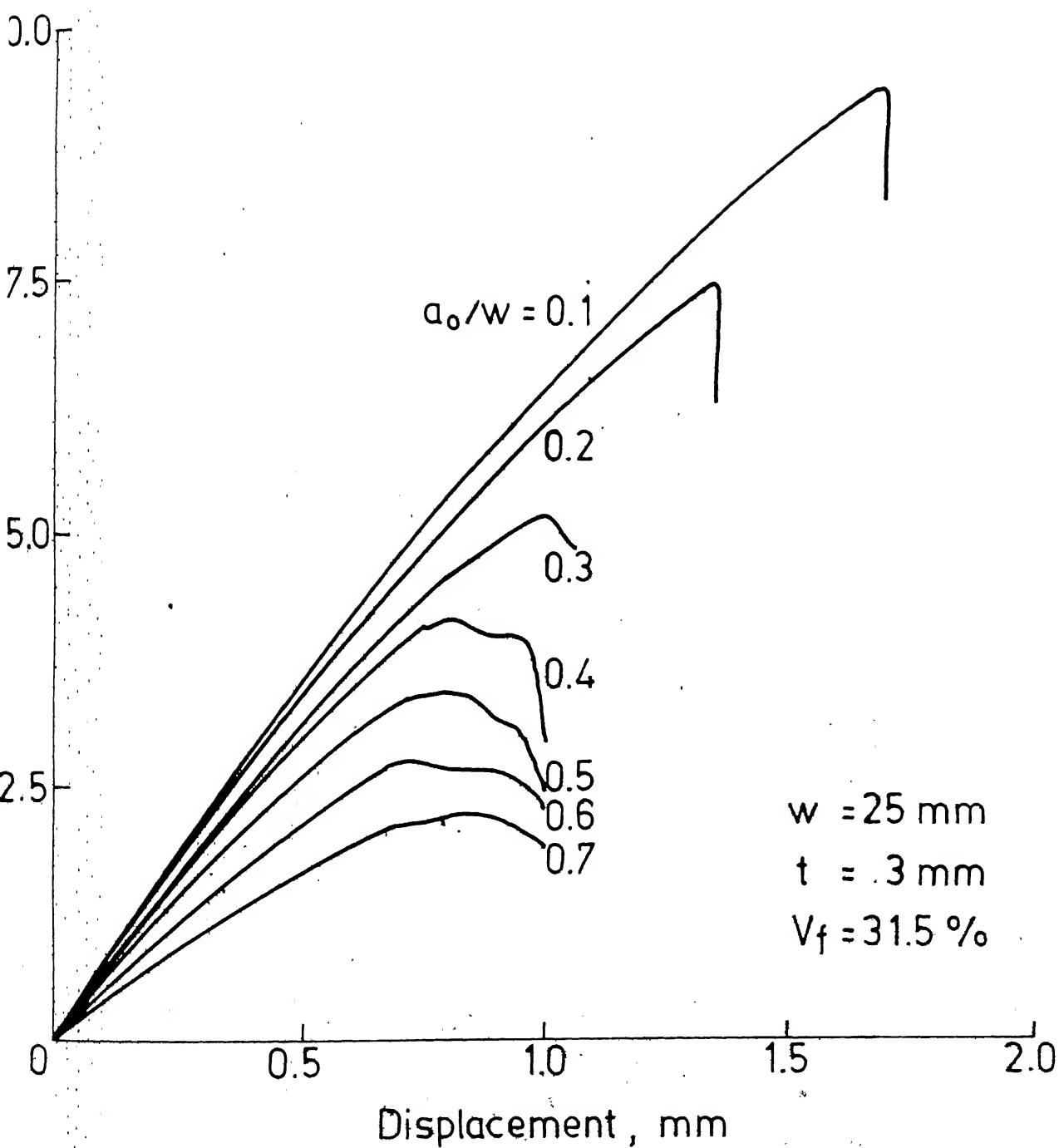
Fig. 4.17 Load displacement curves for specimens with 31.5% fibre volume fraction.
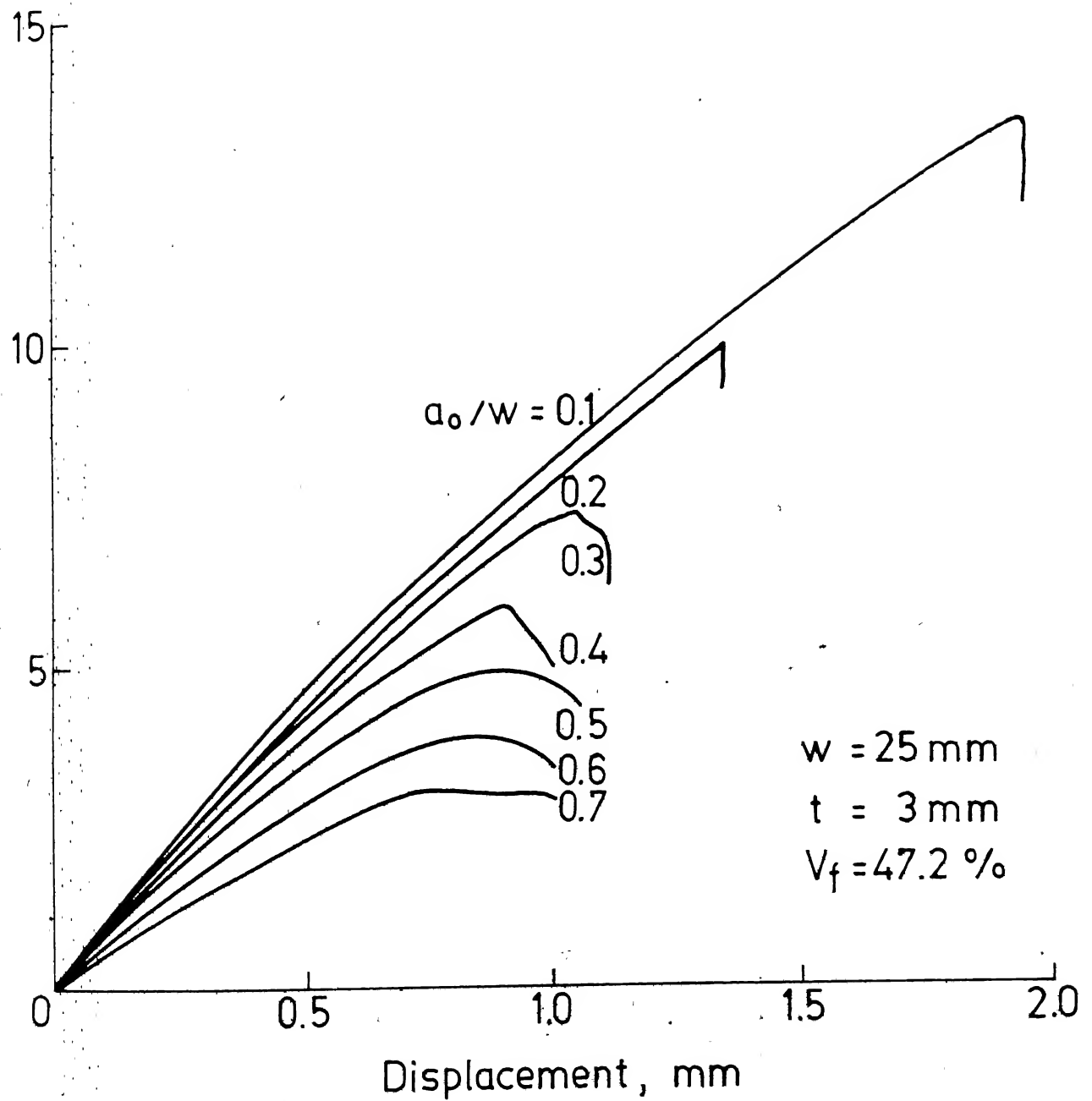
Fig. 4.18 Load displacement curves for specimens with 47.2% fibre volume fraction.
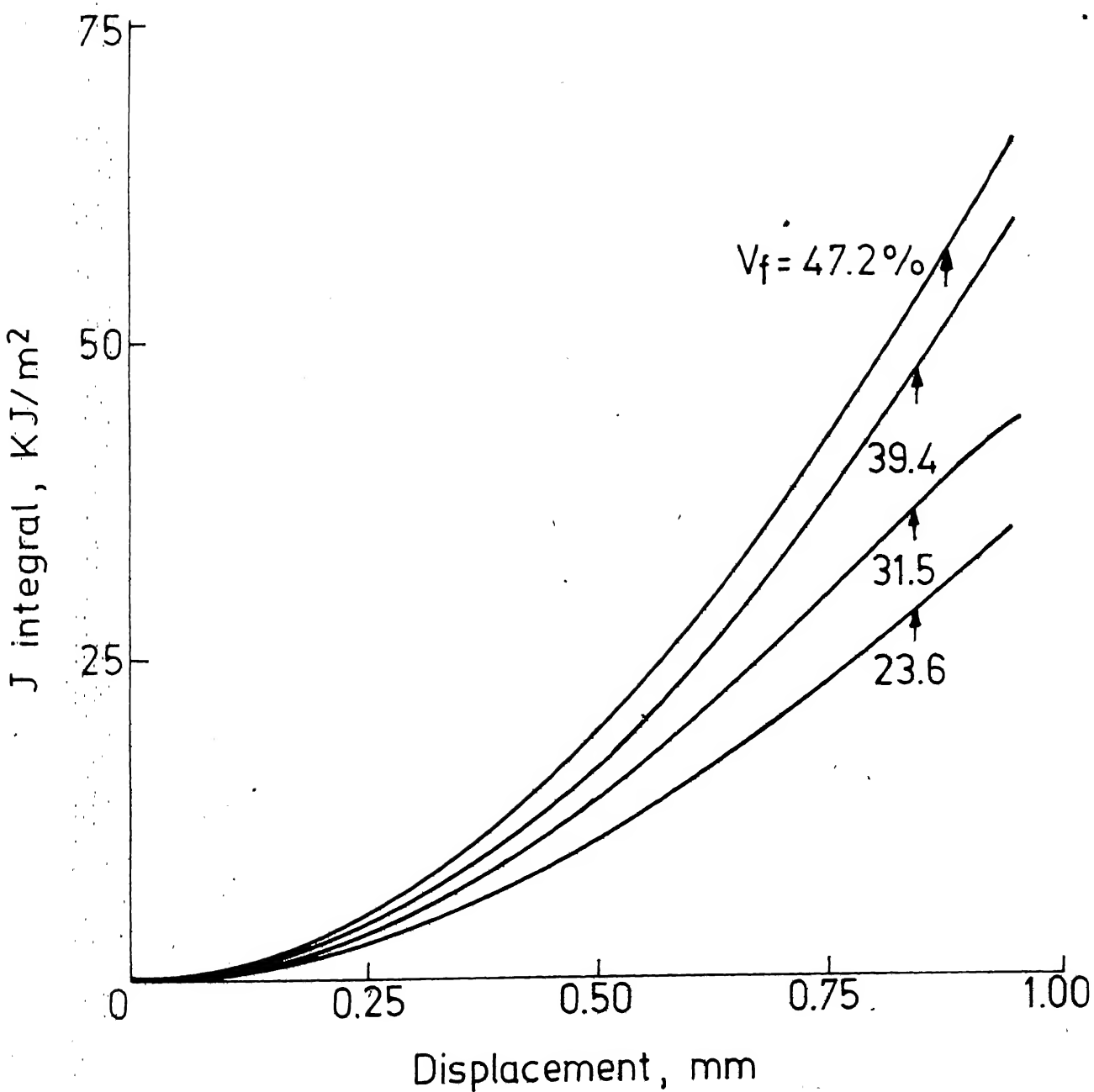
Fig. 4.19 J integral curves for specimens with different fibre volume fractions.

Fig. 4.20 shows a strong dependence on fibre volume fraction.
At $V_f = 47.2\%$, J_c equals 55.8 kJ/m^2 which is double of the
J_c ($= 29$ kJ/m^2) at $V_f = 23.6\%$.

4.5 DISCUSSION

Dependence of J_c on specimen width and thickness and
fibre volume fraction has been investigated in this chapter
by varying one parameter at a time. The specimen width was
varied between 15 and 40 mm, thickness between 1.8 and 9 mm
and fibre volume fraction between 23.6 to 47.2%. The
results show that the J_c is independent of specimen width
and thickness. It has already been shown in Chapter 3 that
J_c is independent of initial crack length and specimen length.
Thus, J_c may be regarded as a material property for short
fibre composites characterizing fracture toughness of the
material.

In composites, the fibre volume fraction is the
single most important variable controlling such material
properties as the strength, modulus etc. The results pre-
sented in this chapter show a strong dependence of J_c on
fibre volume fraction. It increases linearly with fibre
volume fraction. It is known that both the glass fibres
and the epoxy resin are brittle with very low fracture tough-
ness. However, in composites, they interact in such a way
that the fracture toughness of the composite is more than
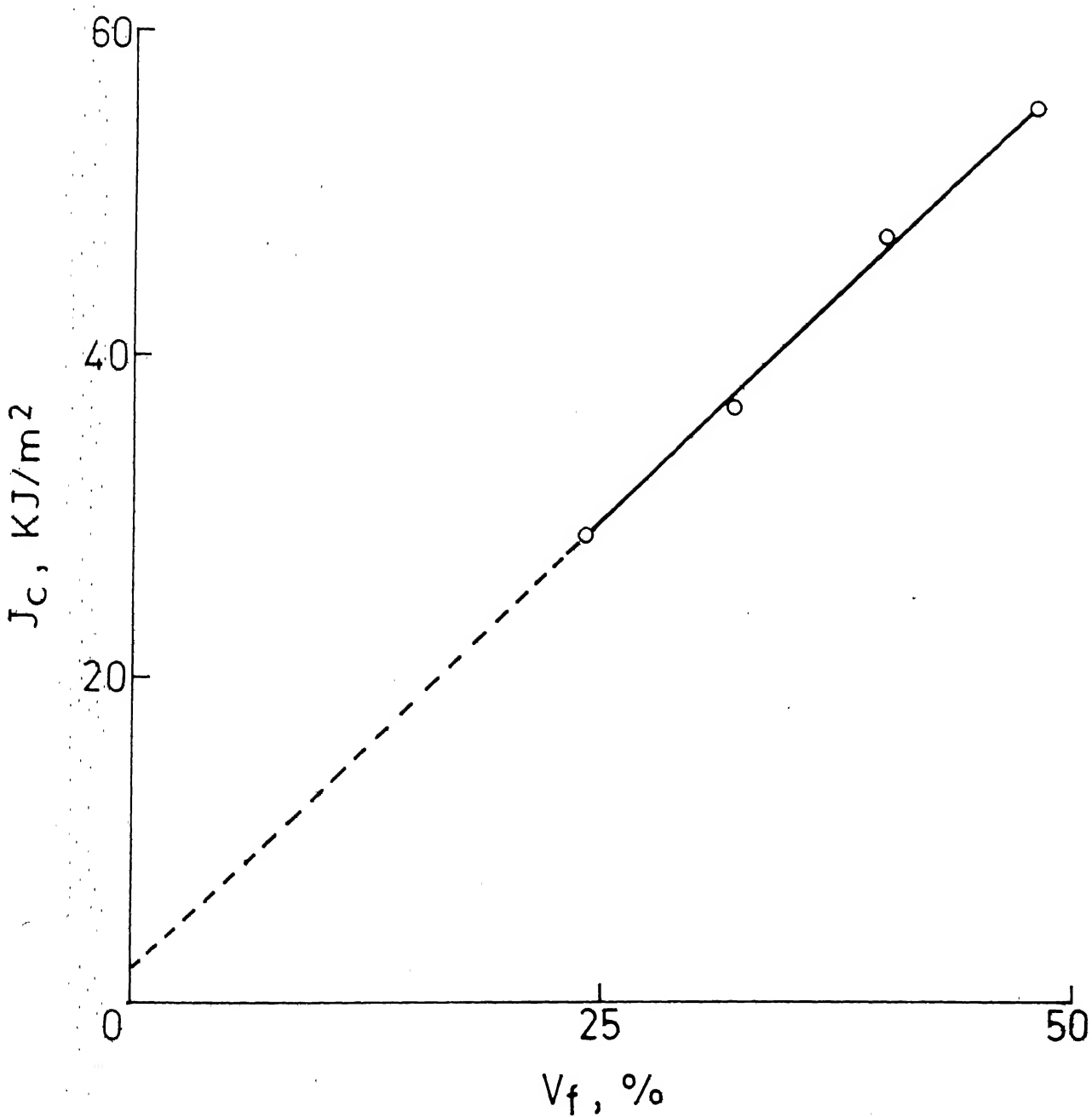
Fig. 4.20 Influence of fibre concentration on J_c.

that of the glass fibres and the epoxy resin. The inter-
action (through the fibre-matrix interface) increases with
fibre volume fraction and hence the increase in fracture
toughness with fibre concentration.

CHAPTER V

FRACTURE TOUGHNESS OF SHORT FIBRE
COMPOSITES USING R CURVE APPROACH

5.1 INTRODUCTION

Fracture characterization of randomly oriented
short glass fibre reinforced composites has been carried out
in the preceeding two chapters using J integral approach.
For comparison of the fracture toughness results using J
integral method, R curve approach has been used for short
fibre composites. In the last 10 years, several investiga-
tors [41 - 53] have carried out fracture tests using R curve
approach. They have considered the effect of various para-
meters, such as thickness, width, temperature, matrix
material, interfacial bond strength etc. on critical crack
growth resistance for these composites. Here, while employ-
ing this approach, an appraisal of the method for short glass
fibre reinforced composites is made, the assumptions involved
are examined and simplification of the procedure is attempted.

5.2 CRACK GROWTH RESISTANCE (R CURVE) PROCEDURE

When a notched specimen with a crack length, a, is
subjected to a load, P, the stress intensity factor (K_I) is
given by

$$K_I = Y \frac{P}{tw} \sqrt{a} \qquad\qquad (5.1)$$

where t and w are specimen thickness and width respec-
tively, Y is a calibration factor to account for the finite
width of the specimen. The applied stress intensity factor
tends to extend the crack and is therefore often referred
to as the crack extension or crack driving force (denoted
by K_1). This tendency of crack extension is resisted by
internal material resistance which is called crack growth
resistance, K_R. The crack growth resistance of the material
can be obtained when the applied force is in equilibrium
with an instantaneous crack length, a_i and is given by

$$K_R = Y \frac{P}{tw} \sqrt{a_i} \tag{5.2}$$

Thus, the crack growth resistance and the crack extension
force are given by the same expression. In calculating the
K_R, actual values of load and crack length are used, while
K_1 may be calculated for any combination of the load and
crack length which may or may not exist in any real situation.

A plot of crack growth resistance against crack
length is referred to as the crack growth resistance curve
(R curve). A plot of crack extension force, for a constant
load, against crack length is crack extension force curve
(K_1 curve).

A typical R curve is shown in Fig. 5.1. The initial
portion AB of the curve is a vertical line representing
increase in K_R due to increase in load without any crack
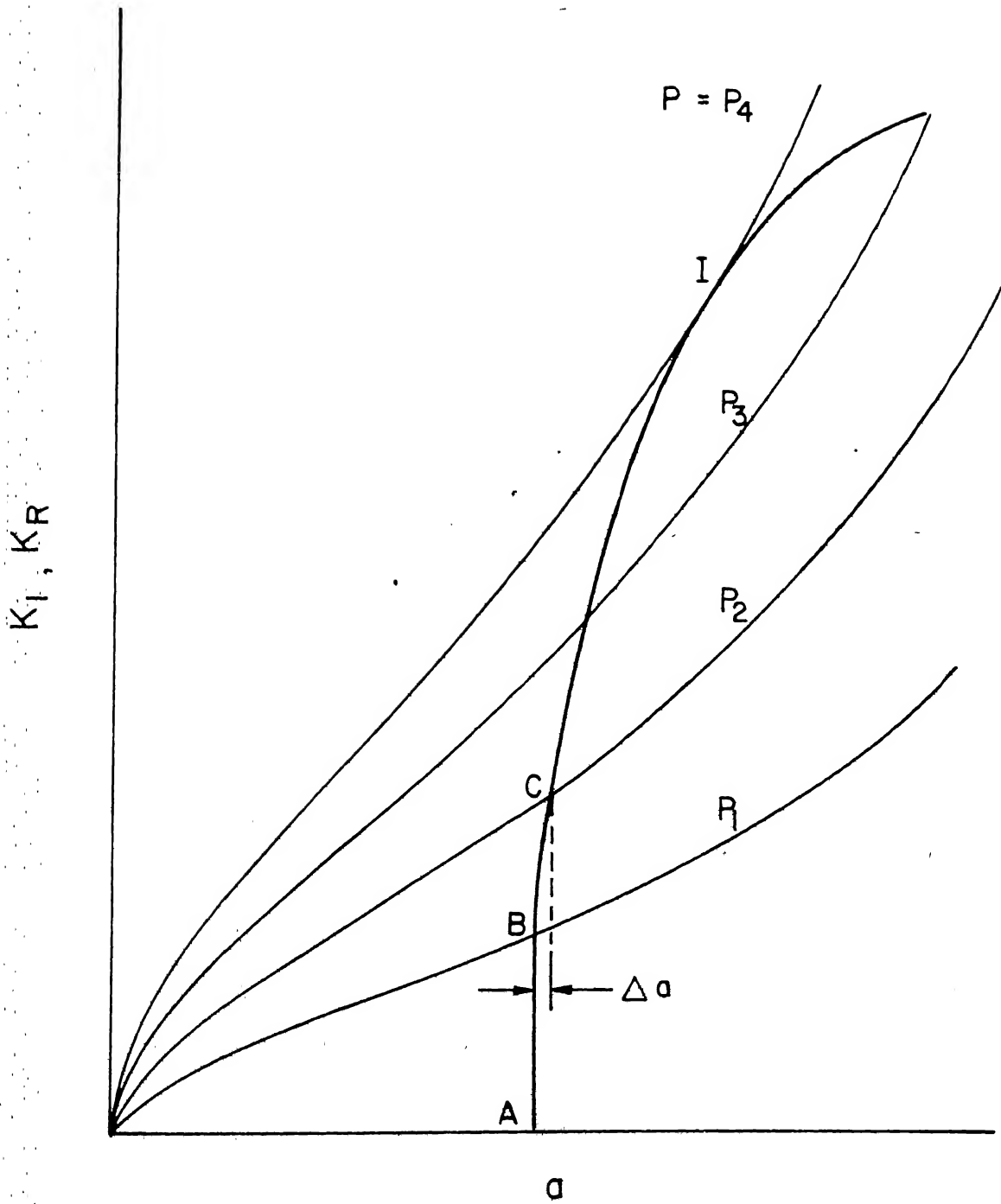
Fig. 5.1 An R curve and a set of K_I curves.

extension. Beyond point B an increase in load causes a crack
extension and corresponding increase in crack growth resis-
tance which is larger than the increase in crack extension
force for a constant load. Thus, this is a stable crack
growth. Further crack growth occurs when crack extension
force is increased by raising the load. The process conti-
nues until point I beyond which crack extension causes a
larger increase in crack extension force than the crack
growth resistance and an unstable crack growth occurs. The
instability criteria at point I may be mathematically repre-
sented by the simultaneous fulfilment of the following two
conditions:

$$K_1 = K_R \qquad (5.3)$$

$$\frac{dK_1}{da} = \frac{dK_R}{da} \qquad (5.4)$$

Thus, at point I, the K_R curve and the K_1 curve have a common
tangent. The point I is located graphically by superimposing
a set of K_1 curves, for different loads, on K_R curve and find-
ing the point of tangency as shown in Fig. 5.1. The crack
growth resistance corresponding to point I is called the critical
crack growth resistance and is a measure of fracture
toughness of the material.

5.3 APPLICATION OF R CURVE APPROACH

The crack growth resistance (R curve) approach
[38 , 39] has been very widely used to analyse fracture test
results on composite materials [40 - 53] . Analysis using
this approach requires measurement of instantaneous crack
length with increasing load in a fracture test. In case of
homogeneous materials the crack is visible and well defined
and can be easily measured at any instant. However, frac-
ture process in composite materials does not proceed by a
simple enlargement of the original crack. Damage progresses
by formation of a large number of microcracks due to debond-
ing, matrix cracking and fibre breaks. An instantaneous
crack length is difficult to define or measure. Consequently,
a procedure for estimating instantaneous crack length must be
adopted. A procedure involving matching of compliance of a
damaged specimen to that of a fresh specimen, generally
referred to as the compliance matching procedure [41] has been
extensively used by researchers to transform the test data
(e.g., the crack mouth opening displacement) into estimated
crack length [41 - 53]. The procedure is explained in the
following paragraphs.

5.4 CONCEPT OF COMPLIANCE MATCHING PROCEDURE

Typical load - COD curves for single edge notched
specimens in tension are shown in Fig. 5.2 for different
initial crack lengths. Initial compliance (based on crack
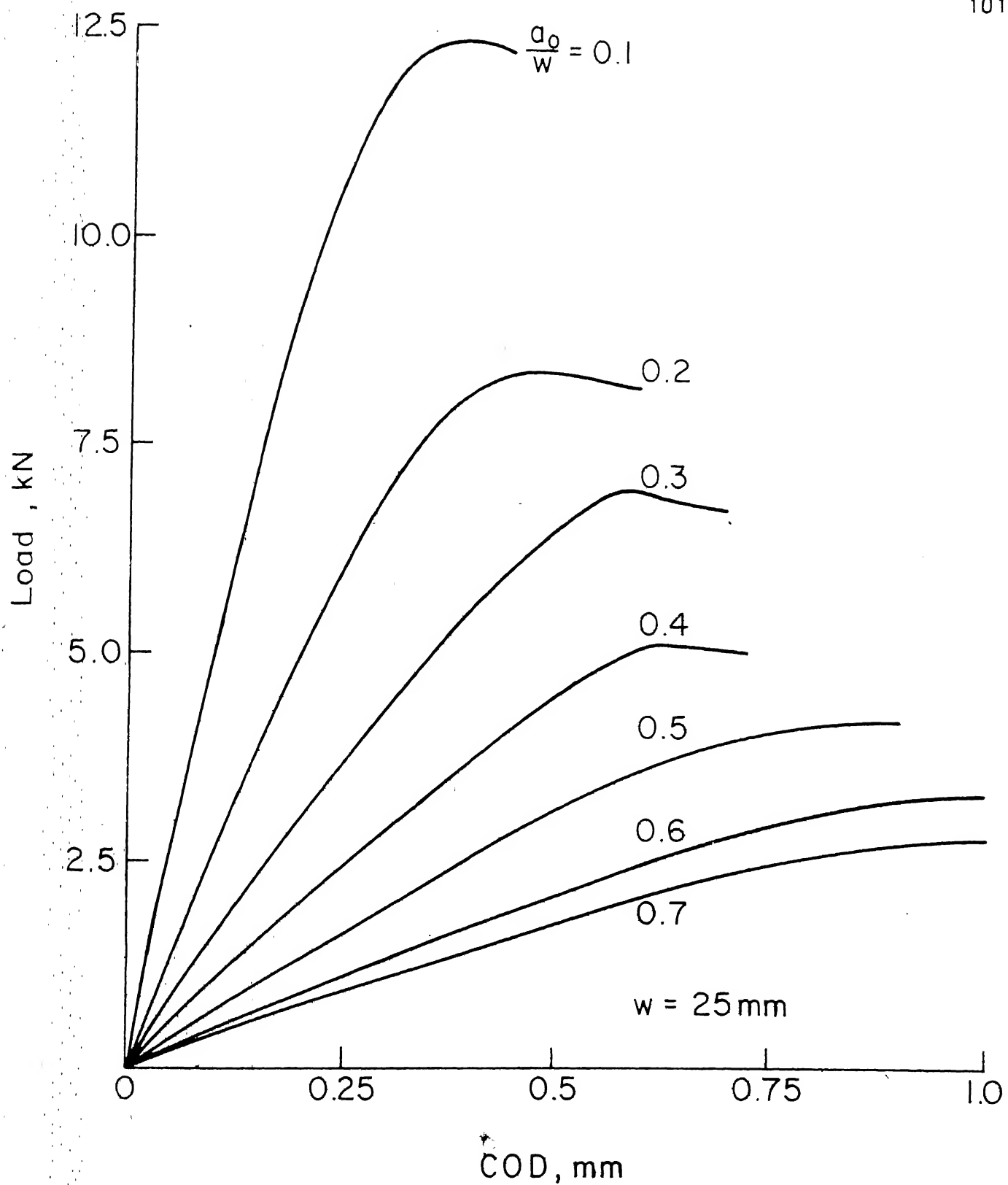
Fig. 5.2   Load - COD curves for 25mm wide specimens with different initial crack lengths.

mouth opening displacement) of specimens changes with length
of initial machined crack. Compliance also changes with
load since the load - COD curves are nonlinear. The damage
to the specimen during loading has the effect of enlargement
of initial crack in changing compliance. The compliance
matching procedure is based on the assumption that the com-
pliance may be taken as a measure of crack length and, hence,
effective crack length in a damaged specimen may be estimated
by matching its compliance with the compliance of a fresh
specimen having machined notch. In the compliance matching
procedure, initial compliance (obtained from the curves in
Fig. 5.2) is first plotted against crack length. This plot
(Fig. 5.3) is referred to as the compliance curve or the
crack length estimation curve. To estimate instantaneous
crack lengths at points P_1, P_2 and P_3 on load - COD curve,
compliances, C_1, C_2 and C_3 of the lines joining P_1, P_2 and
P_3 to the origin are obtained (Fig. 5.4). The crack lengths
a_{e_1}, a_{e_2} and a_{e_3} at points P_1, P_2 and P_3 are then estimated
from the crack length estimation curve (Fig. 5.3) corres-
ponding to compliances C_1, C_2 and C_3 respectively.

The method of estimating crack length through com-
pliance matching procedure assumes that the damaged specimen
behaves like an undamaged specimen with a machined crack of
length equal to the estimated crack length. Therefore the
validity of analysis using R curve approach for composite
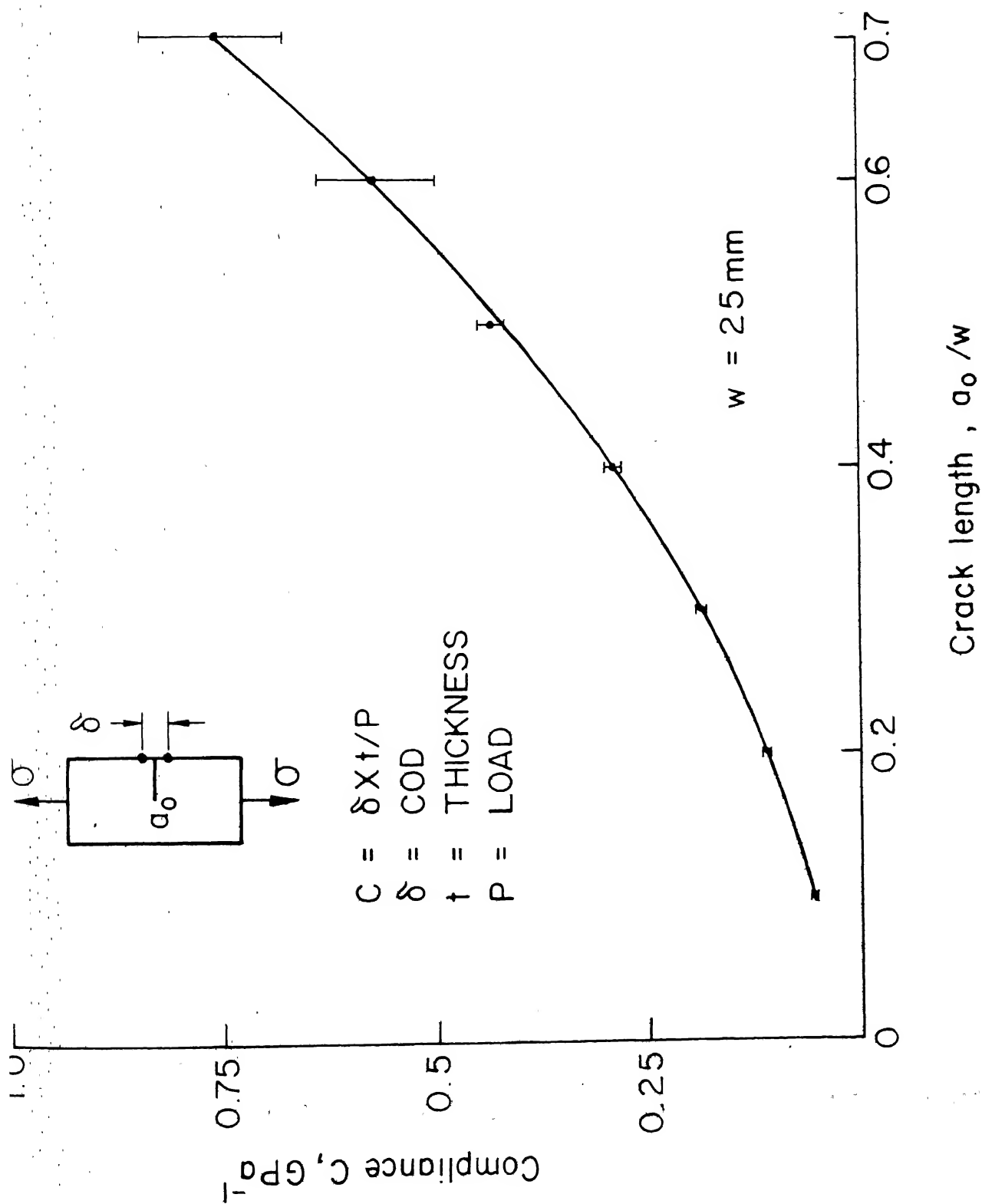
Fig. 5.3   Crack length estimation curve for 25mm wide specimens.
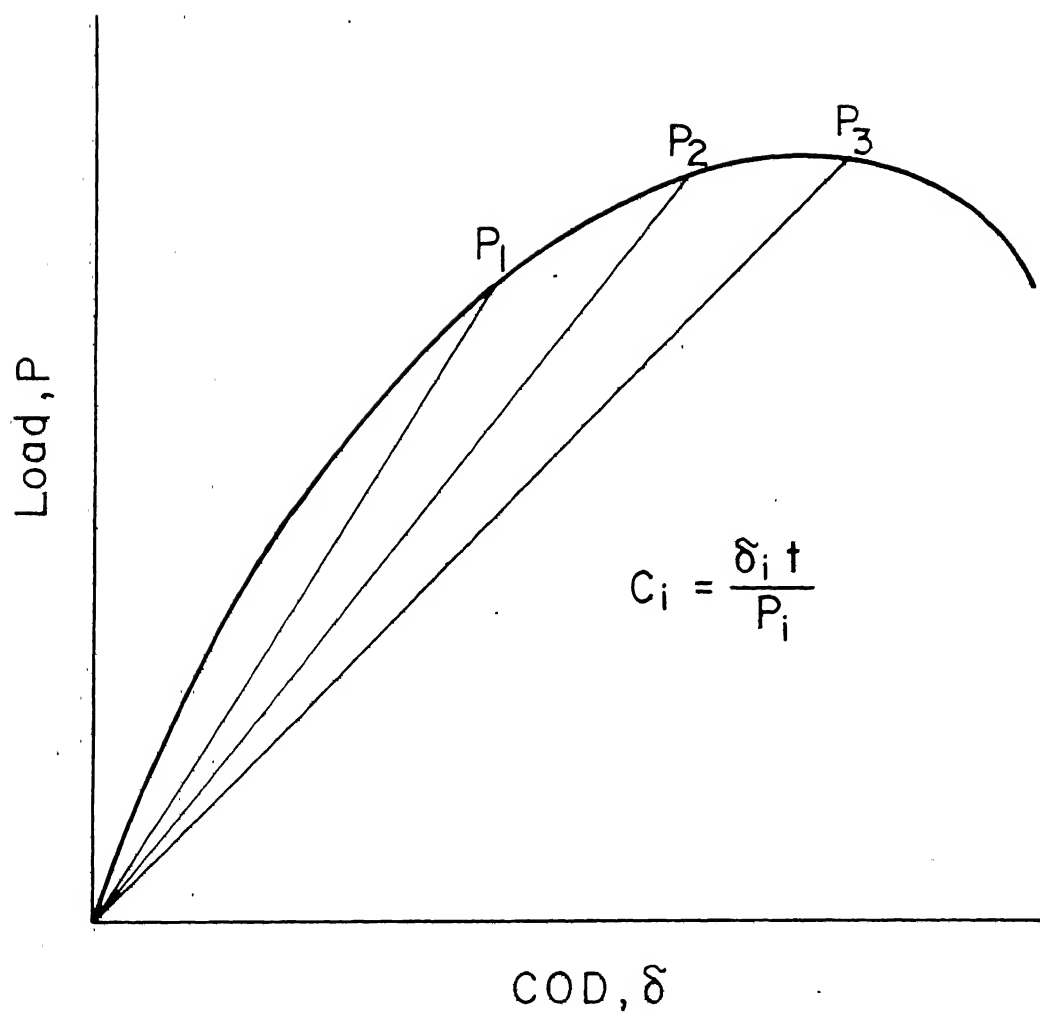
Fig.5.4 Method of evaluting instantaneous compliance.

materials largely depends upon the validity of this compliance
matching procedure which must be carefully examined. Although
the method has been extensively used, its appropriateness does
not appear to have been made systematically. In the present
investigations, the validity of the compliance matching pro-
cedure has been examined.

5.5 VALIDITY OF CRACK LENGTH ESTIMATION PROCEDURE

The method of estimating crack length through com-
pliance matching, as already explained, assumes that the
damaged specimen behaves like an undamaged specimen with a
machined crack of length equal to estimated crack length.
This underlying assumption is examined here through studying
the behaviour of notched specimens in which additional damage
had been produced by loading them in tension and comparing
it with the initial behaviour of fresh specimens as shown
in Figs. 5.2 and 5.3 already referred in the preceding
section. These results are obtained by conducting fracture
toughness test on atleast 6 identical fresh specimens at
each crack length.

Fracture behaviour of damaged specimens was studied
in two ways. First, 12 single edge notched specimens (3
specimens each at 4 different initial crack lengths namely,
5, 10, 12.5 and 15 mm) were loaded in tension to produce
damage ahead of the machined notch. The maximum load on the

specimens before unloading them was varied to different
fractions of their expected fracture loads so that the extent
of damage to the specimens was different in each case. These
damaged specimens were then reloaded to fracture and their
behaviour studied. The second approach involved producing
damage, in the same manner to wider specimens. After unload-
ing, the specimens were reduced in width by cutting off the
notched edge so that a major part of the machined crack was
removed. These reduced width specimens with machined crack
and additional damage were also loaded to fracture and their
behaviour studied. Results of the investigations using both
the approaches are described as follows.

5.5.1 Behaviour of Damaged Specimens Without Changing Width

Typical behaviour of a fresh notched specimen is
illustrated in Fig. 5.5 through loading and unloading paths
for a 25 mm wide specimen having a 5 mm long initial crack.
The specimen was unloaded after subjecting it to about 95 %
of the expected fracture load. Typical behaviour of a damaged
specimen is also illustrated in Fig. 5.5 by superimposing
on it the reloading path of the same specimen. The loading
path of a fresh specimen is linear in the beginning and pro-
gressively deviates from linearity due to increasing damage
to the material. Reloading path of the damaged specimen is
also linear in the beginning but shows a sudden change in
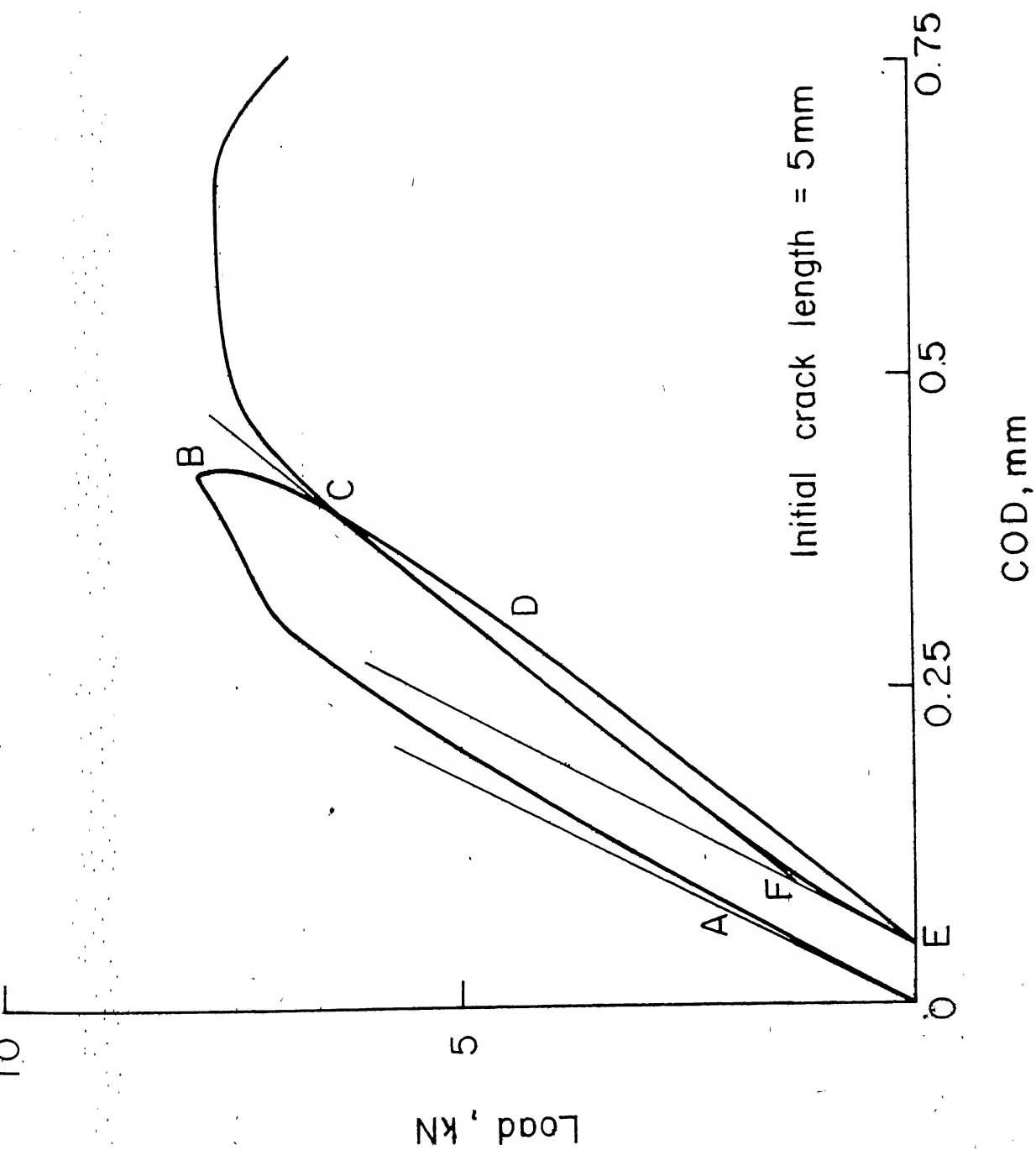
Fig. 5.5 Typical loading, unloading and reloading path for 25mm wide specimens.

Initial crack length = 5mm

COD, mm

Load, kN

slope at a relatively small load. The magnitude of change in slope (sharpness of the knee, F) depends upon the maximum load on the specimen prior to unloading. When the maximum load is small, change in slope is negligible or the knee almost disappears.

To compare the behaviour of damaged and fresh specimens quantitatively, initial compliance of a fresh specimen (C_o), its compliance at maximum load before unloading (C_d), initial compliance of the damaged specimen during reloading (C_{or}) and its compliance corresponding to the straight line portion of load - COD curve beyond the knee (C_{dr}) have been obtained for all 12 specimens. Corresponding to these four compliances, crack lengths have been estimated from the crack length estimation curve (Fig. 5.3) as a_o, a_d, a_{or} and a_{dr} respectively. The estimated crack lengths a_d and a_{or} normalized with respect to initial machined crack, a_o, are plotted (Fig. 5.6) against estimated crack extension, $(a_d - a_o) / a_o$. The two crack lengths are clearly different and the difference between them increases with crack extension. The estimated initial crack length during reloading is independent of the crack extension and is equal to the initial machined crack in the fresh specimen. Thus, the initial behaviour of a damaged specimen does not reflect the extent of damage to the specimen during initial loading. On the other hand the initial behaviour during
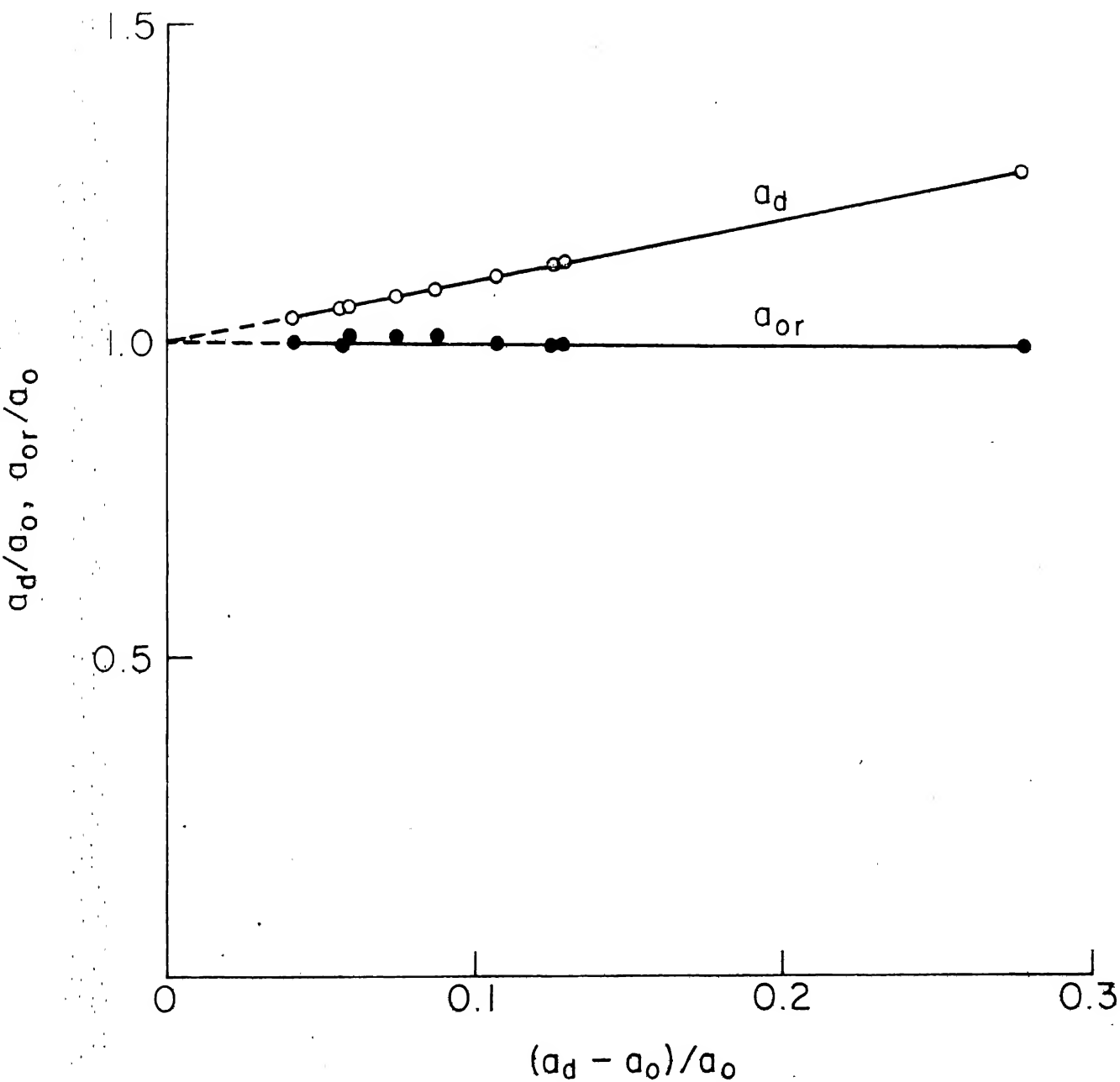
Fig. 5.6 Normalised crack lengths (a_d/a_o and a_{or}/a_o) in fresh and damaged specimens against crack extension.

reloading and the initial loading are the same irrespective of the extent of damage to the specimen. This will be further explained subsequently.

The estimated crack lengths a_d and a_{dr} are plotted in Fig. 5.7. The two crack lengths are overlapping in the range investigated here. This indicates that the extent of damage to the specimen during initial loading is truly reflected during reloading only after the knee (on the load - COD curve) which appears very early. It demonstrates that no additional damage occurs ·during unloading and reloading. The presence of a sharp knee in the reloading path does not signify occurrence of any sudden damage to the material. At small loads prior damage to the specimen does not influence COD. The load - COD curve beyond the knee is, therefore, representative of the damaged specimen.

Fracture load of the damaged specimens, P_f, normalised with respect to the fracture load expected, P_e, for a fresh specimen having the same initial machined crack length, is plotted in Figs. 5.8 and 5.9 against initial crack length and the estimated crack extension prior to unloading respectively. Both the figures show that the fracture load of a damaged specimen is same as the fracture load of a fresh specimen. This observation is independent of initial crack length and the extent of damage to the specimen before unloading. That is, unloading a specimen at any stage of loading does not affect the fracture load.
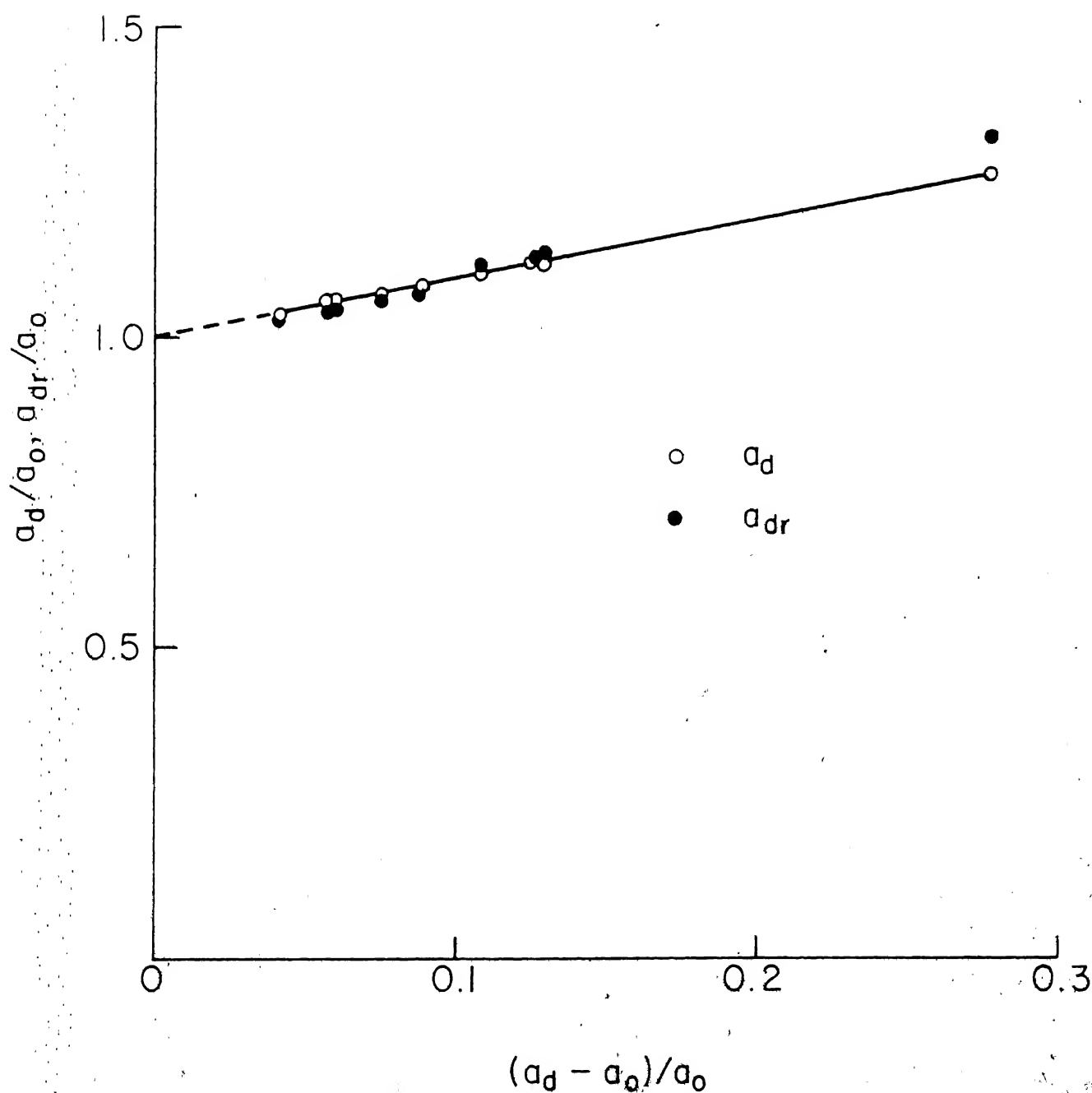
Fig.5.7 Normalised crack lengths (a_d / a_o and a_{dr} / a_o) in fresh
and damaged specimens against crack extension.
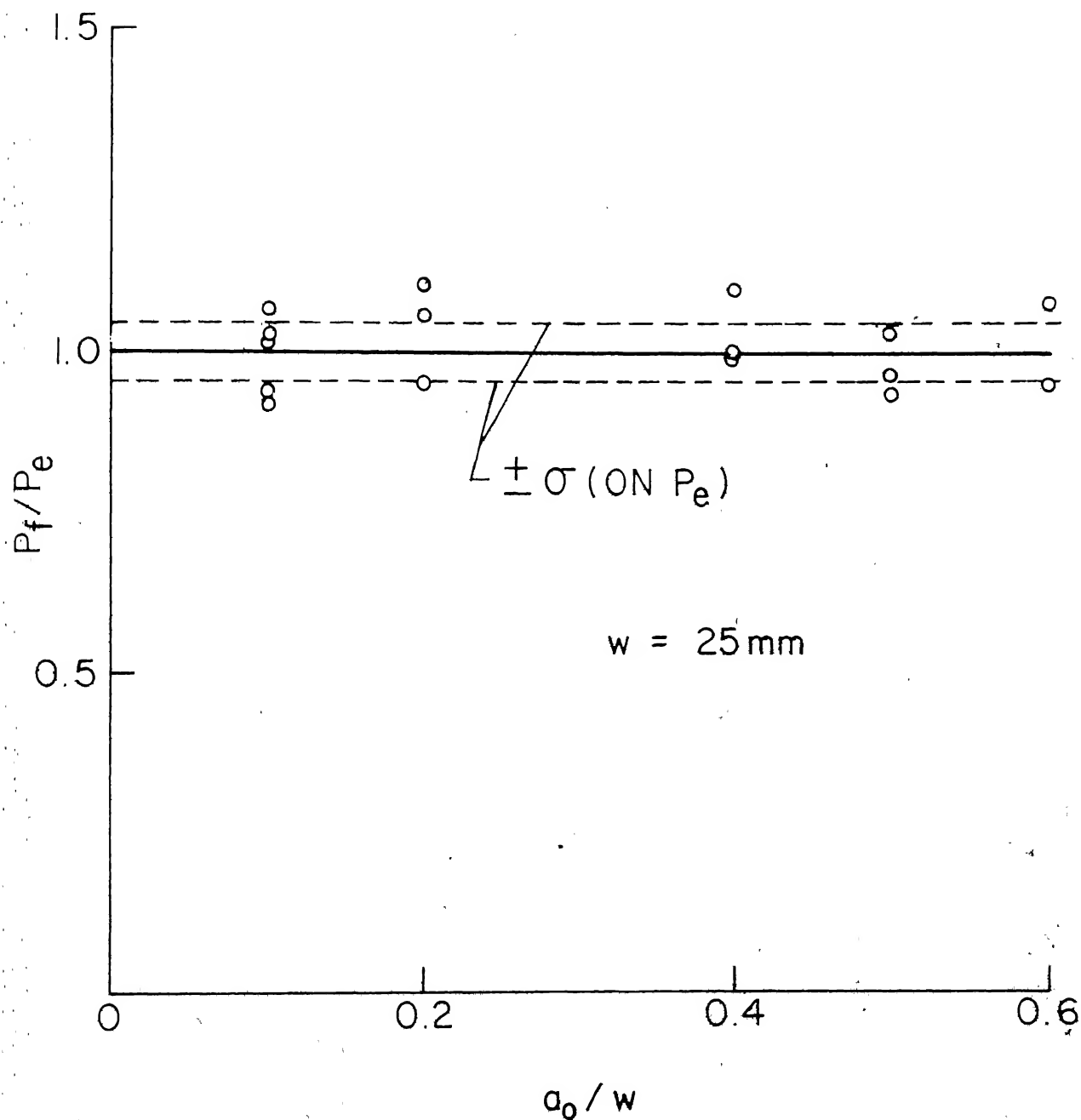
Fig. 5.8 Ratio of fracture loads for damaged and fresh specimens against crack length.
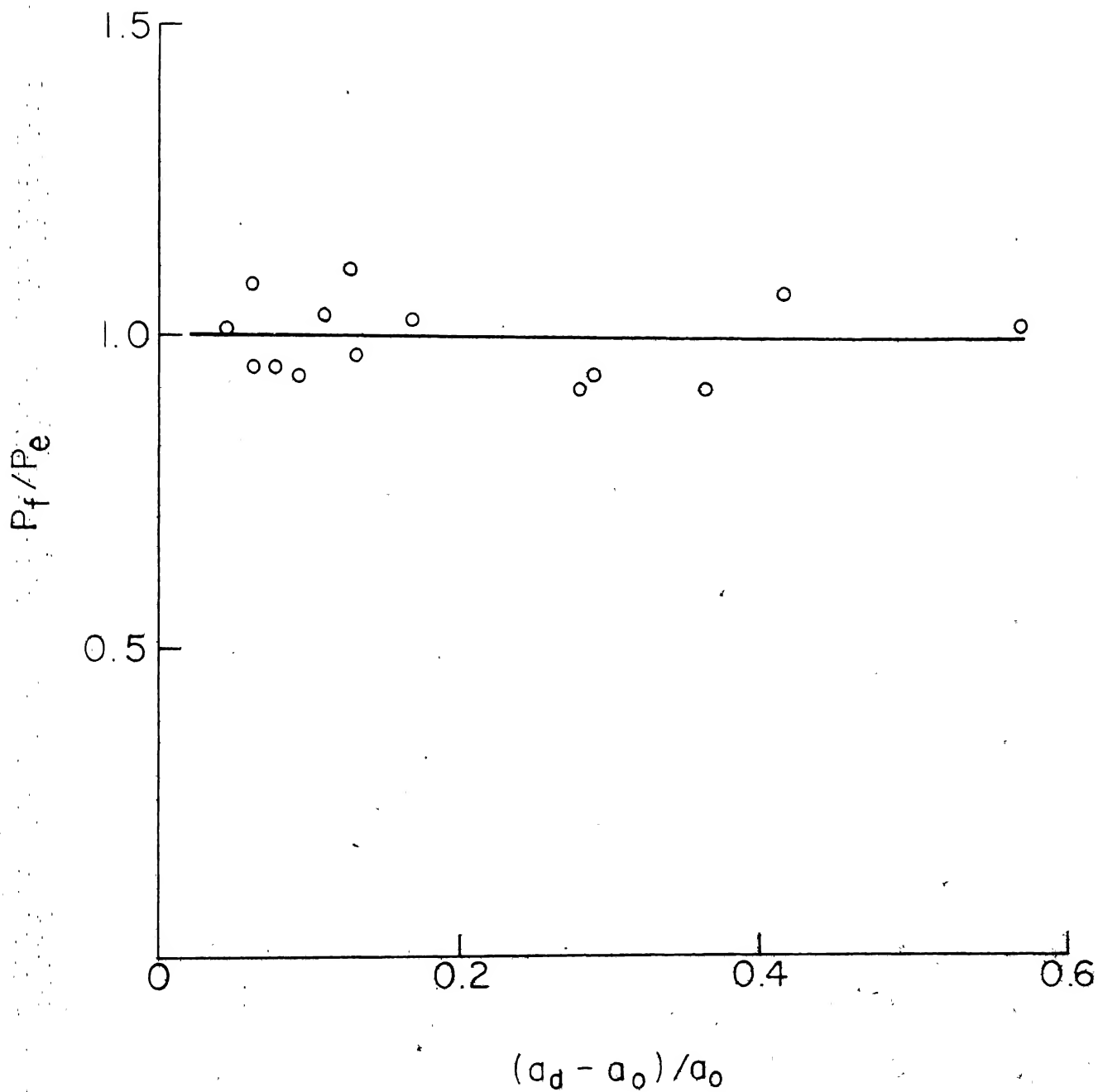
Fig.5.9 Ratio of fracture loads for damaged and fresh specimens against crack extension.

The above observations clearly show that the load - COD behaviour of a damaged specimen is different from that of a fresh specimen having a machined crack of length equal to the estimated length of crack in the damaged specimen. Further, the fracture loads of two such specimens are also different. In fact, fracture load depends only on the length of initial machined crack and is not influenced by additional damage that may be caused to the specimen during loading or unloading. However, it has been demonstrated that the load - COD curve of a damaged specimen can be used to accurately estimate the extent of damage to the specimen caused by earlier loading. Therefore, the use of compliance matching procedure to estimate the instantaneous crack length appears to be justified. This proposition is further examined in the next section using a different approach.

5.5.2 Behaviour of Damaged Specimens after reducing Width

In this approach 10 specimens, 30 mm wide having 7.5 mm long initial machined crack were loaded in tension to produce damage ahead of the crack. The maximum load on the specimen before unloading them was varied to different fractions of the expected fracture load so that the extent of damage was different in each case. In some cases the commencement of unloading was at a load more than the average fracture load or it was past the peak load. This was done to

obtain maximum possible damage to the specimen. This is of particular interest since applicability of the compliance matching procedure in this range may be questionable. At smaller loads the method is expected to yield better results. These 30 mm wide damaged specimens were reduced in width to 25 mm by cutting off a 5 mm wide strip on the notched edge (Fig. 5.10) so that the 25 mm wide reduced width damaged specimens have a machined crack 2.5 mm long and additional damage due to loading. These specimens were loaded in tension to fracture and their behaviour examined. In this approach it is necessary to obtain crack length estimation curves for 30 mm wide as well as 25 mm wide specimens. The crack length estimation curve for 25 mm wide specimens as already shown in Fig. 5.3 was obtained by testing about 40 specimens. For 30 mm wide specimens similar load - COD curves were also obtained by testing additional 42 specimens (Fig. 5.11) with different crack lengths. Crack length estimation curve for 30 mm wide specimens is shown in Fig. 5.12.

It may be pointed out that the length of machined crack in damaged specimens was always 7.5 mm. Other crack lengths showed some practical difficulties in preliminary tests on specimens with different crack lengths. When the initial crack length was 5 mm, the estimated crack length in a reduced width damaged specimen was very small, usually
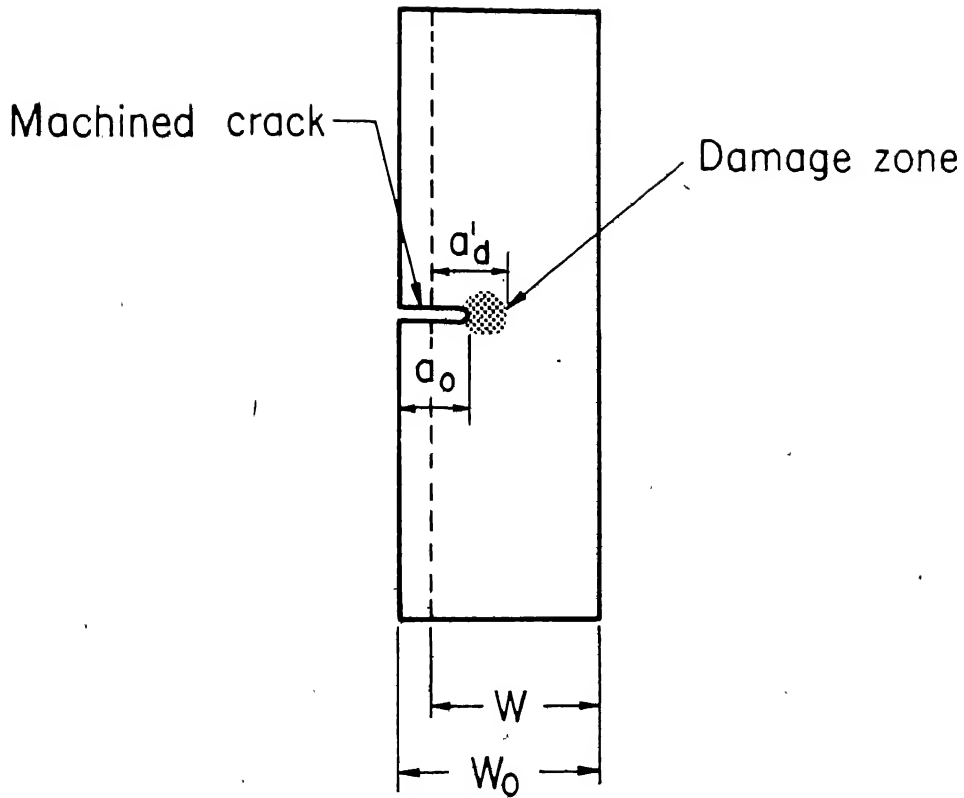
Fig. 5.10   Two stage fracture toughness testing specimen.
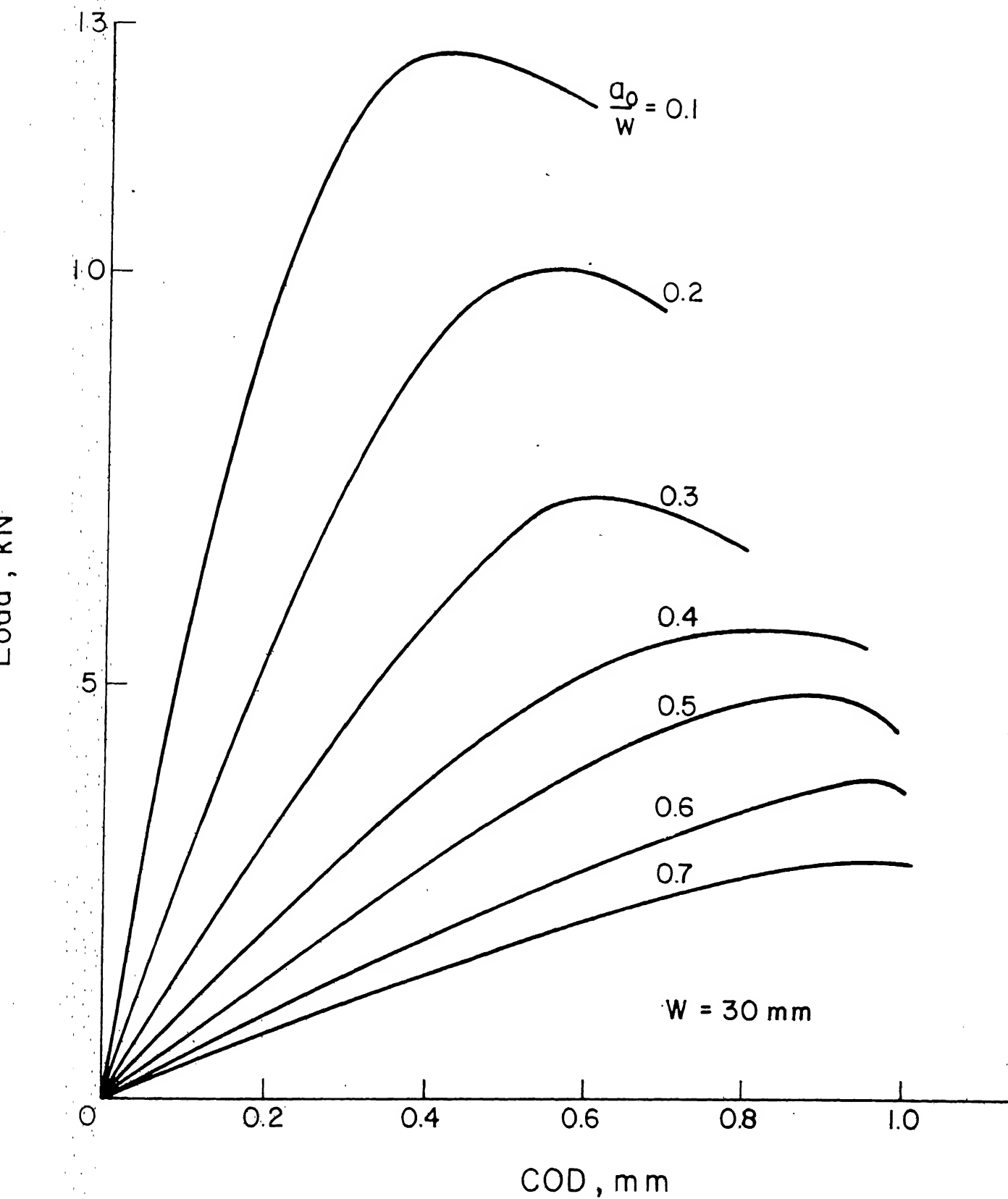
Fig. 5.11   Load–COD curves for 30 mm wide specimens with different initial crack lengths.
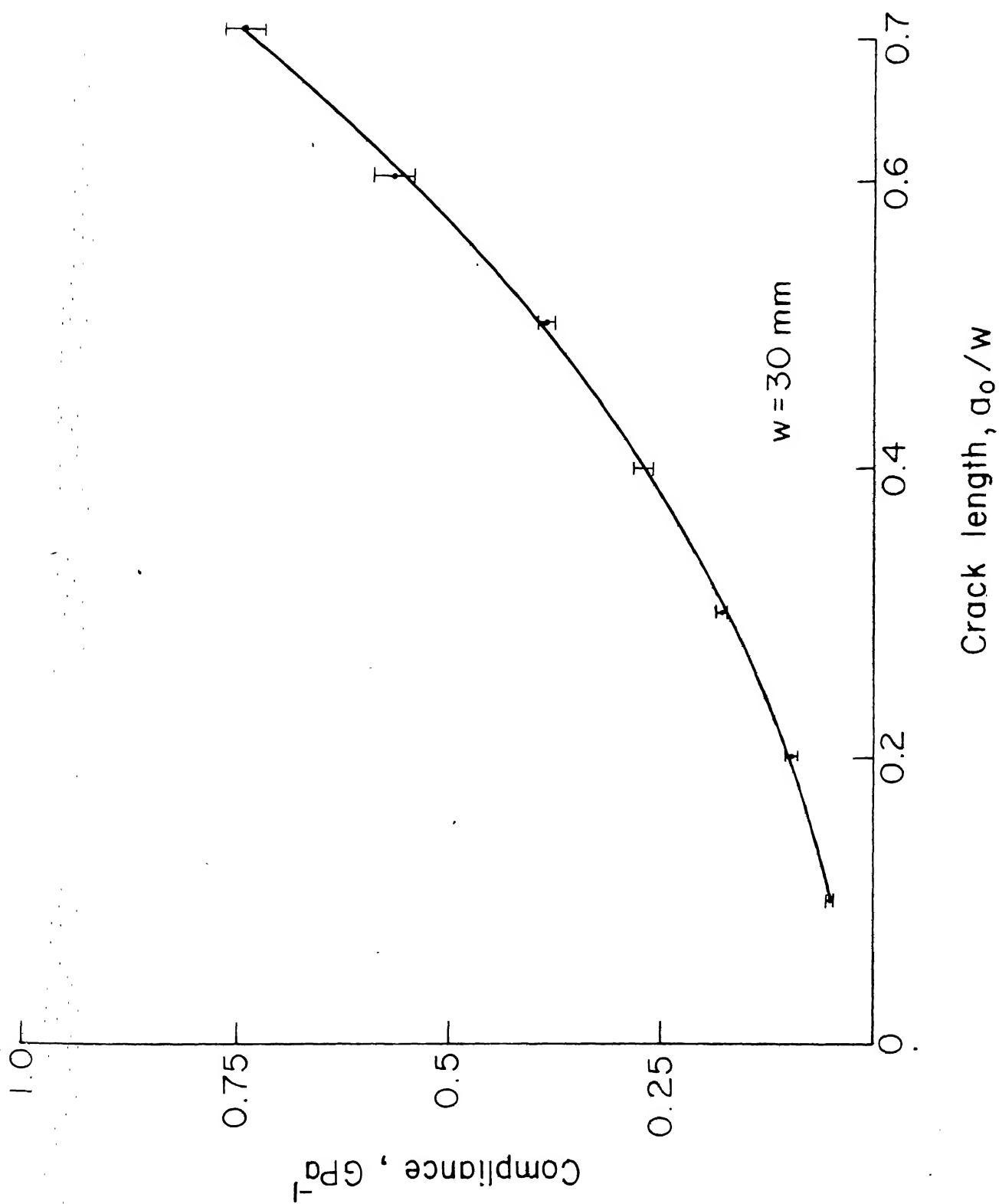
Fig.5.12 Crack length estimation curve for 30mm wide specimens.

less than 2.5 mm and, therefore, their fracture behaviour could not be compared with that of a fresh specimen which is available for initial crack lengths of 2.5 mm or more. On the other hand when the initial crack length was 10 mm or more, the fracture behaviour is dominated by the machined crack and is similar to that obtained in the first approach. Therefore, the initial crack length of 7.5 mm appeared ideally suited. The width of wider specimens was not changed because it would have meant testing additional 40 specimens for each width to obtain crack length estimation curve. In any case the results presented in this section have been obtained from over 100 specimens.

The load - COD curve of a reduced width specimen is shown in Fig. 5.13. It is quite similar to the reloading curve shown in Fig. 5.5. As in the earlier case, a major part of the curve can be approximated by two straight lines. The first straight line with a larger slope describes the initial loading. The slope of second straight line (after the knee) is smaller and covers a major portion of the load - COD curve. The crack lengths estimated by compliance matching procedure corresponding to the two straight lines are denoted by a_{or} and a_{dr} respectively. The crack length estimated at the maximum load during loading of 30 mm wide fresh specimen is denoted by a_d. The estimated crack length in the reduced width damaged specimen is then $a_d - 5$ which
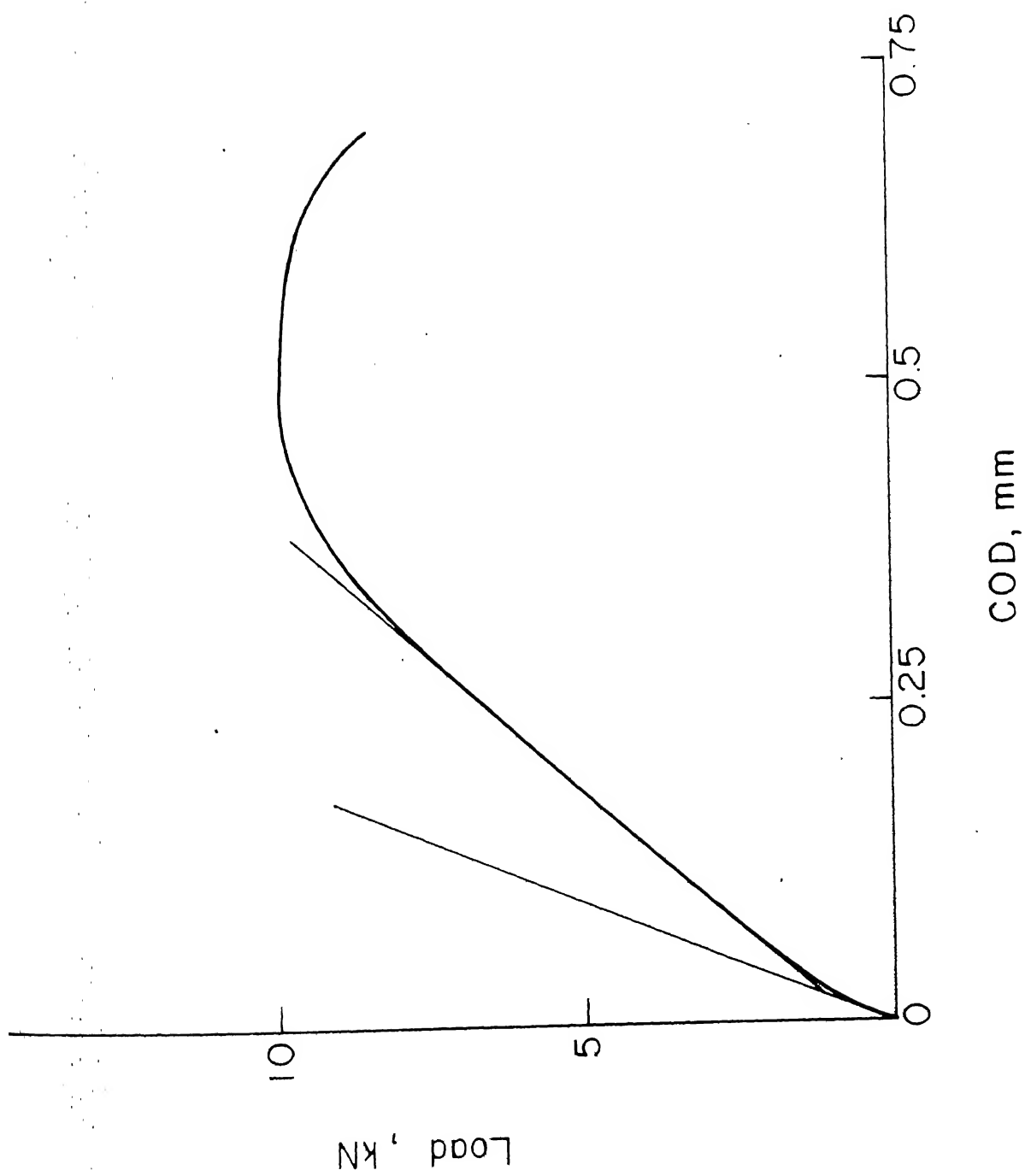
Fig. 5.13   Typical Load-COD behaviour of a reduced width damaged specimen.

120

is denoted by $a_d^!$. The crack lengths a_{or} and a_{dr} normalized with respect to $a_d^!$ are plotted against estimated crack extension in Fig. 5.14. It is observed that the ratio $a_{dr}/a_d^!$ is independent of the extent of damage and is equal to 1 whereas the ratio $a_{or}/a_d^!$ decreases with the increase of damage. These observations indicate that the crack length corresponding to the second straight line, a_{dr} (and not the first) in Fig. 5.13 truly represents the extent of damage. On the other hand a_{or} does not depend upon the extent of damage and its value is 2.5 mm ($\pm 5\%$).

The fracture load of reduced width specimens has also been found to be independent of the extent of damage to the specimen during initial loading. Its average value agrees very well with the average fracture load of 25 mm wide fresh specimens having 2.5 mm long machined crack.

The fracture toughness of all the reduced width specimens was also obtained using R curve method. An average fracture toughness was 25.91 MPa$\sqrt{}$ m (Standard deviation 0.61 MPa$\sqrt{}$ m) which compares well with 25.25 MPa $\sqrt{}$m (Standard deviation 1.25 MPa$\sqrt{}$ m) of 25 and 30 mm wide fresh specimens having 2.5 and 3 mm long machined cracks respectively.

The above observations regarding crack length estimation and fracture load are consistent with the earlier conclusions drawn in the first approach.
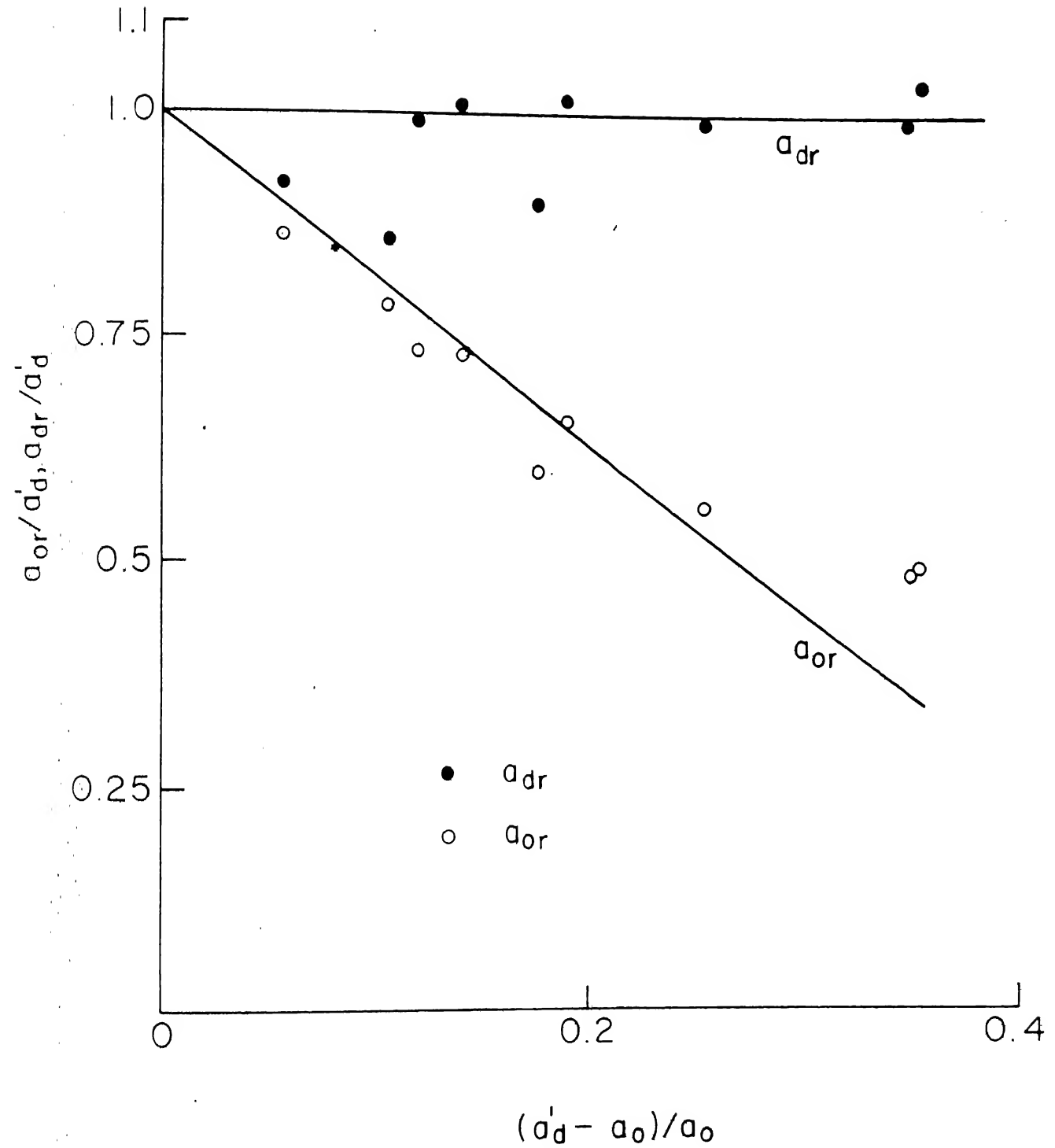
Fig 5.14 Normalised estimated crack lengths in reduced
width damaged specimens.

5.5.3 Discussion

In fracture toughness tests on composite materials, instantaneous crack length is difficult to define or measure. The crack mouth opening displacement is therefore, measured and transformed into estimated crack length through the compliance matching procedure. Validity of this compliance matching procedure has been examined for short fibre composites experimentally by studying the behaviour of damaged specimens in two ways. In both cases the single edge notched specimens were loaded in tension to produce damage ahead of the machined notch. In one case these specimens were reloaded to fracture while in the other case they were reduced in width before reloading so that a major part of the machined crack is removed. Comparison of the behaviour of damaged and fresh specimens shows that the load - COD curve and fracture load of a damaged specimen are different from that of a fresh specimen having a machined crack of length equal to the estimated crack length in the damaged specimen. However, it has been clearly established that the secondary compliance of the damaged specimen can be used to accurately estimate the extent of damage to the specimen by earlier loading. Therefore, the use of the compliance matching procedure appears justified for estimating instantaneous crack length in short fibre composites.

5.6 PREDICTION OF INSTABILITY

The crack length estimation procedure for short fibre composites has been established in the preceding section. With this the crack length can be obtained corresponding to any load in a load - COD curve and therefore, a load - COD curve can be transformed to an R curve. Fracture toughness of the material can be obtained by locating the point of instability on the R curve using the procedure explained in section 5.2. The transformation process is tedious and time consuming. It would, therefore, be of immense help if the point of instability could be directly located on load - COD curve, thus, eliminating the necessity of transforming the entire load - COD curve. This may be expected to increase the accuracy in obtaining the fracture toughness. With this view, the point of instability is mathematically established on the load - COD curve in the following section.

5.6.1 Derivation of Instability Point

The load - COD behaviour of the material is represented qualitatively in Fig. 5.15. The load, P, is a single valued function of COD, δ, and the relationship may be represented by

$$P = P(\delta) \qquad (5.5)$$

The instantaneous crack length at any point on the load - COD

curve is obtained by compliance matching as described earlier. The crack length estimation curve shown in Fig. 5.3 is used for this purpose. The crack length, a, may be written as an explicit function of compliance, c as

$$a = g (c) \tag{5.6}$$

For a given thickness, the compliance may be replaced by ratio δ/P and Eq. 5.6 is rewritten as

$$a = f (\delta/P) \tag{5.7}$$

Equation 5.6 may be represented graphically as shown in Fig. 5.16.

The crack extension force and crack growth resistance are given by

$$K_1 = Y \frac{P}{tw} \sqrt{a} \tag{5.8}$$

$$K_R = Y \frac{P}{tw} \sqrt{a} \tag{5.9}$$

The load - COD curve is transformed to crack growth resistance curve using Eqs. 5.7 and 5.9. The instability condition as stated in section 5.2 are

$$K_1 = K_R \tag{5.10}$$

$$\frac{dK_1}{da} = \frac{dK_R}{da} \tag{5.11}$$

In order to satisfy Eq. 5.11, Eqs. 5.8 and 5.9 are differentiated with respect to crack length, a, as follows
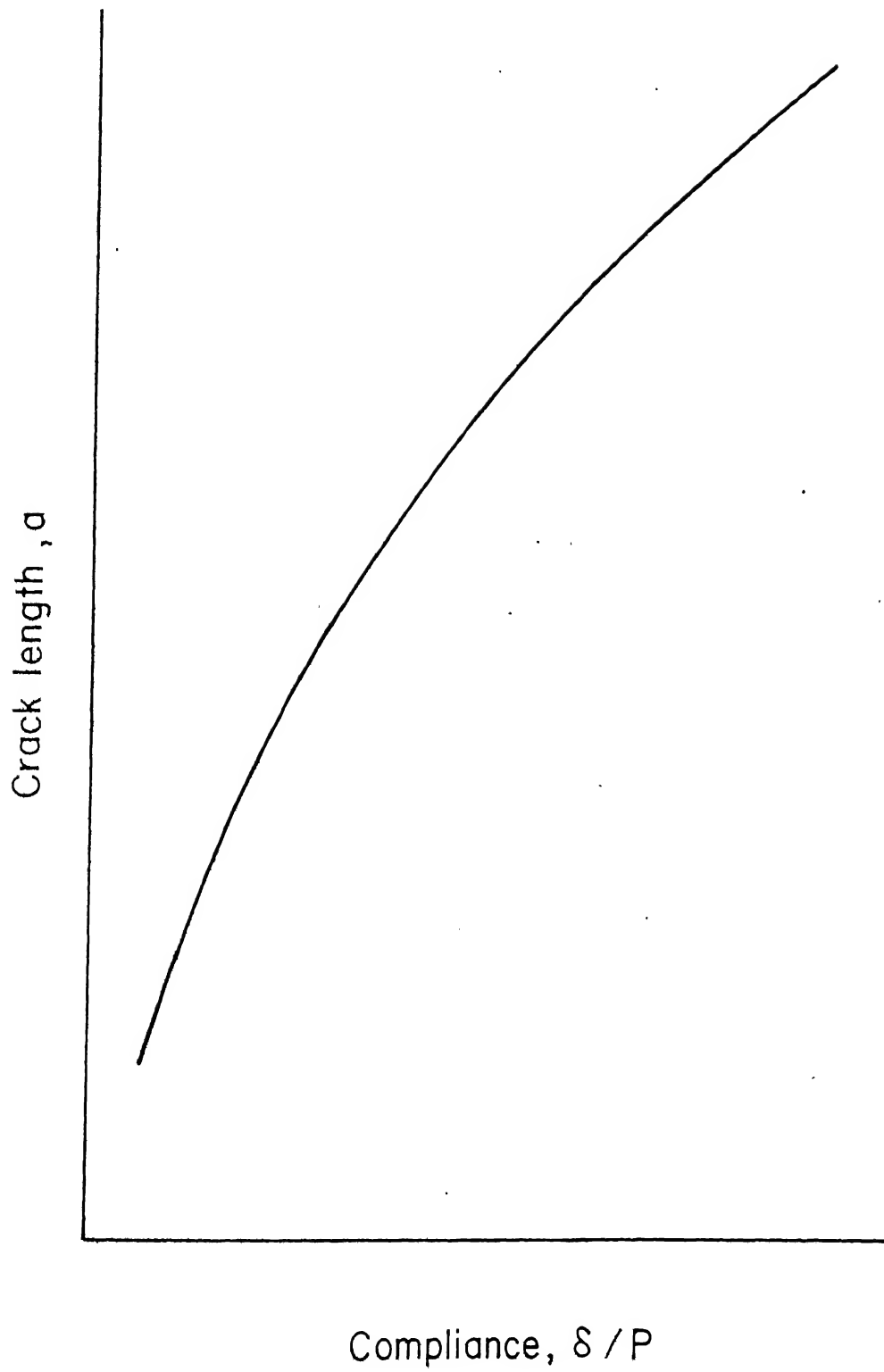
Fig. 5.16 Crack length versus compliance.

$$\frac{dK_1}{da} = \frac{P}{tw}\sqrt{a}\ \frac{dY}{da} + Y\frac{P}{tw}\ \frac{1}{2\sqrt{a}} \tag{5.12}$$

(P is constant on K_1 curve)

$$\frac{dK_R}{da} = \frac{P}{tw}\sqrt{a}\ \frac{dY}{da} + Y\frac{P}{tw}\ \frac{1}{2\sqrt{a}} + Y\frac{\sqrt{a}}{tw}\frac{dP}{da} \tag{5.13}$$

Comparing Eqs. 5.12 and 5.13, instability criterion (Eq. 5.11) reduces to

$$Y\frac{\sqrt{a}}{tw}\ \frac{dP}{da} = 0 \tag{5.14}$$

Since Y, a, t and W are nonzero quantities, Eq. 5.14 becomes

$$\frac{dP}{da} = 0 \tag{5.15}$$

This equation can be evaluated as follows:

$$\frac{dP}{da} = \frac{dP/d\delta}{da/d\delta} = 0 \tag{5.16}$$

Differentiation of Eq. 5.7 yields

$$\frac{da}{d\delta} = f'\ \frac{P - P'\delta}{P^2} \tag{5.17}$$

Substitution of Eq. 5.17 in Eq. 5.16 yields

$$\frac{dP}{da} = \frac{P'\ P^2}{f'\ [P - P'\delta]} = 0 \tag{5.18}$$

In Eq. 5.18, P^2 is definite. The nature of function f (δ/P) is shown in Fig. 5.16 and clearly f' is finite. The term P - P'δ is illustrated in Fig. 5.15 and is also

finite. Therefore, the instability condition reduces to

$$\frac{dP}{d\delta} = 0 \qquad (5.19)$$

That is, the instability point on the load - COD curve has
a horizontal tangent. In other words the peak load repre-
sents instability.

This is a significant result as it eliminates the
necessity of transforming entire load - COD curve to R curve
through a tedius and time consuming process. Now, the
critical crack growth resistance or the fracture toughness
can be obtained by knowing the peak load and estimating the
corresponding crack length. It had already been realized
intuitively that the crack growth resistance at peak load
and the critical crack growth resistance are quite close.

Gaggar and Broutman conducted [44] load controlled
fracture tests and observed that at maximum load, the crack
grows at an accelerated rate and proposed that the crack
growth resistance corresponding to the beginning of accelera-
ted crack growth should be considered critical. Garg [52]
has calculated the crack growth resistance at different
points including that at the maximum load and presented all
of them. Some investigators have used maximum load and
initial crack length [46, 47]. The present results con-
clusively establish a simple method to obtain the critical
crack growth resistance.

5.6.2 Locating Instability Point
On Load - COD Curve

It has been established in the previous section that the fracture toughness can be obtained directly by knowing the peak load and the corresponding COD. Therefore, the accuracy of fracture toughness directly depends upon the accuracy with which the COD corresponding to peak load can be obtained from the load - COD curve. The two types of fracture tests generally performed, the load controlled and the displacement controlled tests, are analyzed here in this light.

Two typical load - COD curves obtained in load controlled and displacement controlled tests are shown in Figs. 5.17 and 5.18. In a load controlled test the machine tries to maintain a constant rate of loading. This causes a sudden increase in COD at nearly constant load close to instability producing a plateau on the load - COD curve (Fig. 5.17). In this case it becomes difficult to accurately determine the COD corresponding to the peak load. The experience shows that transforming such a load - COD curve to an R curve also does not help since locating instability point accurately on the R curve is equally difficult. In a displacement controlled test the load can increase or decrease while the cross head moves with a constant speed. In this case, the COD corresponding to the peak load can be

$a_0 = 5\,\text{mm}$
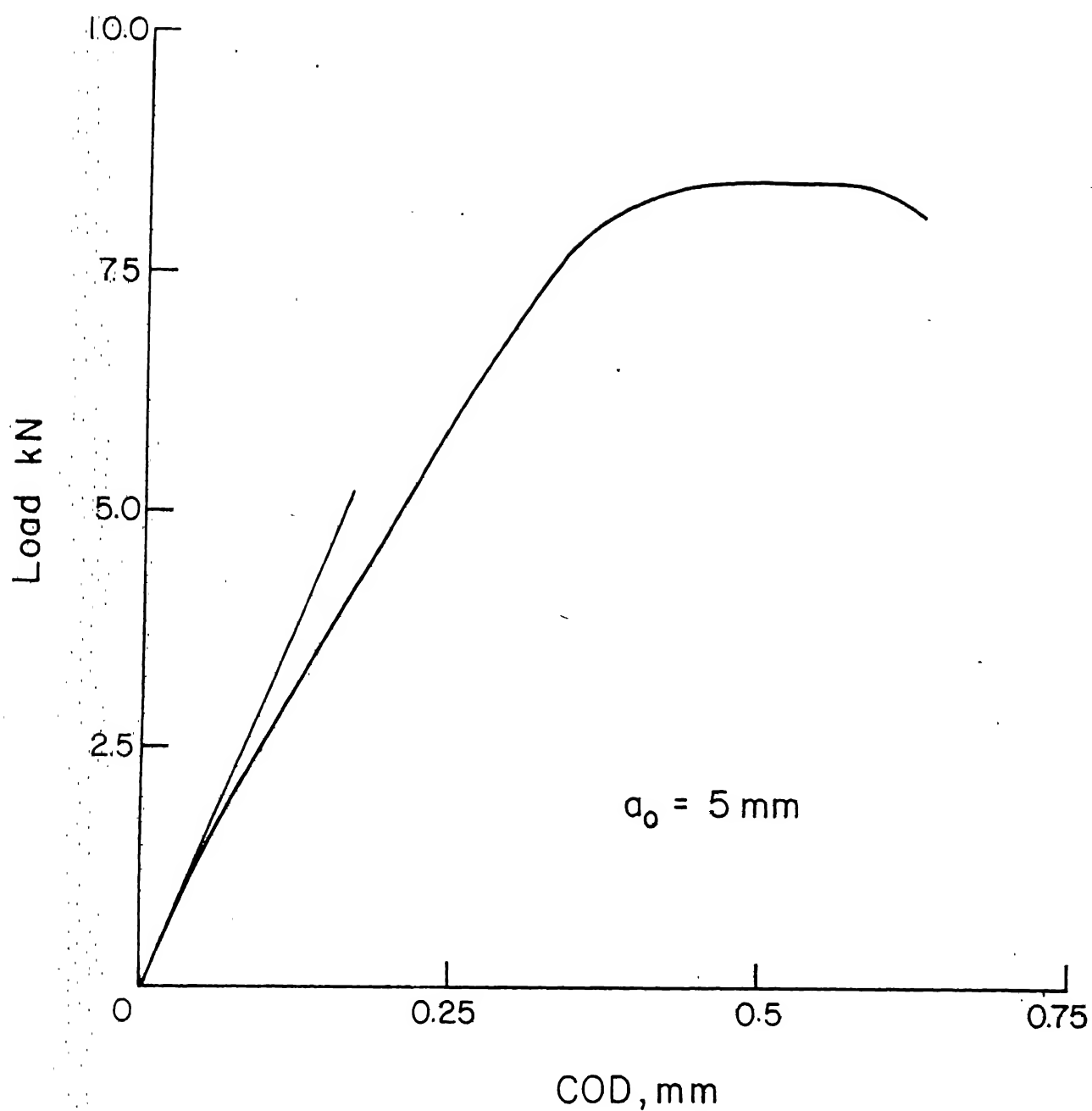
Fig. 5.17   Load – COD curve under load controlled test.
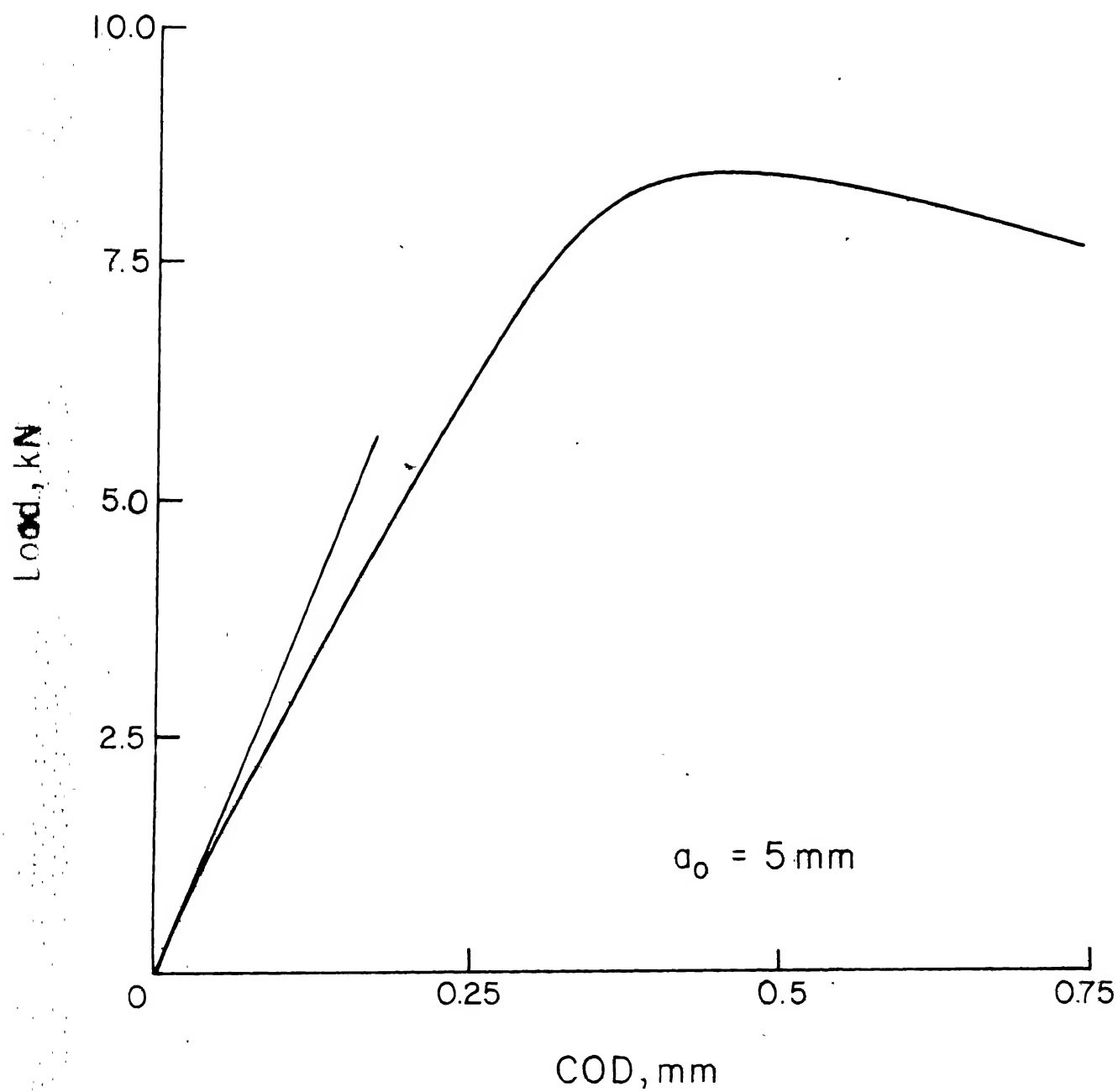
Fig. 5.18   Load – COD curve under displacement controlled test.

identified more accurately (Fig. 5.18). Obviously, therefore, the displacement controlled tests should be preferred to evaluate fracture toughness. In the present investigations, the displacement controlled tests were conducted all along.

5.7 FRACTURE TOUGHNESS RESULTS

Fracture toughness tests were performed on 25 mm and 30 mm wide single edge notched specimens. The ratios of initial crack length to specimen width (a_0/w) were 0.1, 0.2, 0.3, 0.4, 0.5, 0.6 and 0.7. At each crack length at least 4 specimens were tested. The load - COD and the crack length estimation curves have already been referred to and shown in Fig. 5.2, 5.3, 5.11 and 5.12. The critical crack growth resistance, $K_{R(Ins)}$, was calculated from the peak load and estimated crack length at peak load as has been explained in the previous section. It may be mentioned that for several specimens the complete load - COD curves were transformed to the R curves and fracture toughness obtained by locating the instability points on them. Some of these R curves are shown in Fig. 5.19 alongwith the crack extension force curves. The instability points have also been indicated. It was observed that both the approaches give the same results. Therefore, the R curves for other specimens were not obtained.

The fracture toughness of specimens for crack length to width ratios 0.1, 0.2 and 0.3 are given in Tables 5.1,
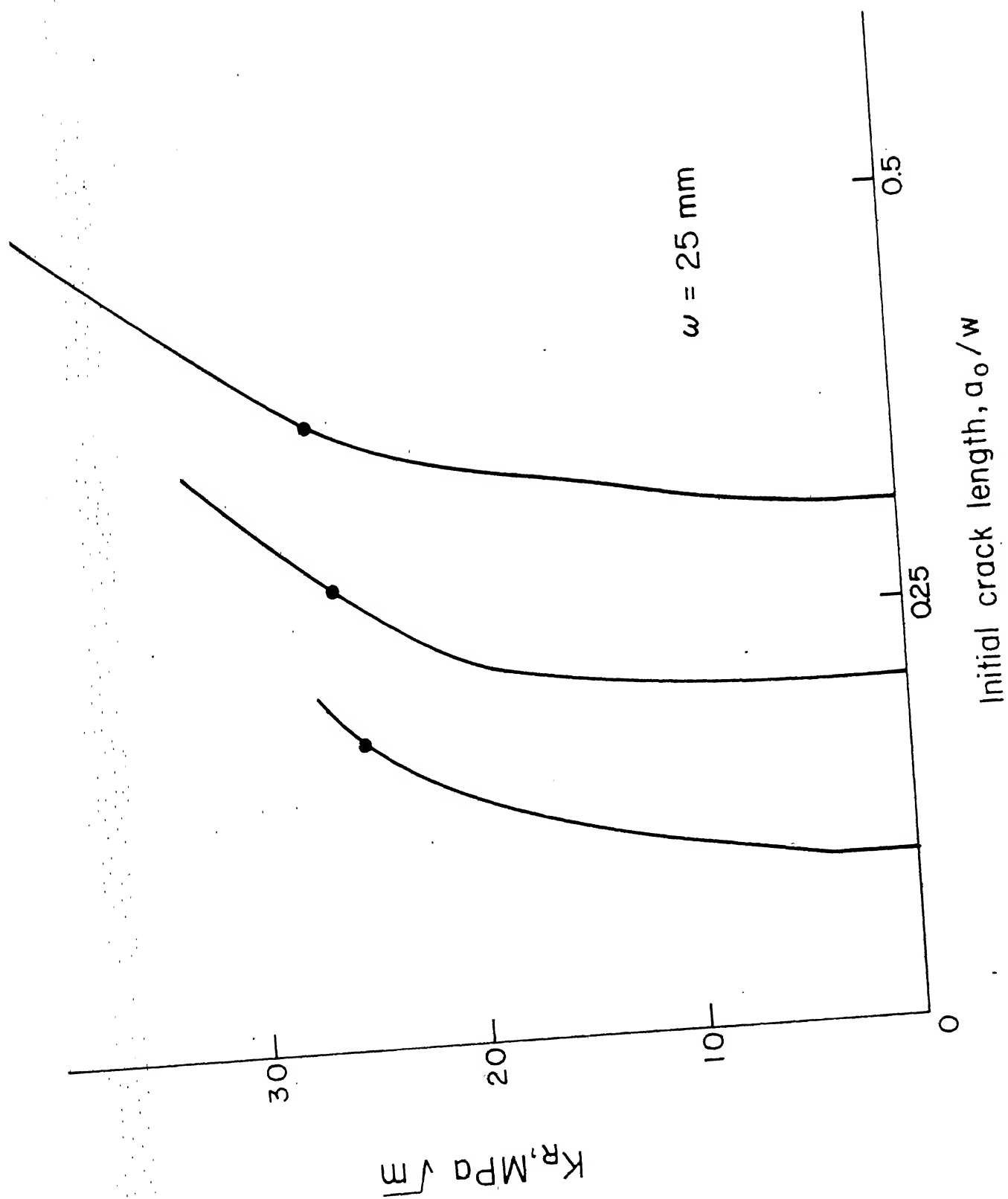
Fig. 5.19 Few crack growth resistance curves.

TABLE 5.1

Fracture Toughness of Specimens with $a_0/w = 0.1$

Sl. No.	Peak load (kN)	Fracture toughness (MPa $\sqrt{m}$)	Mean (MPa $\sqrt{m}$)	Standard deviation
$W = 25$ mm, $a_0 = 2.5$ mm				
1	12.596	26.66		
2	11.497	25.08		
3	12.517	25.22	24.8	1.33
4	11.242	23.83		
5	13.302	23.23		
$W = 30$ mm, $a_0 = 3$ mm				
1	14.107	27.11		
2	12.276	24.12		
3	13.969	25.28	25.698	1.165
4	12.675	25.44		
5	11.988	26.54		

Mean fracture toughness for all specimens = 25.25 MPa $\sqrt{m}$

Standard deviation = 1.25 MPa $\sqrt{m}$.

TABLE 5.2

Fracture Toughness of Specimens with $a_0/w = 0.2$

Sl. No.	Peak load (kN)	Fracture toughness (MPa $\sqrt{m}$)	Mean (MPa $\sqrt{m}$)	Standard deviation
W = 25 mm, a_0 = 5 mm				
1	8.672	28.74		
2	8.456	24.69		
3	8.495	26.12	26.34	1.71
4	7.966	25.81		
W = 30 mm, a_0 = 6 mm				
1	9.3	25.28		
2	10.5	26.65		
3	9.888	25.79	26.18	0.876
4	9.949	26.32		
5	10.197	27.33		

Mean fracture toughness for all the specimens = 26.26 MPa $\sqrt{m}$

Standard deviation = 1.293 MPa $\sqrt{m}$

TABLE 5.3

Fracture Toughness of Specimens with $a_o/w = 0.3$

Sl. No.	Peak load (kN)	Fracture toughness (MPa √m)	Mean (MPa √m)	Standard deviation
W = 25 mm, a_o = 7.5 mm				
1	6.867	25.22		
2	6.494	27.78		
3	7.024	29.98	27.158	1.82
4	6.415	26.37		
5	6.121	26.44		
W = 30 mm, a_o = 9 mm				
1	6.93	27.7		
2	6.57	28.0		
3	7.276	27.65	27.038	1.095
4	6.683	25.39		
5	7.049	26.45		

Mean value of fracture toughness for all the specimens

= 27.098 MPa √m

Standard deviation = 1.4575 MPa √m

5.2 and 5.3 respectively. They are plotted against crack length (a_o/w) in Fig. 5.20. It may be observed from tables 5.1, 5.2 and 5.3 that for a given value of a_o/w, 25 and 30 mm wide specimens give overlapping values of fracture toughness. Therefore, a common average has been plotted in Fig. 5.20. The bars in Fig. 5.20 indicate 68% confidence (i.e., $\pm \sigma$) limits. The fracture toughness increases by about 8% as a_o/w changes from 0.1 to 0.3. This change is comparable with the scatter (standard deviation) of the data. Therefore, it may be considered that the fracture toughness of the short fibre composite is nearly independent of the initial crack length. An average value of the fracture toughness of the material is 26.2 MPa$\sqrt{m}$. The fracture toughness of the same material was obtained using J integral approach in Chapter 3. The critical value J_c was obtained as 51.8 kJ/m^2. The value of J_c can be related to critical crack growth resistance, $K_{R(Ins)}$ through the following relation

$$J_c = K^2_{R(Ins)} / E \qquad\qquad (5.20)$$

where E is the elastic modulus of the material and is equal to 12.5 GPa. Substitution of J_c equal to 51.8 kJ/m^2 in Eq. 5.20, gives $K_{R(Ins)}$ equal to 25.45 MPa $\sqrt{m}$ which compares well with 26.2 MPa $\sqrt{m}$ obtained by the R curve approach. Therefore, the J integral and R curve approach lead to the same fracture toughness value for the material investigated here.
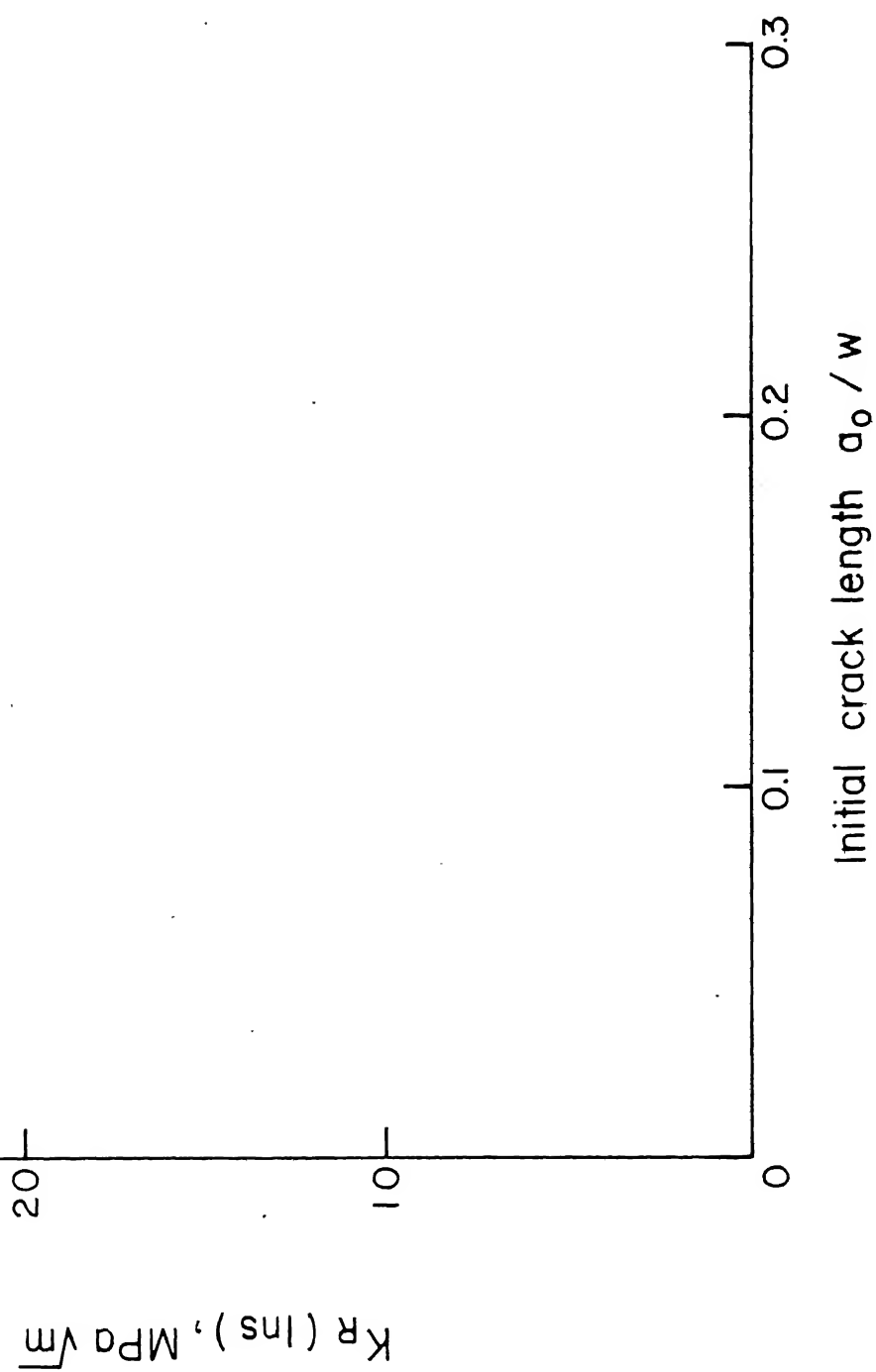
Fig 5.20 Variation of $K_R(\text{Ins})$ with initial crack length.

Initial crack length a_o / w

$K_R(\text{Ins})$, MPa $\sqrt{m}$

5.8 CONCLUDING REMARKS

Fracture toughness of the glass epoxy composite has been obtained using the R curve approach in this chapter. The motivation for initiating these studies had been to compare the fracture toughness results obtained using the J integral approach (Chapter 3) which is being applied to composite materials for the first time. For uniformity, the results for both the approaches were obtained from the same specimens. During all the fracture toughness test on single edge notched specimens, load, load point displacement and COD were measured. The load - displacement records are used for J integral approach and load - COD records for the R curve approach. Both the approaches lead to the same fracture toughness values and thus validate the results of each other.

Although the R curve approach has been applied to composites by several investigators, two major contributions have been made in the present study. One relates to the validity of a vital step in employing the approach and the other simplifies the application of this approach to the composites. An additional outcome of the latter is to evolve a better understanding of the test procedure.

Analysis using the R curve approach requires measurement of instantaneous crack length with increasing load. In composite materials the crack length can not be measured

directly. Consequently the crack length is estimated through the compliance matching procedure. The validity of analysis, therefore, rests upon validity of this step. The present study examines the compliance matching procedure in this light and provides a justification for its use for short fibre composites.

In R curve approach, the fracture toughness of the material is obtained by locating the point of instability on the crack growth resistance curve. However, for composite materials, obtaining the full R curve itself is tedious and time consuming due to the indirect method of determining the instantaneous crack length. The present study mathematically establishes that the peak load point on the load - COD curve is the instability point and that the fracture toughness can be obtained from the peak load and the corresponding COD. This greatly simplifies the application of R curve approach to composites. It has also been shown that for better accuracy the fracture toughness tests should be performed under displacement controlled conditions (constant cross-head speed),

CHAPTER VI

FRACTURE TOUGHNESS OF SHORT CARBON FIBRE REINFORCED EPOXY RESIN

6.1 INTRODUCTION

Carbon fibres are high strength, high stiffness and low specific gravity fibres. Their strength is quite comparable with that of glass fibres. Their stiffness is 4 to 6 times larger. Their specific gravity is about 1.8 to 1.9 compared to 2.54 for glass fibres. Also, the strength and stiffness of carbon fibres can be obtained in many different combinations by controlling the manufacturing parameters. Thus, carbon fibres are very attractive reinforcements. The use of carbon fibre composites is rapidly increasing particularly in structures where dimensional accuracy and low weight are important as in aerospace applications. The fracture toughness of short carbon fibre reinforced epoxy resin has been investigated here.

Fracture toughness of short glass fibre reinforced epoxy resin composites has been obtained by J integral as well as R curve methods. J integral is employed for randomly oriented short carbon fibre reinforced epoxy resin composites. The J integral results are compared with those obtained from the linear elastic fracture mechanics methods.

6.2 STRESS STRAIN BEHAVIOUR

A typical stress strain curve for the short carbon fibre reinforced epoxy resin ($V_f = 20.8\%$) is shown in Fig. 6.1. The stress strain curve is initially linear but progressively deviates from linearity. The constitutive relation can be described by Ramberg Osgood type relation [6]

$$\frac{\sigma}{13.08} = \left(\frac{\epsilon}{0.08}\right)^{0.935} \qquad (6.1)$$

where σ is the composite stress in MPa and ϵ is the strain in percent. The constants 13.08 MPa for stress and 0.08 percent for strain correspond to the end of linear portion of the stress-strain curve. The exponent $n = 0.935$ for the carbon fibre composite is larger than that for the glass fibre composite ($n = 0.83$). This indicates that carbon fibre composite is less nonlinear than the glass fibre composite ($n = 1$, represents linear relationship). This relation (Eq. 6.1) is shown superimposed on the actual stress-strain curve in Fig. 6.1. It is seen that the actual and idealized stress-strain curves are very close to each other to such an extent that for a major portion one curve can not be distinguished from the other. The usefulness of the nonlinear stress-strain behaviour for application of J integral approach has already been discussed in Chapter 3 and is not repeated here.

$$\frac{\sigma}{13.08} = \left(\frac{\epsilon}{0.08}\right)^{0.935}$$

— — — $\frac{\sigma}{13.08} = \left(\frac{\epsilon}{0.08}\right)^{0.935}$
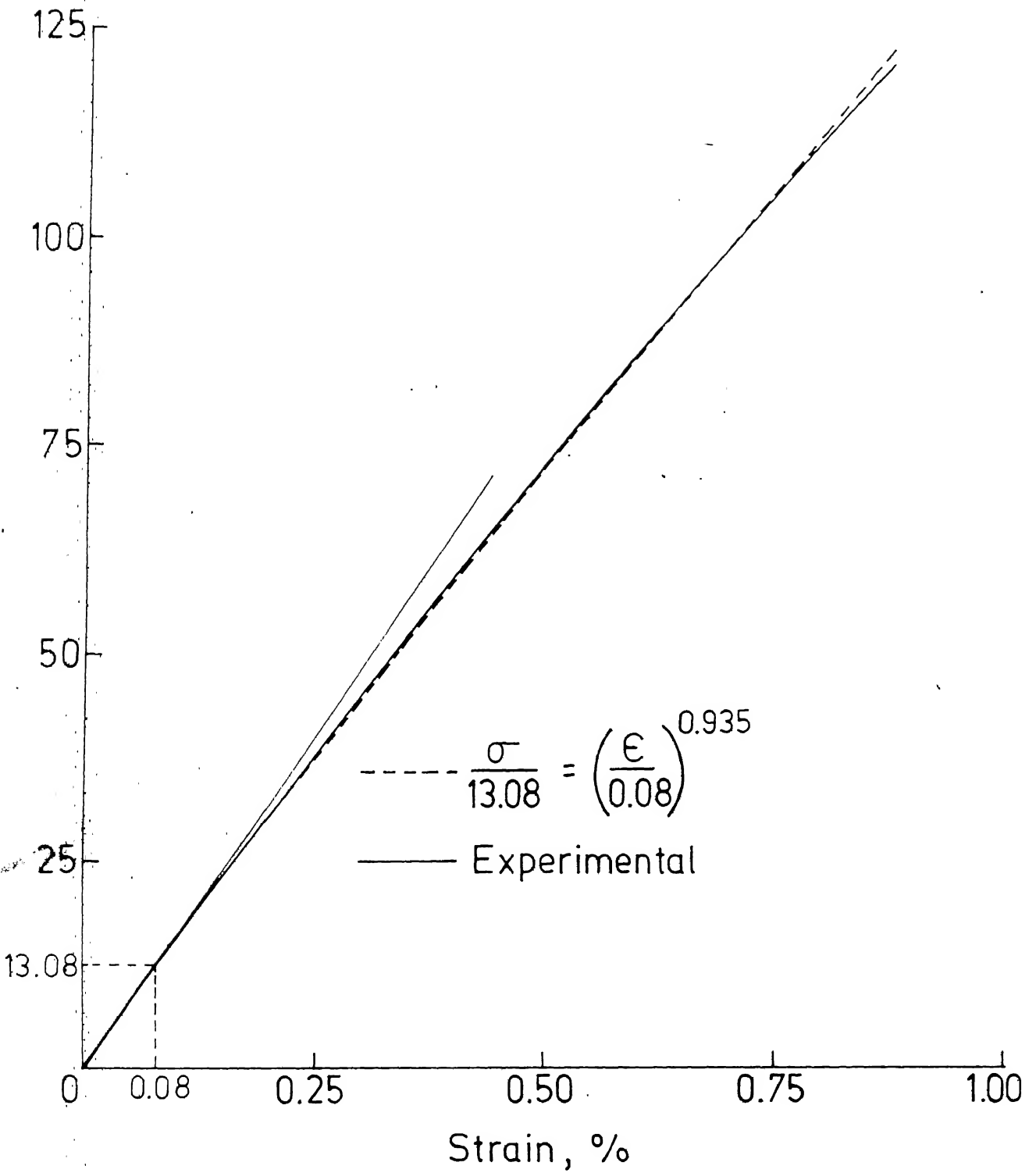
—— Experimental

g. 6.1 Experimental and idealized stress-strain relations for short carbon fibre reinforced composites.

6.3 FRACTURE TOUGHNESS USING J INTEGRAL

Typical load-displacement (at the load point) curves for specimens with different crack lengths are shown in Fig. 6.2. The specimens undergo a catastrophic failure irrespective of crack length. Specimens with small cracks have a slightly nonlinear behaviour but the load-displacement relation for specimens with crack lengths 10 mm or longer is almost linear.

The observed fracture load is plotted against crack length in Fig. 6.3 alongwith the fracture load that would be expected if the strength was unaffected by the crack; that is, the fracture load obtained by multiplying the net cross sectional area and the unnotched strength. The observed fracture load is smaller than the expected indicating that the crack reduces the fracture load far greater than can be accounted for by the reduction in cross sectional area. The extent of this influence is illustrated in Fig. 6.4 through the ratio of observed to expected fracture loads. The decreasing ratio indicates the increasing influence of cracks which stabilizes for cracks equal to and longer than 10 mm. The ratio of observed to expected fracture load for the glass fibre composite is also shown in the figure for comparison. It is seen that the cracks reduce the fracture load much more in carbon composite than in glass fibre composite.
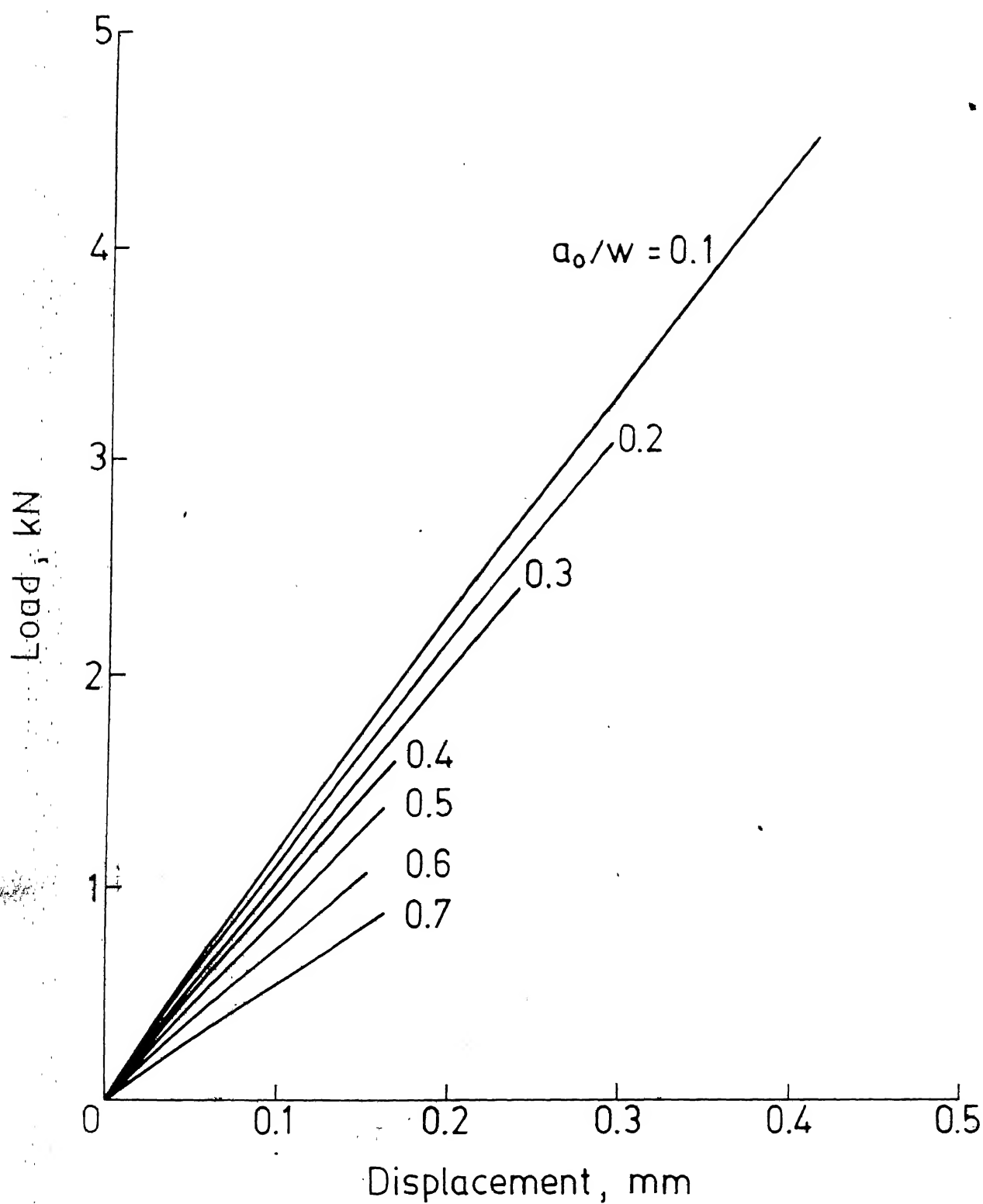
Fig. 6.2 Load displacement curves for different initial crack lengths.
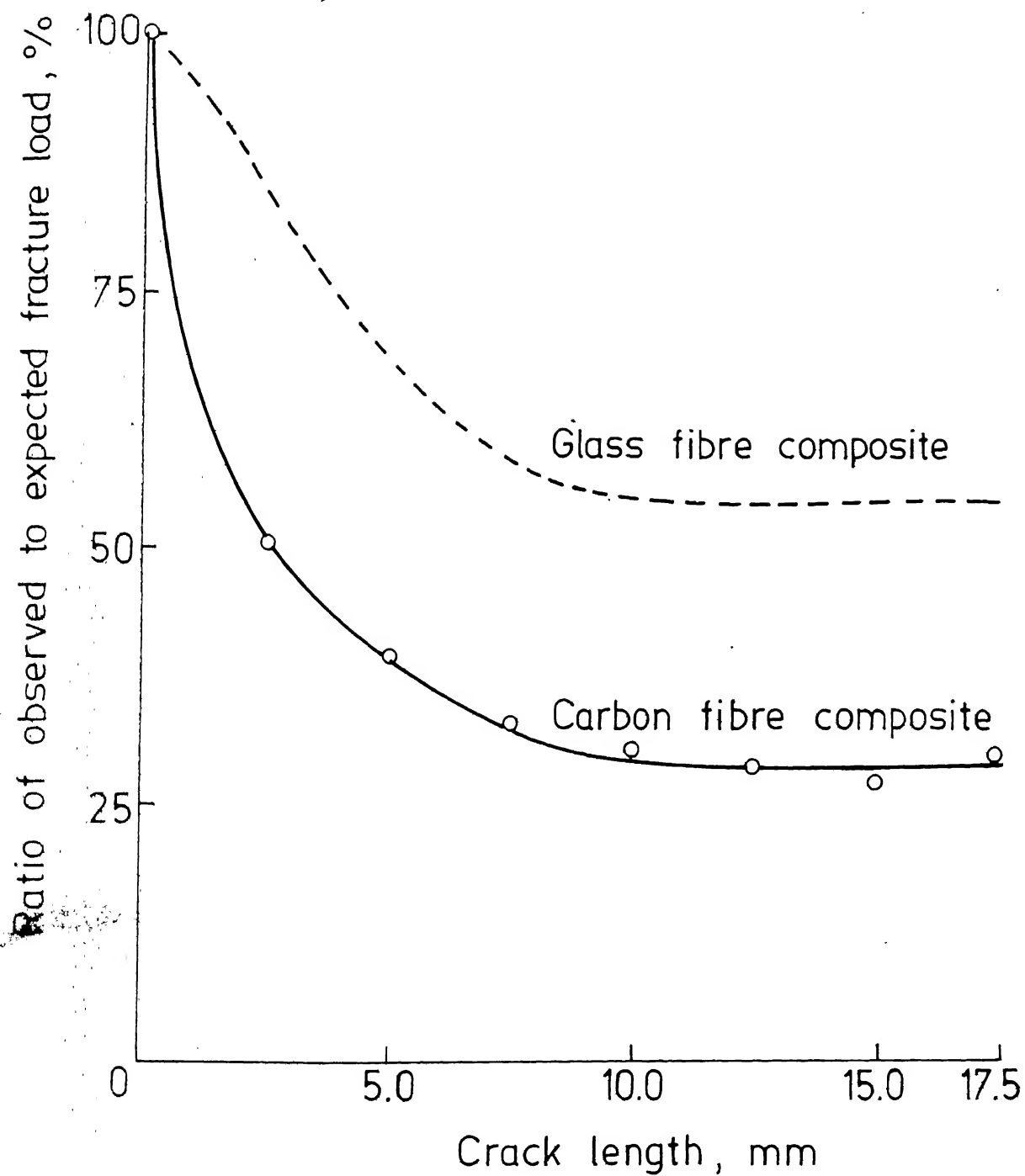
Fig. 6.4 The ratio of observed to expected fracture load as a function of crack length.

The critical displacement is plotted against crack length in Fig. 6.5. Initially, the critical displacement decreases with increase in crack length and remains constant for 10 mm cracks and longer. The initial variation in critical displacement occurs due to deformation away from the crack plane because of larger loads. The constant value of critical displacement for carbon fibre composite (0.167 mm) is much smaller than that for the glass fibre composite (about 0.9 mm). The critical value of J integral is obtained corresponding to this constant critical displacement (0.167 mm).

The procedure of obtaining J integral experimentally through its energy rate interpretation using the load displacement curves was described in Chapter 3. The area under the load displacement curves is obtained and plotted against crack length for several displacements (Fig. 6.6). For a given displacement, energy absorbed by a specimen decreases as the crack length increases because smaller loads are required. The variation in strain energy is less for cracks shorter than 10 mm compared to that for longer cracks because the energy absorbed is essentially in the vicinity of crack tip and is thus strongly influenced by the crack length.

The J integral is obtained from its energy rate interpretation through slopes of the strain energy curves in
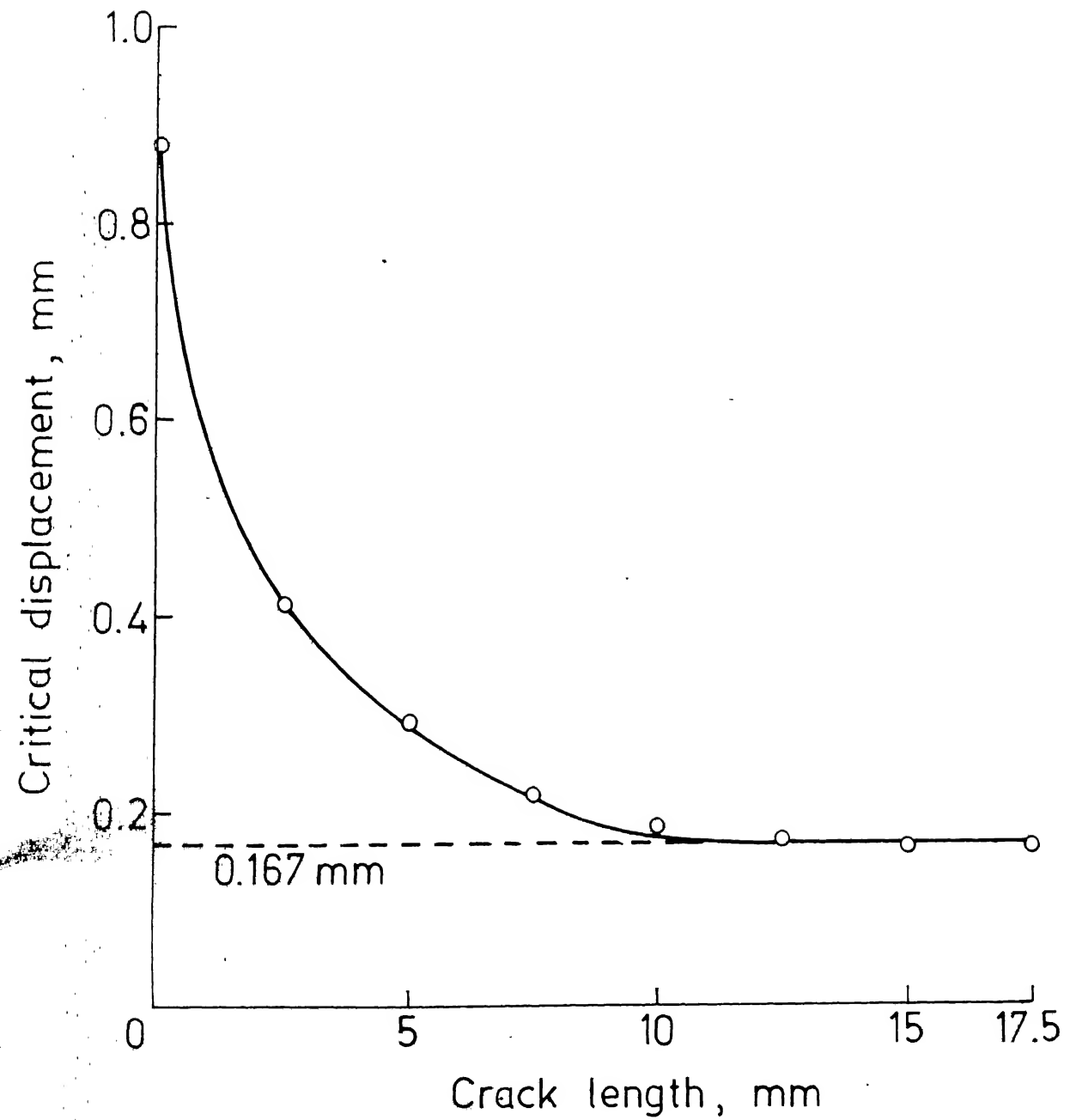
Fig. 6.5 Effect of initial crack length on critical displacement.
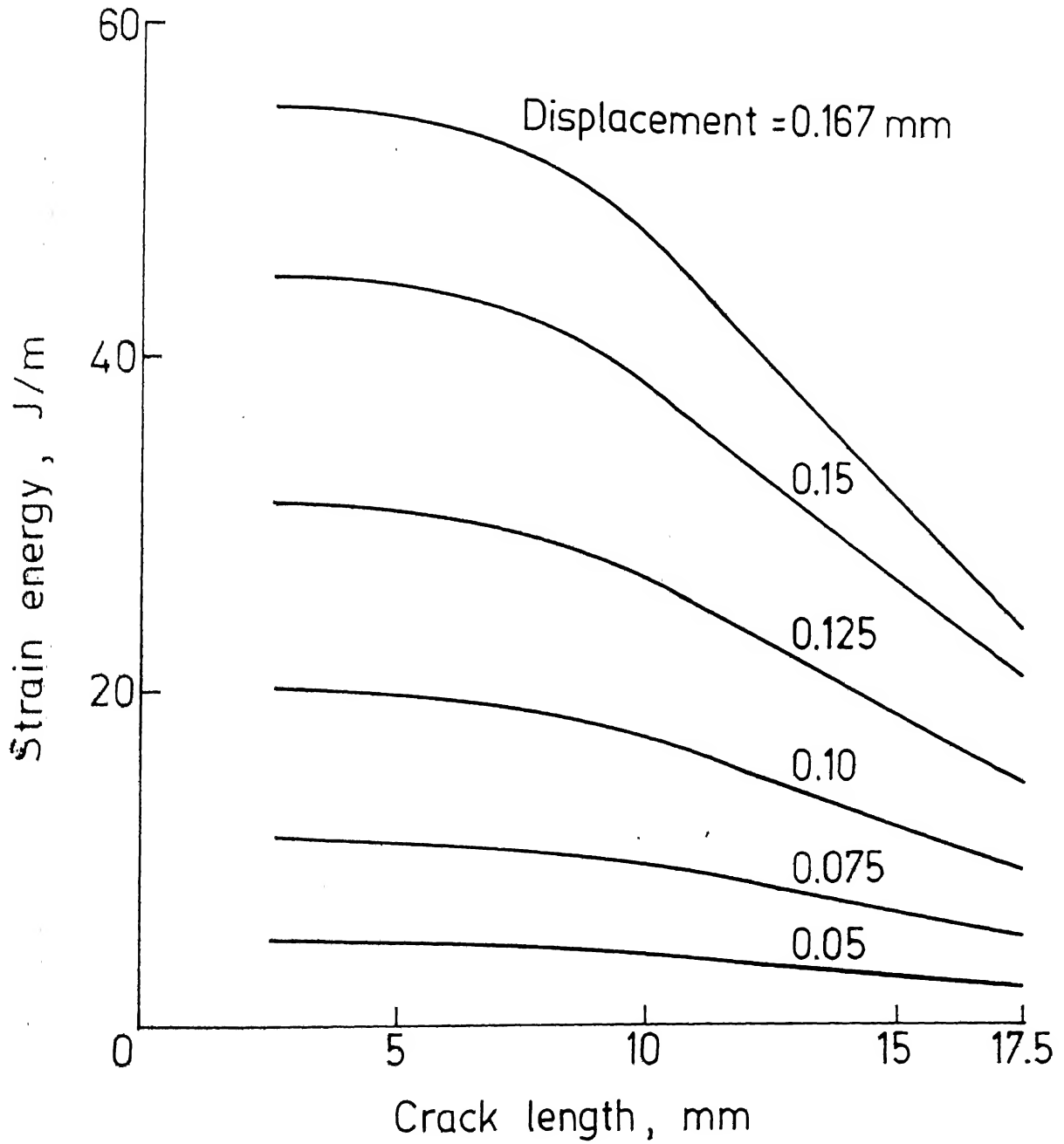
Fig. 6.6 Strain energy as a function of displacement.

Fig. 6.6. The J integral is independent of crack length for cracks larger than or equal to 10 mm since the strain energy curves are straight lines in this range (Fig. 6.6). The variation of J with displacement is shown in Fig. 6.7. The critical value of J corresponding to the critical displacement of 0.167 mm is 3.225 kJ/m^2. This critical value of J integral for carbon fibre composite is nearly an order of magnitude smaller than that for the glass fibre reinforced composite materials.

This may be expected due to very small fracture strain of carbon fibres which have comparable strength with glass fibres but are nearly 4 to 6 times stiffer. The unnotched strengths of carbon and glass fibre composites are quite comparable when fibre concentrations are same. However, in the presence of cracks the fibre composite behaves in a brittle fashion. The fracture occurs at very small displacements. The damage during fracture is confined to a very narrow band as shown in Fig. 6.8. Therefore, the energy absorbed for fracture is quite small.

6.4 LEFM APPROACH

In the case of carbon fibre composites, there is no slow crack growth. This is reflected in load-crackmouth opening displacement curves as shown in Fig. 6.9. For smaller crack lengths of 2.5, 5 and 7.5 mm, the load-COD curves are linear upto fracture indicating no crack growth.
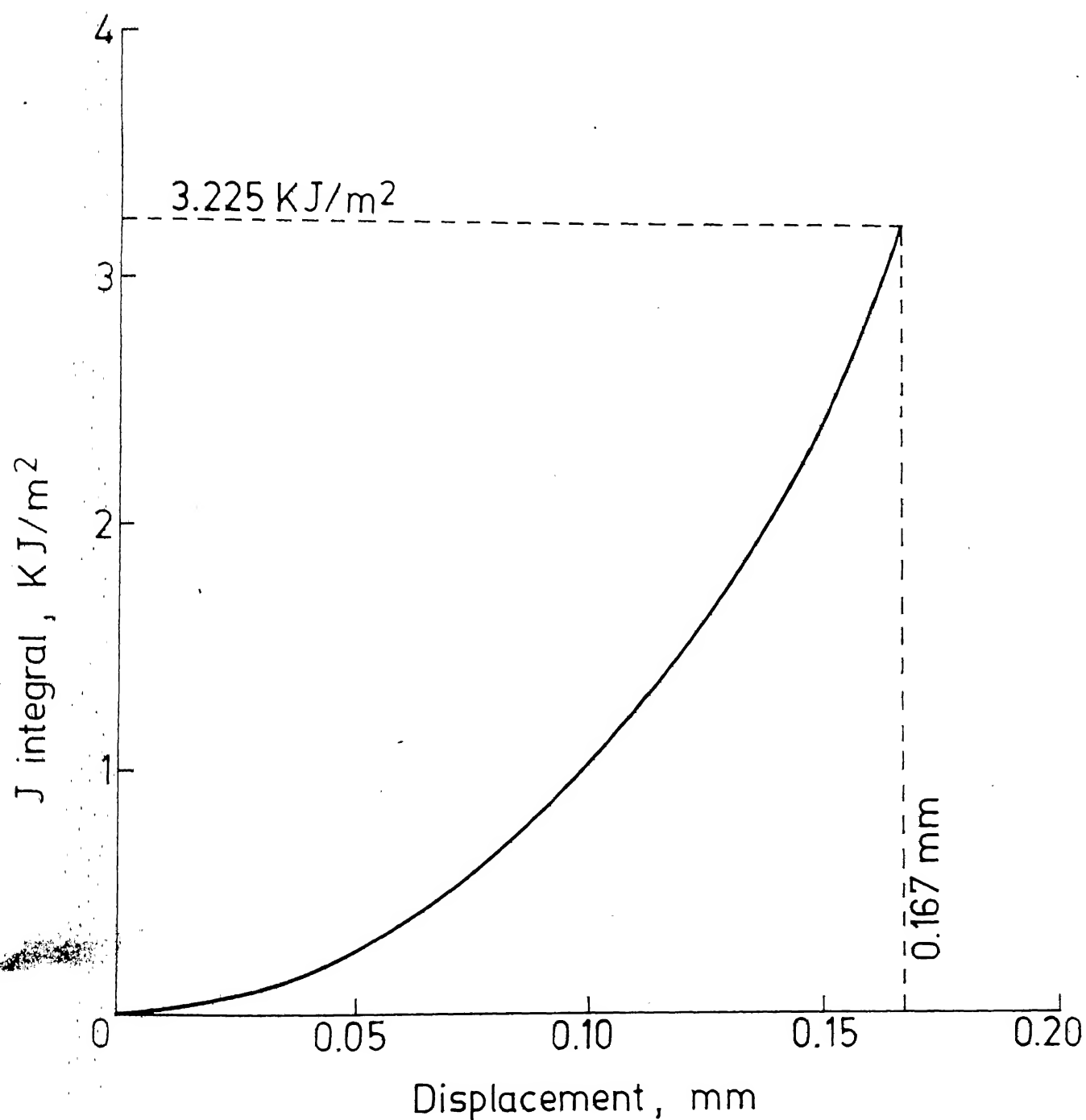
Fig. 6.7 J integral as a function of displacement.
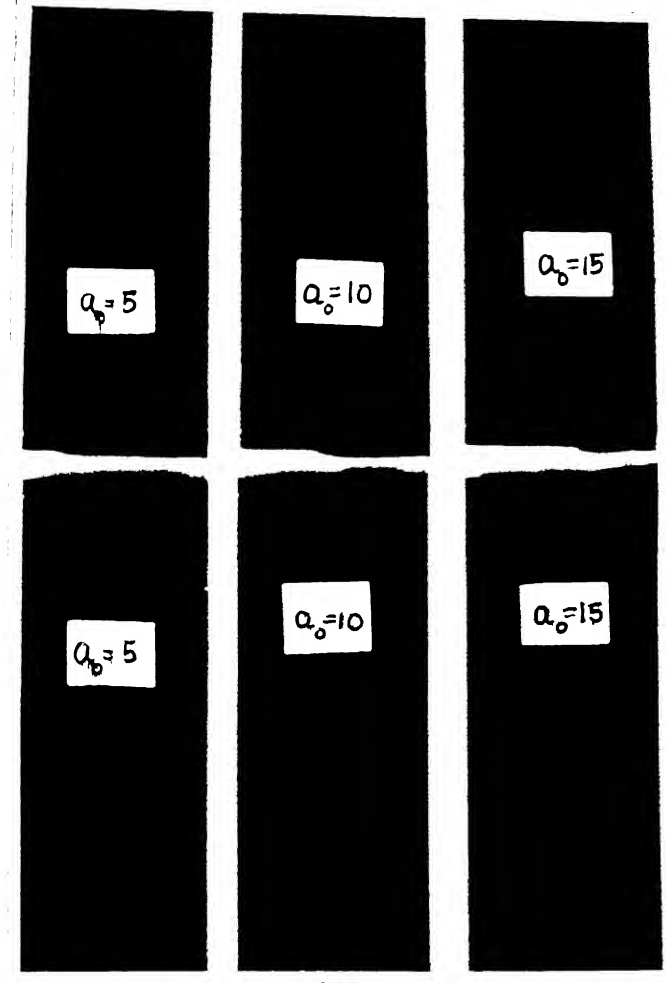
Fig. 6.8 Photograph of fractured short carbon fibre
composite specimens.
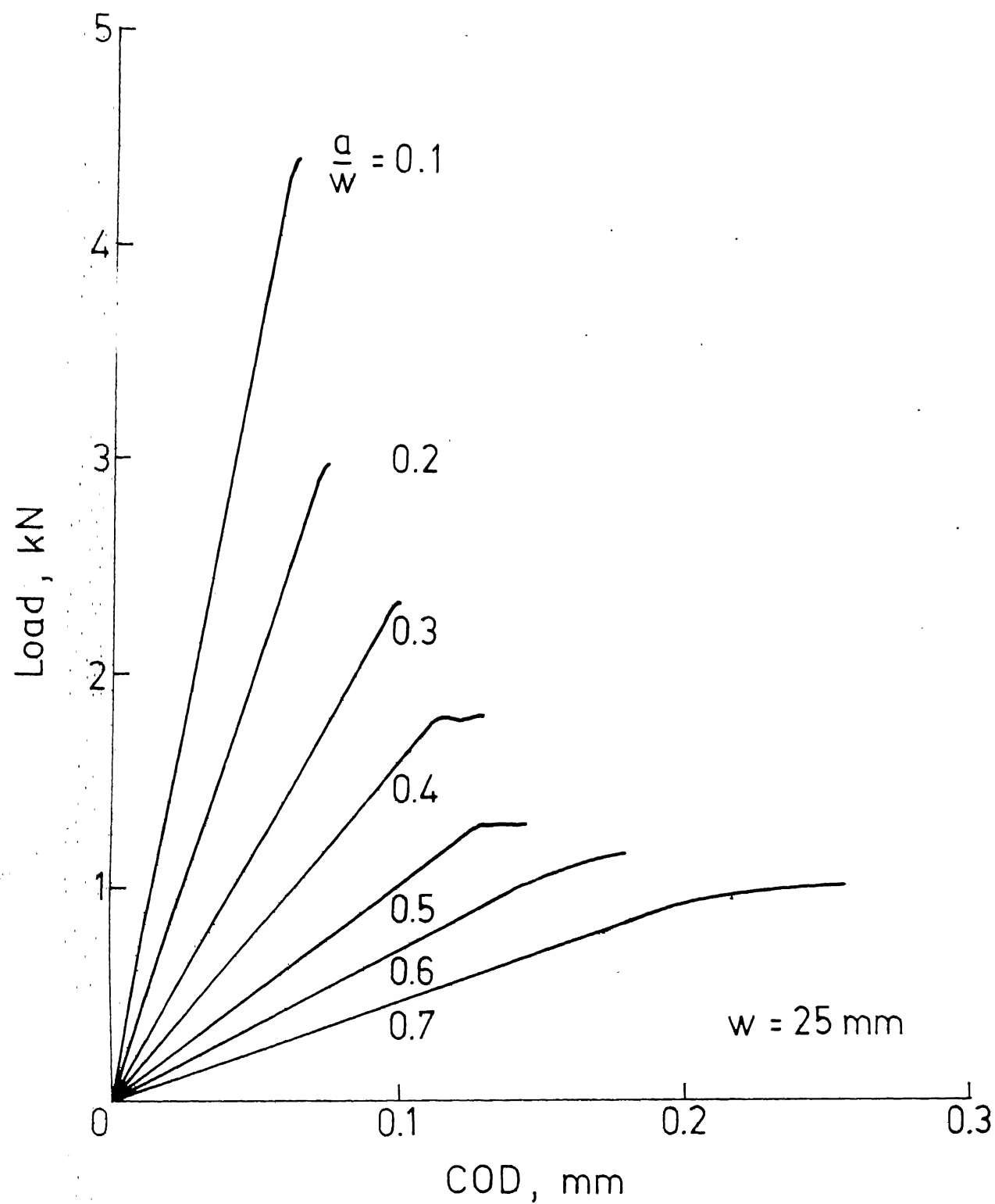
Fig. 6.9 Load-COD curves for different crack lengths.

In these cases R - curve approach is not necessary and critical stress intensity factor can be evaluated from fracture load and initial crack length. For 10 mm and higher crack lengths, the load - COD curves are linear for a large portion but at fracture load, they level off. In this region the equivalent crack length can be estimated from the crack length estimation curve shown in Fig. 6.10. However, it is not necessary to use the concept of instantaneous crack length because LEFM approach may not be applicable for specimens with comparatively large initial crack lengths.

Critical stress intensity factor, K_c, can be evaluated for the fracture load, P_c, and the initial crack length, a_0, using the following well known relation [40]

$$K_c = Y \frac{P_c}{tw} \sqrt{a_0} \qquad (6.2)$$

Fracture toughness values for 2.5, 5 and 7.5 mm crack length specimens are evaluated. For each crack length 5 specimens were tested. The average critical stress intensity factor alongwith the standard deviation are shown in Fig. 6.11. It is observed that increase in K_c with crack length is small. The mean values of K_c for 2.5, 5 and 7.5 mm crack lengths are 6.025, 6.825 and 7.4 MPa $\sqrt{m}$ respectively.
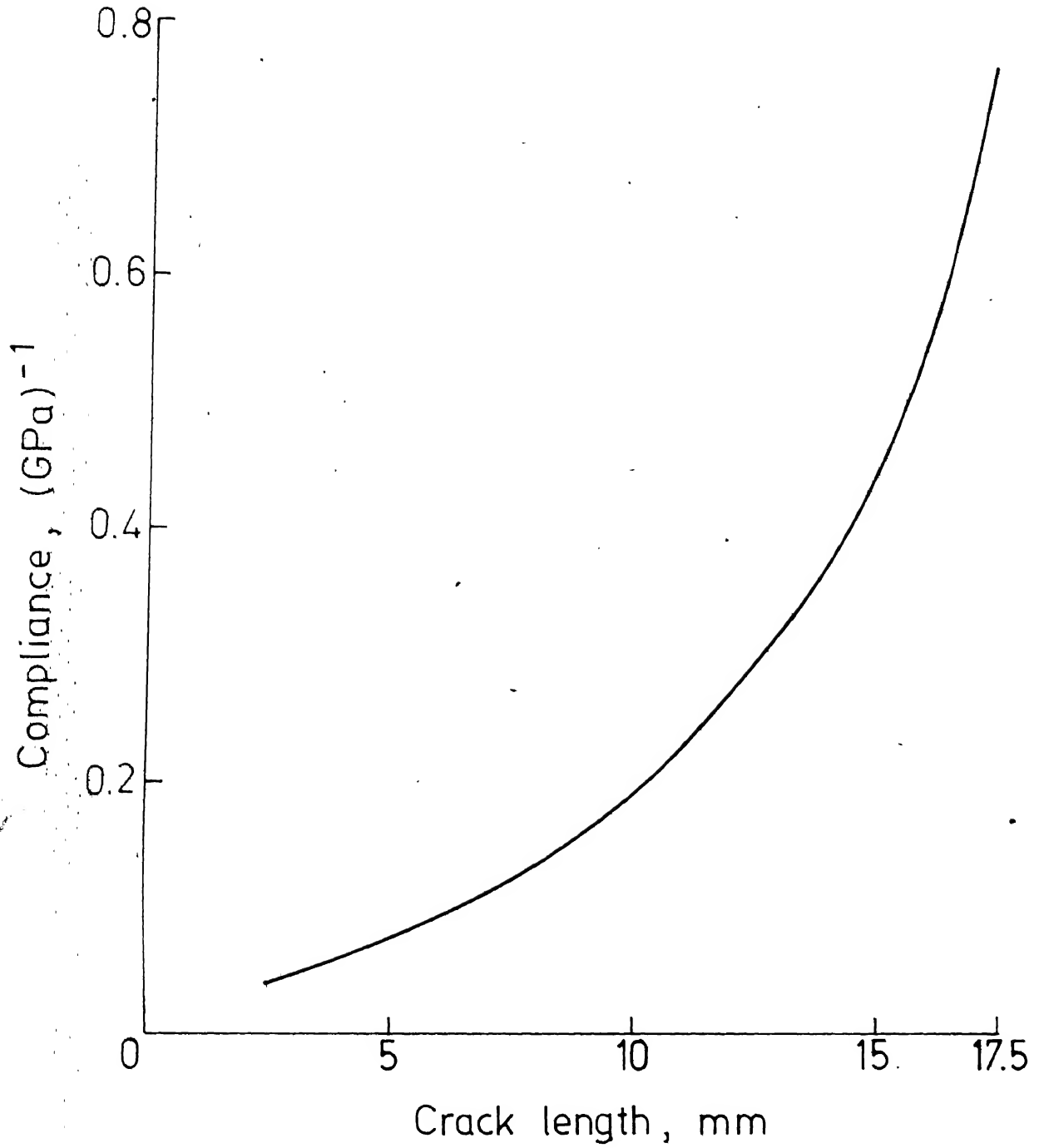
Fig. 6.10 Crack length estimation curve for short carbon
fibre rainforced composites.
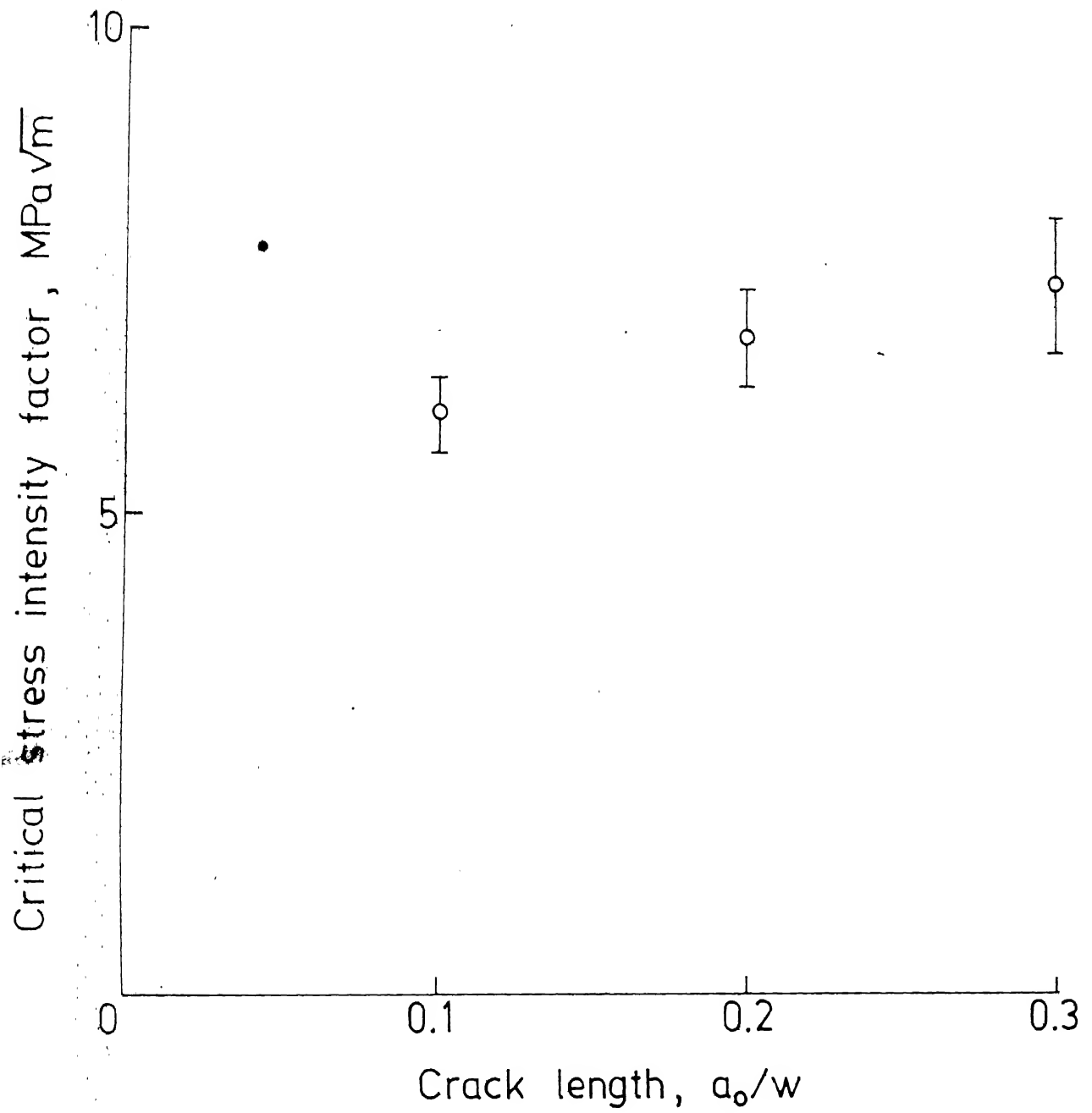
Fig. 6.11 Variation of critical stress intensity factor with crack length.

6.5 DISCUSSIONS

The critical value of J integral, J_c, and critical stress intensity factor, K_c have been evaluated in the preceeding sections. For plane stress case, the relation between them is given by [5]

$$J_c = K_c^2 / E \qquad (6.3)$$

The elastic modulus of the composite is 14 GPa.

Corresponding to J_c value of 3.225 kJ/m^2, the K_c value obtained by using Eq. 6.3 is 6.72 MPa$\sqrt{m}$. This compares very favourably with K_c value of 6.75 MPa$\sqrt{m}$ obtained as average values for all the specimens.

The above results show that J integral method and LEFM approach yield the same results. In fact the two methods compliment each other as is further discussed in the following paragraph.

The load displacements plots are nonlinear for 2.5 to 7.5 mm crack lengths and linear for 10 to 17.5 mm crack lengths ($a/w \geq 0.4$). For higher crack lengths the net section ultimate stresses and critical displacements are the same and J integral method is applicable in this range. Linear elastic fracture mechanics approach, on the other hand, is applicable for 7.5 mm cracks or less ($a/w \leq 0.3$). In this range the load-COD curve is linear indicating no crack extension before catastrophic fracture. However, for

higher crack lengths (a/w $\geq$ 0.4), the load-COD curves deviate: from linearity towards the end. Secondly linear elastic fracture approach is only applicable when crack length is small compared to the width of the specimen.

The J integral method has proved successful for randomly oriented short glass fibre reinforced epoxy resin exhibiting nonlinear load-displacement and load-COD behaviour. A comparison of J_c with K_c obtained by R - curve approach demonstrates the equality between them. The J integral method has also been found effective for short carbon fibre composites as it yields the same results as obtained by using LEFM approach.

CHAPTER VII

CONCLUSIONS AND SCOPE FOR FURTHER RESEARCH

7.1 CONCLUSIONS

Fracture toughness of randomly oriented short glass and carbon fibre reinforced epoxy composites has been investigated experimentally. The composite material plates were fabricated in the laboratory. A total of about 1000 single edge notched specimens were tested at different stages of the investigations. Emphasis was placed on developing the J integral as a fracture criterion but the measurements during tests were made such that the data could be analysed using J integral as well as R curve approach and the results compared.

While applying the R curve method to short glass fibre composites, attention was focussed mainly on two aspects in the present study:

1. The compliance matching procedure has been widely used by several investigators to estimate instantaneous crack length in composites during fracture toughness tests. Validity of this procedure has been examined and established.

2. It has been mathematically established and
   experimentally verified that the peak load point
   on the load-COD curve indeed corresponds to the
   instability point on R curve and that the fracture
   toughness can be determined at this point. This
   eliminates the necessity of obtaining the full R
   curve through a tedious and time consuming process.

It may be mentioned that to locate the peak load
point and the corresponding COD accurately, the fracture
toughness tests performed under displacement controlled
conditions are better suited than the load controlled tests.

Successful application of the results obtained
using R curve approach (LEFM approach) requires an accurate
analysis of the crack tip region which presents many prac-
tical difficulties even for homogeneous isotropic materials
and more so for heterogeneous composites where crack tip
geometry is more complicated. A characterization of the
crack tip area by a parameter calculated without focussing
attention directly at the crack tip would provide a more
useful method for analysing fracture. The well known J
integral is often used to characterize fracture of metals
under conditions of large scale yielding. Its value depends
on the near tip stress strain field but its path indepen-
dent nature allows an integration path, taken sufficiently
far from the crack tip, to be substituted for a path close

to the crack tip region. With this in mind, the experimental data have been analysed using the J integral approach through its energy rate interpretation. The following observations have been made:

1. When $a_o/w > 0.4$, the material damage is confined to the crack tip region and J integral is independent of crack length. Since in this range, the critical displacement is independent of initial crack length, the critical value of J integral (J_c) is also independent of crack length.

2. When $a_o/w < 0.4$, general material damage away from crack tip also influences the energy absorbed significantly. In this range, J_c value is higher than the constant value of J_c obtained earlier. Therefore, the use of J_c obtained for higher crack lengths would lead to conservative (safe) design.

3. When $a_o/w < 0.4$, an extrapolation method has been developed through which the crack tip energy may be separated from the energy absorbed due to general material damage and J_c evaluated directly. This J_c value is independent of crack length and is the same as that obtained without extrapolation for $a_o/w > 0.4$.

In composites, the fibre volume fraction is the single most important variable controlling such material properties as the strength, modulus etc. The results on the glass fibre composites show that J_c increases linearly with fibre volume fraction.

7.2 SCOPE FOR FURTHER RESEARCH

The J integral approach applied here to short fibre composites shows a great promise. For greater confidence further investigations should be carried out using different material and specimen variables. Some of the aspects which may be investigated are mentioned below.

1. Influence of specimen width on J_c has been investigated in the range of 15 to 40 mm. A larger variation in width upto about 100 or 150 mm is desirable.

2. Influence of matrix material on J_c may be investigated. Effect of thermosetting resins such as polyesters as well as thermoplastic matrices such as nylon, polypropylene etc. should be studied.

3. Fibre length is an important parameter affecting the properties of short fibre composites. Its influence on fracture toughness should be investigated.

4. The J integral approach should be applied to
    other reinforcement systems such as woven fabric
    and continuous fibres.

5. Influence of such environmental variables such
    as moisture, saline water, acids and oils should
    be investigated. The effect of temperature on J_c
    need be established.

REFERENCES

1. A.A. Griffith, "The Phenomena of Rupture and Flow in Solids", Phil. Trans. Roy. Soc. of London, A 221, 1920, pp. 163 - 197.

2. G.R. Irwin, "Analysis of Stresses and Strains Near The End of A Crack Traversing A Plate", Trans. ASME, J. Applied Mechanics, Vol. 24, 1957, pp. 361 - 364.

3. E. Orowan, "Energy Criteria of Fracture", Welding Journal, Vol. 34, 1955, pp. 157S - 160S.

4. J.R. Rice, "A Path Independent Integral and The Approximate Analysis of Strain Concentration by Notches and Cracks", J. Applied Mechanics, Vol. 35, 1968, pp. 379-386.

5. J.R. Rice, "Mathematical Analysis in The Mechanics of Fracture", Chapter 3, Fracture , Vol. II, Ed. H. Liebowitz, Academic Press, New York, 1968, pp. 191 - 311.

6. J.W. Hutchinson, "Singular Behaviour at The End of a Tensile Crack In a Hardening Material", J. Mechanics and Physics of Solids, Vol. 16, 1968, pp. 13-31.

7. J.R. Rice and G.F. Rosengren, "Plane-Strain Deformation Near a Crack Tip in a Power Law Hardening Material", Ibid, pp. 1-12.

8. F. McClintock, "Plasticity Aspects of Fracture", Chapter 2, Fracture, Vol. III, Ed. H. Liebowitz, Academic Press, New York, 1971, pp. 47-225.

9. K.B. Broberg, "Crack Growth Criteria and Nonlinear Fracture Mechanics", J. Mechanics and Physics of Solids, Vol. 19, 1971, pp. 407-418.

10. J.A. Begley and J.D. Landes, "The J Integral as a Fracture Criterion", Fracture Toughness, ASTM STP 514, American Society for Testing and Materials, Philadelphia, 1972, pp. 1-20.

11. J.D. Landes and J.A. Begley, "The Effect of Specimen Geometry on J_{IC}", Fracture Toughness, ASTM STP 514, American Society for Testing and Materials, Philadelphia, 1972, pp. 24-39.

12. J.D. Landes and J.A. Begley, "Recent Developments in J_{IC} Testing", <u>Developments in Fracture Mechanics Test Methods Standardization</u>, ASTM STP 632, American Society for Testing and Materials, Philadelphia, 1977, pp. 57-81.

13. M.E. Waddoups, J.R. Eisenmann and B.E. Kaminski, "Macroscopic Fracture Mechanics of Advanced Composite Materials, J. Composite Materials, Vol. 5, 1971, pp. 446-454.

14. M.J. Owen and P.T. Bishop, "Critical Stress Intensity Factors Applied to Glass Reinforced Polyester Resin", J. Composite Materials, Vol. 7, 1973, pp. 146-159.

15. P.K. Mallik and L.J. Broutman, "The Influence of the Interface on the Fracture Toughness of Low Aspect Ratio Fibre Composites", Fibre Science and Technology, Vol. 8, 1975, pp. 113-144.

16. G.C. Sih, P.D. Hilton, R. Badaliance, P.S. Shenberger and G. Villareal, "Fracture Mechanics fof Fibrous Composites", <u>Analysis of the Test Methods for High Modulus Fibers and Composites</u>, ASTM STP 521, American Society for Testing and Materials, 1973, pp. 98-132.

17. J.F. Madell, S.S. Wang and F.J. McGarry, "The Extension of Crack Tip Damage Zones in Fiber Reinforced Plastic Laminates", J. Composite Materials, Vol. 9, 1975, p. 266.

18. M.D. Snyder and T.A. Cruse, "Boundary Integral Equation Analysis of Cracked Anisotropic Plates", International Journal of Fracture, Vol. 11, 1975, pp. 315-328.

19. H.J. Konish, Jr., "Mode I Stress Intensity Factors for Symmetrically - Cracked Orthotropic Strips", <u>Fracture Mechanics of Composites</u>, ASTM STP 593, American Society for Testing and Materials, 1974, pp. 99-116.

20. J.M. Slepetz and L. Carlsen, "Fracture of Composite Compact Tension Specimens", <u>Fracture Mechanics of Composites</u>, ASTM STP 593, American Society for Testing and Materials, 1974, pp. 143-162.

21. N.R. Adsit and J.P. Waszczak, "Fracture Mechanics Correlation of Boron/Aluminium Coupons Containing Stress Risers", <u>Fracture Mechanics of Composites</u>, ASTM STP 593, American Society for Testing and Materials, 1974, pp. 163-176.

22. C.T. Sun and K.M. Prewo, "The Fracture Toughness of Boron Aluminium Composites", J. Composite Materials, Vol. 11, 1977, pp. 164-175.

23. J. Awerbuch and H.T. Hahn, "K - Calibration of Unidirectional Metal Matrix Composites", J. Composite Materials, Vol. 12, 1978, pp. 222-237.

24. Y.J. Yeow, D.H. Morris and H.F. Brinson, "The Fracture Behaviour of Graphite/Epoxy Laminates", Experimental Mechanics, Vol. 19, 1979, pp. 1-8.

25. D.F. Devitt, R.A. Schapery and W.L. Bradley, "A Method of Determining the Mode I Delamination Fracture Toughness of Elastic and Viscoelastic Composite Materials", J. Composite Materials, Vol. 14, 1980, pp. 270-285.

26. C. Bathias, R. Esnault and J. Pellas, "Application of Fracture Mechanics to Graphite Fibre-reinforced Composites", Composites, 1981, pp. 195-200.

27. S. Guofang, "Fracture of Fibreglass Reinforced Composites", J. Composite Materials, Vol. 15, 1981, pp. 521-530.

28. J.M. Whitney and R.J. Nuismer, "Stress Fracture Criteria for Laminated Composites Containing Stress Concentrations", J. Composite Materials, Vol. 8, 1974, pp. 253-265.

29. R.J. Nuismer and J.M. Whitney, "Uniaxial Failure of Composite Laminates Containing Stress Concentrations", ASTM STP 593, American Society for Testing and Materials, Philadelphia, Pa., 1975, pp. 117-142.

30. R.J. Nuismer and J.D. Labor, "Application of the Average Stress Failure Criterion: Part I - Tension", J. Composite Materials, Vol. 12, 1978, pp. 238-249.

31. G.S. Giare, Some Experimental Investigation Concerning Fracture Mechanics of Short Fibre Composites, Ph.D. Thesis, Indian Institute of Technology, Kanpur, India, May, 1980.

32. H.F. Brinson and Y.T. Yeow, "An Experimental Study of the Fracture Behaviour of Laminated Graphite/Epoxy Composites", Composite Materials Testing and Design (Fourth Conference), ASTM STP 617, American Society for Testing and Materials, Philadelphia, Pa., 1977, pp. 18-38.

33. R.B. Pipes, R.C. Wetherhold and J.W. Gillespire, Jr., "Macroscopic Fracture of Fibrous Composites", Material Science and Engineering, Vol. 45, 1981, pp. 247-253.

34. E.M. Wu, "Strength and Fracture of Composites", Composite Materials, Vol. 5, Ed. L.J. Broutman, Academic Press, New York, 1974, pp. 191-247.

35. G.C. Sih, Editor, Mechanics of Fracture, Vol. 6, Martiness Nijhoff Publishers, The Hague, 1981.

36. I.M. Daniel, R.E. Rowlands and J.B. Whiteslide, "Effect of Material and Stacking Sequence on Behaviour of Composite Plates with Holes", Experimental Mechanics, Vol. 14, 1974, pp. 1-9.

37. P.W.R. Beaumont, "Fracture Mechanisms in Fibrous Composites", Fracture Mechanics, Current Status, Future Prospects, Proc. Conf. Cambridge University, Ed. R.A. Smith, March 1979, pp. 211-233.

38. R.H. Heyer, "Crack Growth Resistance Curves (R - Curves) Literature Review", Fracture Toughness Evaluation by R-Curve Methods, ASTM STP 527, American Society for Testing and Materials, 1973, pp. 3-16.

39. W.F. Brown and J.E. Srawley, "Plane Strain Crack Toughness Testing of High Strength Metallic Materials", Fracture Toughness Testing, ASTM STP 410, American Society for Testing and Materials, 1966, p. 1.

40. B.D. Agarwal and L.J. Broutman, Analysis and Performance of Fiber Composites, John Wiley and Sons, New York, 1980.

41. S.K. Gaggar and L.J. Broutman, "Crack Growth Resistance of Random Fiber Composites", J. Composite Materials, Vol. 9, 1975, pp. 216-227.

42. S.K. Gaggar and L.J. Broutman, "Effect of Crack Tip Damage on Fracture on Random Fiber Composites", Materials Science and Engineering, Vol. 21, 1975, pp. 177-183.

43. S.K. Gaggar and L.J. Broutman, "Strength and Fracture Properties of Random Fibre Polyester Composites", Fibre Science and Technology, Vol. 9, 1976, pp. 205-224.

44. S.K. Gaggar and L.J. Broutman, "Fracture Toughness of Random Glass Fiber Epoxy Composites : An Experimental Investigation", Flow Growth and Fracture, ASTM STP 631, American Society for Testing and Materials, 1977, pp. 310-330.

45. D.H. Morris and H.T. Hahn, "Fracture Resistance Characterization of Graphite/Epoxy Composites", Composite Materials : Testing and Design, ASTM STP 617, American Society for Testing and Materials, Philadelphia, 1977, pp. 5-17.

46. J.M. Mahishi and D.F. Adams, "Micromechanical Predictions of Crack Initiation, Propagation and Crack Growth Resistance in Boron/Aluminium Composites", J. Composite Materials, Vol. 16, 1982, pp. 457-469.

47. S. Ochiai and P.W.M. Peters, "Tensile Fracture of Centre-notched Angleply $(0/\pm 45/0)_s$ and $(0/90)_{2s}$ Graphite-epoxy Composites", J. Material Science, Vol. 17, 1982, pp. 417-428.

48. B.D. Agarwal and G.S. Giare, "Crack Growth Resistance of Short Fibre Composites : I - Influence of Fibre Concentration, Specimen Thickness and Width", Fibre Science and Technology, Vol. 15, 1981, pp. 283-298.

49. B.D. Agarwal and G.S. Giare, "Crack Growth Resistance of Short Fiber Composites: II - Influence of Test Temperature", Fibre Science and Technology, Vol. 16, 1982, pp. 19-28.

50. B.D. Agarwal and G.S. Giare, "Fracture Toughness of Short Fibre Composites in Modes II and III", Engineering Fracture Mechanics, Vol. 15, 1981, pp. 219-230.

51. B.D. Agarwal and G.S. Giare, "Effect of Matrix Properties on Fracture Toughness of Short Fibre Composites", Material Science and Engineering, Vol. 52, 1982, pp. 139-145.

52. A.C. Garg and C.K. Trotman, "Fracture Resistance of Random Fiber Glass Composites", Fracture Mechanics and Engineering Application, Ed. G.C. Sih and S.R. Valluri, Sijthoff and Noordhoff, 1979, pp. 373-385.

53. Yanada and Homma, "Study of Fracture Toughness Evaluation of FRP", Journal of Material Science, Vol. 18, 1983, pp. 133-139.

54. R.J. Lee and D.C. Phillips, "Fracture Toughness Testing of High Performance Laminates", Conference on Testing Evaluation and Quality Control of Composites, held at Guildford, September, 1983.

55. M.J. Owen and R.J. Cann, "Fracture Toughness and Crack-growth Measurement in GRP", Journal of Material Science, Vol. 14, 1979, pp. 1982-1996.

56. C.E. Harris and D.H. Morris, "The Effect of Laminate Thickness on the Fracture Behaviour of Composite Laminates", in Composite Structures (2), Edited by I.H. Marshall, Applied Science Publishers, 1983, pp. 511-523.

57. W.I. Griffith, M.F. Kanninen and E.F. Rybicki, "A Fracture Mechanics Approach to the Analysis of Graphite/Epoxy Laminated Precracked Tension", Nondestructive Evaluation and Flaw Criticality for Composite Materials, ASTM STP 696, R.B. Pipes, Ed., American Society for Testing and Materials, 1979, pp. 185-201.

58. G. Smith, A.K. Green and W.H. Bowyer, "The Fracture Toughness of Glass Fabric Reinforced Polyester Resins", Fracture Mechanics in Engineering Practice, Ed. P. Stanley, Applied Science Publishers, 1977, pp. 271-287.

59. B.D. Agarwal, P. Kumar and B.S. Patro, "The J Integral as a Fracture Criterion for Composite Materials" in Composite Structures 2, Edited by I.H. Marshall, Applied Science Publishers, 1983, pp. 486-499.

60. B.D. Agarwal, B.S. Patro and Prashant Kumar, "J Integral as a Fracture Criterion for Short Fibre Composites: An Experimental Approach", Engineering Fracture Mechanics, In Press.